UNIVERSITY COLLEGE LONDON

Modelling and management of multi-modal urban traffic

by

Shuai Li

A thesis submitted in partial fulfillment for the
degree of Doctor of Philosophy

in the
Faculty of Engineering Science
Civil, Environmental and Geomatic Engineering

February 2016

Declaration of Authorship

I, SHUAI LI, declare that this thesis titled, 'Modelling and management of multi-modal urban traffic' and the work presented in it are my own. I confirm that:

- This work was done wholly or mainly while in candidature for a research degree at University College London.
- Where any part of this thesis has previously been submitted for a degree or any other qualification at University College London or any other institution, this has been clearly stated.
- I have acknowledged all main sources of help, especially my supervisor Andy Chow who introduced me the high-level research directions on variational theory and bus holding control strategies, established the CTM-based simulation platform and contributed to the development of Chapter 3.
- Where I have consulted the published work of others, this is always clearly attributed.
- Where I have quoted from the work of others, the source is always given. With the exception of such quotations, this thesis is entirely my own work.

Signed:

Date:

"Be yourself; everyone else is already taken."

Oscar Wilde

UNIVERSITY COLLEGE LONDON

Abstract

Faculty of Engineering Science

Civil, Environmental and Geomatic Engineering

Doctor of Philosophy

by Shuai Li

This research aims to model and manage bus regularity with consideration of the interaction between buses and surrounding traffic in an integrated multi-modal system. A parsimonious macroscopic simulation framework is first developed to estimate multi-modal road traffic conditions and the bus-traffic interaction based on the variational formulation of kinematic waves. The proposed simulation platform can capture shocks, dispersion of vehicle platoons, moving bottlenecks and traffic characteristics effectively with data collected from Central London. Second, different bus holding strategies are implemented on the proposed simulation platform in order to evaluate and compare their performance on improving bus service regularity and impact on transport system efficiency. It is shown that the two-way holding strategy performs the best in terms of regulating headway at low-traffic level. At high-traffic level, the two-way holding strategy and the forward holding strategy have a similar performance. However, the efficiency of buses and road traffic can be severely compromised due to bus holding at stops and the consequential delay on road traffic, especially under heavy traffic conditions. In order to mitigate these challenges, the third part of this thesis presents a range of signal-based bus holding strategies which are responsive to road traffic dynamics. Proposed control strategies are implemented on the proposed simulation platform to evaluate their performance. They are also compared with traditional stop-based holding strategies and numerical results suggest improved bus service regularity and transport efficiency.

Acknowledgements

I would like to acknowledge Andy Chow's contribution in this thesis. As my academic adviser, Andy Chow has been very inspirational and insightful to motivate me to expand boundaries and broaden horizons. I sincerely appreciate his advice and guidance for the past few years. I also value the guidance from my secondary supervisor Liora Malki-Epshtein and discussion with Professor Benjamin Heydecker and Professor Nick Tyler. In the postgraduate school, I received a lot of support from other PhD students including Rui Sha, Ying Li, Lei Wang and Aris Pavlides and research associates including Fang Xu, Kun Liu and Ziyi Jiang. I am also grateful for Angela Cooper and Hale Cuss for helping me improve my academic writing. My colleagues in Room 302 of Chadwick Building have created a good working environment to conduct research and write thesis. I would also like to thank Liz Jones, Sarah Davies and Mike Dunderdale among others for their administrative support. This research is funded by the Dean's Award of UCL Faculty of Engineering and China Scholarship Council. Transport for London also provided field data to support this research.

I am very grateful for Professor Burcin Becerik-Gerber and Professor Henry Koffman who introduced me to academia and helped me develop the research skills for future success. Professor Shouqing Wang, Professor Zan Yang and Professor Siqi Zheng have provided me with generous guidance and recommendation since undergraduate school. I am very privileged to receive generous help and support from the Cheveley's family and Karl Grossfield for the past few years in London. I would also like to say thank you to Eve Lin, Qing Dou and Nan Li for their friendship and advice throughout the PhD journey.

Finally, I want to thank my parents, Angus Cepka, Heather Crichton, Edward Cepka and Sebastian Cepka for their unconditional love, company and support throughout my undergraduate and postgraduate school. Thank you so much for creating the best environment for me to grow up and always encouraging me to become a better person.

Contents

Declaration of Authorship i

Abstract iii

Acknowledgements v

List of Figures ix

List of Tables xi

Abbreviations xii

Symbols xiv

1 Introduction 1
- 1.1 Background and motivation . . . 1
  - 1.1.1 General background . . . 1
  - 1.1.2 Academic challenges . . . 4
- 1.2 Research questions and objectives . . . 8
- 1.3 Research contribution . . . 9
- 1.4 Thesis outline . . . 10

2 Literature Review 11
- 2.1 Introduction . . . 11
- 2.2 Traffic flow models . . . 12
  - 2.2.1 Microscopic Models . . . 12
  - 2.2.2 Macroscopic models . . . 16
- 2.3 Bus system . . . 26
  - 2.3.1 Performance indicators . . . 26
  - 2.3.2 Bus control . . . 29
- 2.4 Discussion . . . 33
  - 2.4.1 Research gap . . . 33

2.4.2 Research motivation 35

3 Modelling urban traffic dynamics 40
3.1 Introduction 40
3.2 Background 40
3.3 Dynamic network model 42
3.3.1 Node model 42
3.3.2 Link model 44
3.3.3 Numerical implementation 50
3.4 Numerical examples 52
3.4.1 Viscosity at shocks 54
3.4.2 Platoon dispersion 56
3.4.3 Error Analysis 59
3.4.4 Bus-traffic interaction 62
3.5 Real-world application 66
3.5.1 Traffic data 67
3.5.2 Building traffic models 69
3.5.3 Results 72
3.6 Conclusion 78

4 Evaluation of bus holding control 80
4.1 Introduction 80
4.2 Background 81
4.3 Development of VMBus platform 82
4.3.1 Interface of micro buses and macro traffic 82
4.3.2 Implementation of bus holding strategies 84
4.3.3 Performance indicators 92
4.3.4 VMBus simulation platform 94
4.4 Evaluation of holding strategies 95
4.4.1 Sensitivity analysis 96
4.4.2 Evaluation of holding strategies 114
4.5 Real-world application 120
4.6 Conclusion 125

5 Signal-based control 127
5.1 Introduction 127
5.2 Background 128
5.2.1 Stop-based holding strategies 128
5.2.2 iBus 129
5.3 Control rules 132
5.3.1 Control actions 132
5.3.2 Control strategies 136
5.4 Numerical test 141
5.4.1 Test setting 141
5.4.2 Test results 143

5.4.3 Discussion 149
5.5 Real-world application 152
5.6 Conclusion 155

6 Conclusions **158**
6.1 Summary 158
6.2 Contribution 160
6.3 Assumption and limitation 161
6.4 Future work 162

References **165**

Journal publication paper **181**

List of Figures

2.1 Vehicle order index in microscopic models 13
2.2 Demonstration of macroscopic variables in time-space plane 17
2.3 The triangular fundamental diagram 19
2.4 Basic concept of the variational method 23
2.5 Concept of cost function in the variational method 24
2.6 Bus bunching in London bus transit system (27/11/2012) 28
2.7 Illustration of bus headways 32
2.8 Thought process to identify the proposed research framework and direction, adapted from Law *et al.* (2015) 36

3.1 Cell representation of a signal-controlled link 45
3.2 Components of the proposed simulation platform 51
3.3 Network of the numerical case 52
3.4 Fundamental diagrams with different numbers of segments 53
3.5 Density maps (in: vpm) generated by CTM with different fundamental diagram specifications 55
3.6 Density maps (in: vpm) generated by variational method with different fundamental diagram specifications 55
3.7 Outflow profiles generated with different fundamental diagram specifications 58
3.8 The transitioning zone from free flow state to congestion 60
3.9 Formation of the transitioning zone 61
3.10 N value [in: veh] at the points in the transitioning zone 61
3.11 Illustration of bus-traffic interaction 63
3.12 Transition of traffic states associated with the slow-moving bus . . . 64
3.13 Simulation of impact of a slow-moving bus under variational method 65
3.14 Simulation of impact of a slow-moving bus under CTM representation 65
3.15 Tottenham Court Road (TCR), London, UK (1:10000) 66
3.16 Sensitivity analysis of estimation errors with respect to choice of saturation flow (at Goodge Street) 71
3.17 MAPE of journey time estimates with different wave speeds 73
3.18 Comparison of TCR journey times (5 June 2013) 74
3.19 Flow estimates by CTM with three-segment fundamentals 76
3.20 Flow estimates by variational method with three-segment fundamentals 77

4.1 Bus control in a multi-modal system . . . 82
4.2 Bus control in a multi-modal system . . . 85
4.3 Illustration of bus control strategies . . . 87
4.4 Representation of traffic delay . . . 93
4.5 Sample output of the VMBus simulation platform . . . 94
4.6 Components of the VMBus simulation platform . . . 94
4.7 Configuration of the base case . . . 97
4.8 Fundamental diagram of experiment test . . . 98
4.9 Bus trajectories with $\sigma(\beta_s)/\bar{\beta}_s = 1$ . . . 99
4.10 Bus headway variance with temporal passenger deviation . . . 100
4.11 Bus headway variance with temporal passenger deviation . . . 101
4.12 Bus headway deviation observed at Stop 4 under fixed traffic demands 102
4.13 Traffic congestion region upstream of bus dwelling . . . 103
4.14 Base case fundamental diagram . . . 103
4.15 Bus HD under stochastic traffic demands . . . 105
4.16 Configuration of midblock inflow . . . 106
4.17 Bus HD with midblock traffic inflow ratios . . . 106
4.18 Bus headway variance with different passing rate . . . 107
4.19 Impact of different passing rates on buses and surrounding traffic . 108
4.20 Specification of piecewise linear FDs with multiple segments . . . 109
4.21 Fixed parameters of multi-segment FDs . . . 110
4.22 Bus HD with multi-segment FDs . . . 110
4.23 AJT of buses with underlying traffic . . . 116
4.24 Average traffic delay of different scenarios . . . 117
4.25 JTD of bus operation with different traffic loads . . . 118
4.26 HD of buses operation with $d/Q = 25\%$ . . . 118
4.27 HD of buses operation with $d/Q = 75\%$ . . . 119
4.28 Bus stops in TCR (1:10000) . . . 121

5.1 iBus architecture for bus priority. Source: TfL (2006) . . . 130
5.2 Implementation of differential priority by iBus and SCOOT . . . 131
5.3 Extension of green light . . . 133
5.4 Recall of green light . . . 134
5.5 Extension of red light . . . 135
5.6 Recall of red light . . . 136
5.7 Scenario to apply SIG-1 control . . . 137
5.8 Scenario to consider traffic factor . . . 139
5.9 Scenario to apply insertion in SIG-3 control . . . 140
5.10 Numerical Test Setting . . . 142
5.11 Average bus journey time . . . 144
5.12 Average traffic delay . . . 144
5.13 Bus journey time deviation . . . 144
5.14 Bus headway deviation . . . 145
5.15 Recommendation chart of holding strategies . . . 151

List of Tables

2.1 Reciprocals of macroscopic variables 17

3.1 Summary of different FD specifications 56
3.2 Analytical solutions of platoon arrival times 58
3.3 Estimation of saturation flows on Tottenham Court Road 70
3.4 MAPE of journey time estimate by different methods 75
3.5 MAPE of flow estimates aggregated in 3 cycles 78

4.1 Evaluated factors on bus regularity 97
4.2 Summary of different FD specifications 109
4.3 Average deviation of dwelling time and cruising time (sec) 111
4.4 Comparative performance ranking 112
4.5 Specification of test scenario 115
4.6 Impact of different bus holding strategies 120
4.7 TCR Bus route ID 122
4.8 AJT of TCR bus route under different holding strategies (sec) . . . 123
4.9 Average traffic delay on TCR under different holding strategies (sec) 124
4.10 JTD of the bus routes under different holding strategies (sec) 124
4.11 TCR bus route HD under different holding strategies (sec) 125

5.1 Differential priority levels of iBus 131
5.2 Signal-based control strategies 137
5.3 Evaluation of different signal-based control strategies 145
5.4 Comparison and signal-based control and stop-based control 147
5.5 Comparison of signal-based control and iBus 148
5.6 Summary of control strategy effects 150
5.7 Average bus journey time under signal-based control (sec) 153
5.8 Average traffic delay under signal-based control (sec) 153
5.9 Journey time deviation under signal-based control (sec) 154
5.10 Average bus journey time under signal-based control (sec) 156

Abbreviations

AD	**A**verage **D**elay
AFC	**A**utomatic **F**are **C**ollection
AJT	**A**verage **J**ourney **T**ime
ANPR	**A**utomatic **N**umber **P**late **R**ecognition
AVL	**A**utomatic **V**ehicle **L**ocation
BRT	**B**us **R**apid **T**ransit
CTF	**C**umulative **T**raffic **F**low
CFL	**C**ourant **F**riedrichs **L**ewy
CTM	**C**ell **T**ransmission **M**ethod
DVLA	**D**river and **V**ehicle **L**icensing **A**gency
DfT	**D**epartment **f**or **T**ransport
FIFO	**F**irst-**I**n-**F**irst-**O**ut
FD	**F**undamental **D**iagram
GHR	**G**azis **H**erman **R**othery
GPS	**G**lobal **P**ositioning **S**ystem
HD	**H**eadway **D**eviation
HJB	**H**amilton **J**acobi **B**ellman
ITS	**I**ntelligent **T**ransport **S**ystem
JTD	**J**ourney **T**ime **D**eviation
LCAP	**L**ondon **C**ongestion **A**nalysis **P**roject
LWR	**L**ighthill **W**hitham **R**ichards
MAPE	**M**ean **A**bsolute **P**ercentage **E**rror
PDE	**P**artial **D**ifferential **E**quation
PSD	**P**hase **S**pace **D**ensity

RHS	**R**ight **H**and **S**ide
TCR	**T**ottenham **C**ourt**R**oad
TfL	**T**ransport **f**or**L**ondon
TSP	**T**ransit **S**ignal**P**riority
VM	**V**ariational **M**ethod
UTC	**U**rban **T**raffic **C**oontrol

Symbols

c	signal cycle time
d	traffic demand
e	mean absolute percentage error
g	green light time
h	headway
$\bar{h}$	average headway
h^T	target headway
h^M	minimum headway
i	cell index
M	moving bottleneck
n	vehicle index
N	accumulative traffic flow
q	traffic flow
q_B	bottleneck capacity/passing rate
q_M	capacity/passing rate with moving buses
q^R	traffic flow to receive
q^S	traffic flow to send
Q	saturation flow
r	red light time
s	stop index
t	time instant
t^A	actual arrival time
t^S	scheduled arrival time

t^D	departure time
T	time duration
T^C	bus cruising time
T^D	bus dwell time
T^H	bus holding time
T^J	journey time
T^L	bus loading time
T^S	slack time
T^W	passenger waiting time
u	free flow speed
v	traffic speed
w	backward wave speed
x	location
ρ	traffic density
ρ_c	critical density
ρ_j	jam density
Φ	fundamental diagram
Θ	cost function (variational formulation)
β	bus loading time factor
ε	bus headway discrepancy
α	bus control parameter
η	traffic split parameter
σ	standard deviation
Δt	time step
Δx	space step (cell size)

Dedicated to my parents

Chapter 1

Introduction

1.1 Background and motivation

1.1.1 General background

Road traffic volume is currently increasing at a rapid speed. In 2011, the overall motor vehicle traffic volume in the United Kingdom was 303.8 billion vehicle miles, which was about 7 times that of the road traffic volume in 1951 (DfT, 2012*a*). This growing traffic demand is mainly driven by three forces which are population, GDP per capita and fuel price. In the United Kingdom, the population is estimated to rise from 62 million in 2010 to 74 million in 2033 (ONN, 2009). Between 2009 and 2013, GDP per capita increased by 4.5%, and the growing trend is likely to continue due to a strong economy after crisis. With the recent drop in oil price and increase in energy efficiency, the fuel cost of driving is expected to decline in the near future (OBR, 2014). The Department for Transport (DfT) forecast that road traffic will be 46% higher in 2040 compared to 2010 (DfT, 2013). Overall, the trend of growing traffic demand will continue for the next few decades.

The ever-increasing road traffic generates a negative impact on the well-being of societies. Despite the peak-car phenomenon, Goodwin (2012) pointed out that traffic growth can still exist in most countries and cities. Since 2010, the increasing

traffic demand has been identified as one of the top challenges faced by the civil engineering community (Becerik-Gerber *et al.*, 2013). Negative consequences of high-level traffic demand include traffic congestion, journey time delay, energy consumption rise and pollution emission. In 2010, transport accounted for 26% of the total greenhouse gas emissions in the United Kingdom (DfT, 2012*a*). A government report published by the Prime Minister's Strategy Unit reveals the economic impact of worsening urban traffic conditions. Excessive traffic delay is estimated to cost £12.0 billion, and poor air quality due to traffic emission is estimated to cost £4.5 to 10.6 billion (PMSU, 2009). Therefore, the increasing traffic places the UK economy, environment and society under pressure.

A bus system is an important transport mode in an integrated multi-modal transport system. Buses can make more efficient use of road space compared to private vehicles in terms of the number of passengers conveyed over a unit length of road.The benefit of the bus system has been outlined by DfT as:

> "Economically, supporting buses increases the attractiveness of bus travel relative to car travel, which in turn helps alleviate congestion, including for those still in the car. Environmentally, the increased attractiveness of bus travel relative to car travel helps reduce pollution. Socially, the existence of a bus service increases the accessibility of non-car owners to social services and employment opportunities" (DfT, 2012*b*).

Given its importance in our society, a regular bus service is critical to satisfy the expectations of both travelling passengers and transport agencies. Service regularity is generally considered to be the most important performance measure of an operating bus system (Bowman and Turnquist, 1981). With a regular bus system, passengers can plan their journey effectively without excessive waiting time, and they can arrive at their destinations at appointed times. If the regularity of a bus service is not satisfactory, passengers may shift from buses to other modes such as private cars. In this case, an increasing amount of traffic demand is

added to the existing road of limited capacity. From the agencies' perspective, enhanced bus regularity is beneficial with reduced labour hours assigned due to service uncertainty and an increasing utilization rate of the bus operating service. London bus service regularity level declined in 2015 with the excess passenger waiting time at bus stops increased by 7% from 61.2 seconds to 65.4 seconds (TfL, 2015). In order to maintain service frequency, highly irregular bus routes require additional buses to meet heavy and irregular passenger demand. In London, the capital and operational costs of running one additional bus are about £120,000 every year which shows that irregular bus service imposes strong financial pressure on the operating agency. Overall, service regularity is widely recognized as the primary goal to achieve in a bus system.

In order to ensure bus service regularity, various strategies have been implemented and proposed. These strategies can generally be divided into two categories. The first category focuses on expanding or improving the road space where buses operate. Example policies in this category include separate bus lanes, development of rapid transit system, and improvement of road geometry design. The second category employs efficient design and management strategies of the bus system to enhance service performance. For instance, the development of an automatic fare collection system can reduce bus delay caused by passenger payment. With advanced information technology, recent decades have witnessed a growing trend for an intelligent transport system which is installed in roads and operating buses. For example, transit signal priority can utilize real-time bus information to adjust traffic signals in transport networks to assign priority to buses. The i-Bus system deployed by Transport for London (TfL) can monitor bus locations and apply control strategies accordingly.

However, improvement strategies which focus on expanding or improving existing roads are not sustainable from a long-term perspective. Continuous expansion and construction of transport infrastructure are challenged by spatial constraints, financial limits, as well as environmental regulations (Hau, 1998). As new infrastructure is completed, induced traffic demand can offset its effectiveness to reduce traffic congestion. Therefore, public transport agencies and academic researchers

have turned to developing effective control strategies that can improve service efficiency and regularity.

Among a wide variety of bus control strategies, bus headway control is commonly used to regulate the bus service, especially for high-frequency urban bus routes. Bus headways are directly related to the waiting time of passengers at bus stops. Strong bus headway deviation leads to excess passenger waiting time at a bus stop. Moreover, bus headway deviation leads passengers to experience stronger perceptions of bus delays and irregular service compared to time table adherence (Diab *et al.*, 2015). Headway-based bus holding strategies can significantly improve bus headway regularity in an urban transport system. There are three main headway-based holding strategies which are forward, backward and two-way holding strategies. The forward holding strategy aims at regulating headways with their leading buses; the backward with their following buses; the two-way with both leading and following buses.

In a multi-modal urban transport system where buses and other road traffic share the limited road space together, the outcome of bus headway control can be either positive or negative given the interaction of different transport modes. Headway control strategies in favour of buses can potentially affect private vehicles negatively by increasing their delay. Moreover, predefined headway control strategies might not be effective in a congested urban road where bus movement is constrained by their surrounding traffic. In order to successfully develop and implement a bus headway control strategy, it is important for policy makers to fully understand its comprehensive impact on various transport modes in a multi-modal transport system in different traffic conditions.

1.1.2 Academic challenges

In order to establish an effective headway control strategy, there are three academic challenges to overcome, which are below based on the logical order to tackle the outlined problem.

- An integrated simulation platform which is simple[1] to deploy and accurate to estimate multi-modal[2] urban traffic conditions and interaction between buses and their surrounding traffic.

- An effective[3] framework to evaluate effectiveness of bus holding strategies to understand their performance under different traffic conditions and impact on various transport modes in an integrated system.

- Innovative bus holding strategies which are responsive to road traffic dynamics and effective in improving bus service regularity without compromising transport efficiency.

Since buses are usually integrated with general road traffic, it is necessary to accurately estimate underlying urban traffic conditions in which buses operate. Most traffic models researching into traffic conditions focus on motorways or road segments (Daganzo, 2005*b*; Laval and Leclercq, 2013). Modelling of integrated urban transport systems with roads, intersections and signals is more complicated compared to motorways, and consequently there is relatively less research in this area. If a section of motorway can be considered as a one-direction transport corridor which carries vehicles from fixed entrances to exits, then an integrated urban network is structured by multiple transport corridors connected through transport intersections. Traffic control by signals at intersections further increases the complexity of modelling. Moreover, vehicles in an urban network can travel towards different directions with multiple combinations of origins and destinations compared to one-direction motorway. In order to develop and evaluate a bus headway control strategy, it is fundamental to establish a comprehensive urban transport framework to accurately estimate urban traffic conditions.

[1] a simple simulator is a relative term compared with microscopic simulators. It requires fewer parameters, calibration efforts and faster computational capability to reproduce essential traffic features for research interests

[2] multi-modal is defined as mixed traffic flows of buses and other road traffic without consideration of pedestrians or cyclists from here and onwards in this thesis

[3] effective means that the proposed simulation framework can capture essential traffic features (such as moving bottlenecks and shock waves) with high accuracy according to the underlying theoretical model compared to the competing simulation framework

It is necessary to develop a simple and effective platform which can represent the dynamics of interaction between buses and private vehicles in an integrated transport system. Bus service operating in mixed traffic is the predominant practice in most cities. Modelling of bus-traffic[4] interaction serves as the mechanism to estimate bus movement in multi-modal traffic flow. Therefore, an accurate representation of bus-traffic interaction is the prerequisite condition to develop an effective headway control strategy. It can help us evaluate the impact on bus operations under certain control strategies, for example, if a bus dwells at a curbside bus stop to pick up passengers. Vehicles following the bus need to take corresponding actions to surpass the bus from other lanes or to stop behind it. Most research on urban traffic control focuses on only one transport mode, either the buses (Daganzo, 2009; Daganzo and Pilachowski, 2011; Xuan *et al.*, 2011) or the general road traffic (Balijepallia *et al.*, 2013*a*; Chow *et al.*, 2015). An effective dynamic framework is still unavailable which can model a multi-modal transport system including both microscopic buses and macroscopic traffic.

There have been several microscopic and macroscopic simulation platforms to model bus-traffic interaction proposed by various researchers (Sibley, 1985; Hossain and McDonald, 1998; Kosonen, 1999; Silcock, 1993; Fellendorf, 1994; Valencia, 2012; Gu *et al.*, 2013; TRL, 2014) which, however, cannot represent traffic conditions and interactions in a simple and effective way. For microscopic simulation, it calls for a large number of detailed parameters which are difficult to calibrate or collect in reality. It is also more expensive and time-consuming to build a microscopic simulator into a large-scale network, such as a comprehensive urban transport network, given its requirement for complicated parameter calibration and an intense computing capability requirement. Moreover, existing microscopic simulation represents traffic interactions among individual vehicles which does not take into account bus-specific characters (Silva, 2001). For macroscopic simulation, most existing simulators do not consider buses or simply take buses as a separate overlay of vehicle stream which does not interact with the rest of road

[4]traffic here refers to the road traffic excluding buses

traffic (TRL, 2014). Other macroscopic simulators represent bus-traffic simulation in a static framework which cannot be implemented in a dynamic transport system.

The comprehensive impact of headway control strategies on both buses and other road traffic concurrently in a multi-modal transport system remains unknown. Since implementation of bus headway control strategies introduces perturbation to the transport system, not only buses but also the rest of road traffic are affected. Bus control such as holding buses at bus stops can potentially delay other road traffic due to the bus-traffic interaction. However, evaluation of bus control impact on both bus service and traffic delay in actual field tests can be very time-consuming and cost-inefficient which makes it hard to be carried out in reality. Therefore, there is a need for an evaluation framework to efficiently assess the comprehensive impact of different headway control strategies in a multi-modal urban transport system. Policy makers can gain insights into the internal mechanism of how an urban transport system responds to different headway control strategies through the process of formulating, calibrating and deploying this evaluation framework. Policy makers can thus further improve the intelligence of bus headway control strategies based on different objectives to achieve.

Moreover, there is a need for innovative bus control strategies which are responsive to road traffic conditions and effective to improve bus service regularity without compromising transport efficiency. How to incorporate road traffic conditions to develop an effective bus headway control strategy remains a challenge. Most headway control strategies focus on holding buses at bus stops for an extra amount of time in order to even bus headways. A predefined amount of time, called slack time, is assigned to bus stops to hold buses even if they arrive without delay. To ensure stop-control holding effectiveness, the predefined slack time is large enough so that calculated holding time is always positive. Bus service efficiency under these holding strategies is greatly compromised because the predefined slack time slows down the commercial speed of bus service and reduces bus service efficiency. Holding buses at a bus stop after all passengers are loaded or alighted can also be annoying for onboard passengers.

Lastly, various advanced transport systems have been developed and implemented in the world such as the London iBus system and Sydney Coordinated Adaptive Traffic System. Among these systems, London iBus has been recognized as an effective tool to help improve bus service efficiency and regularity (Hounsell *et al.*, 2008*a*). Used mainly for assigning priority to buses, iBus' potential in regulating bus service has not been fully explored and more innovative bus control strategies can be developed. Proposed innovative strategies should leverage existing iBus infrastructure and achieve higher bus service regularity compared to existing iBus-based control strategies.

1.2 Research questions and objectives

The main research question is how to develop an effective control strategy to improve bus service regularity in a multi-modal urban transport system. In order to answer this main question, there are 3 sub research questions to address:

1. What are urban traffic conditions given existence of buses and other road traffic?
2. How do different holding strategies perform and affect other road traffic?
3. How to control bus headways effectively without compromising transport system efficiency?

In order to address these research questions, the following research objectives are proposed:

1. Establish a parsimonious[5] simulation framework to estimate multi-modal road traffic conditions and bus-traffic interaction in an integrated urban transport system.

[5]the term parsimonious means that the simulation framework is both simple and effective

2. Evaluate the effects of different bus holding strategies and understand their performance and impact on multi-modal traffic.

3. Develop a range of bus schedule control strategies which are responsive to road traffic dynamics, effective to improve bus service regularity and reduce traffic delay.

1.3 Research contribution

First, the proposed simulation platform in this research can help estimate traffic conditions more accurately in an urban transport network compared to other competing macroscopic simulation platforms, especially with the presence of buses among other road traffic. It is particularly more accurate to estimate urban traffic flow volume upon being released from signalized junctions when traffic lights switch from red to green.

Second, the proposed VMBus simulation platform is effective in estimating bus holding strategy outcomes and impacts in an integrated urban transport system. To the researcher's best knowledge, no other simulation platforms can provide an equivalently comprehensive evaluation in terms of bus regularity, bus commercial speeds and overall traffic delay as the proposed VMBus platform does.

Third, more innovative bus holding strategies are proposed based on traffic signal adjustment. Proposed strategies are relatively cost-efficient to implement as they only require the existing iBus system and no other additional infrastructure. Compared to classical bus holding strategies, they do not compromise bus commercial speeds in order to achieve bus service regularity and they are responsive to real-time traffic dynamics.

1.4 Thesis outline

In Chapter 2, a literature review is presented with an aim to understand different existing traffic flow models and how bus-traffic interaction is represented under different models. This chapter also reviews the bus control strategies with a focus on bus headway control. Based on findings from the literature review, research gaps and challenges are identified as motivation for this study.

In Chapter 3, a macroscopic simulation framework is developed for estimating road traffic conditions with the input of boundary traffic demand. The macroscopic simulator is further extended to incorporate public transport (e.g. buses) and reproduce interaction between buses and their surrounding traffic based on bottleneck models. The simulation framework is validated with numerical examples and a real-world case with field data provided by TfL.

In Chapter 4, a set of existing bus headway control strategies are implemented in the proposed simulation platform and evaluated in terms of their effectiveness and efficiency under different traffic conditions, passenger demands and various transport characteristics. Simulation tests based on hypothetical networks and real-world settings are conducted to quantify control performances and impacts. Research findings are compared with previous findings with analytical discussions of traffic flow.

In Chapter 5, a set of new bus headway control strategies are proposed and evaluated based on the developed simulation platform. They are further compared with existing headway control strategies and iBus to identify their advantages and disadvantages in various scenarios. The impact on different traffic modes in terms of regularity and efficiency is identified and validated in real-world settings.

In Chapter 6, research conclusions and contributions are drawn; assumptions and limitations of this study are listed and future directions in terms of short-term, middle-term and long-term plans are discussed.

Chapter 2

Literature Review

2.1 Introduction

The objective of this chapter is to establish foundation for this doctoral research. The specific objectives are:

1. To review existing academic research in traffic flow modelling and bus control strategies
2. To identify knowledge and research gaps for us to mitigate
3. To provide the knowledge basis to carry out our research activities

Section 2.2 reviews traffic flow models and the bus-traffic representations. Section 2.3 presents various bus control strategies categorised by priority improvement strategies. Section 2.4 discusses the research gaps identified through the literature review and how they motivate the development of the proposed research.

2.2 Traffic flow models

Traffic flow models are mathematical representations of traffic to estimate road traffic conditions in which buses operate. In this research, the review was conducted based on the scale of traffic representation which is arguably the most classical and popular categorization.

Traffic flow models are divided into two categories: microscopic models and macroscopic models. Microscopic models represent each vehicle separately and trace individual vehicle behaviour. Macroscopic models treat traffic as continuous fluid and study traffic dynamics in an aggregated manner.

2.2.1 Microscopic Models

A large class of microscopic models are vehicle-following models which trace individual behaviour of each vehicle and focus on depicting the relationship between the motion of two successive vehicles. Car following models are of crucial value to traffic simulation since they can reproduce behaviour of each individual vehicle to a great length of details. Therefore, the microscopic simulator is an effective tool to validate detailed design of transport infrastructure and specific transport operations.

In microscopic models, each vehicle is indexed with a number based on their order entering the simulated system. Figure 2.1 illustrates a scheme of 4 vehicles in different locations of a section of road at time t. Vehicle n at location x_n follows vehicle $n-1$ at location x_{n-1}, and vehicle x_{n+1} follows vehicle n at location x_n.

Location, speed and acceleration are variables considered in microscopic models. Taking vehicle n in Figure 2.1 as an example, and assuming that it moves a distance of Δx from time t to time $t+\Delta t$, its speed v_n and acceleration a_n at time t can be calculated by Equation 2.1 and Equation 2.2.

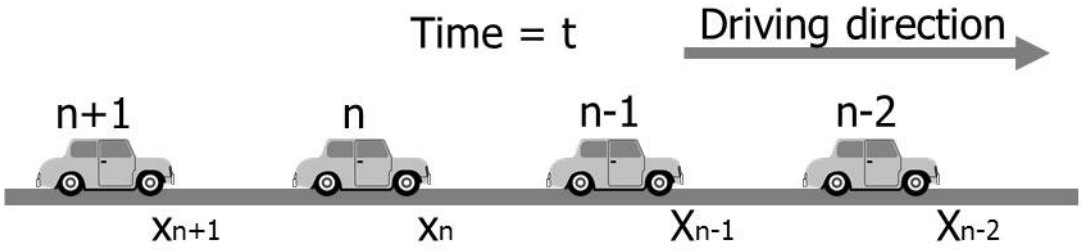

FIGURE 2.1: Vehicle order index in microscopic models

$$v_n = \frac{dx_n}{dt} = \lim_{\Delta t \to 0} \frac{\Delta x}{\Delta t} \tag{2.1}$$

$$a_n = \frac{dv_n}{dt} = \frac{d^2 x_n}{dt^2} \tag{2.2}$$

The mechanism of vehicle-following models is essentially a stimulus-response process which can be generally expressed as:

$$\text{Response (later)} = \text{Sensitivity} \times \text{Stimulus (now)}$$

Upon receiving a stimulus from their surrounding traffic, a driver can respond with a variety of actions such as braking, accelerating and changing lanes. Car following models can be differentiated by different stimulus elements such as safety following distance, relative speed, and relative spacing among others.

There are different approaches in vehicles following models depending on the stimulus elements such as safety following distance, relative speed and relative spacing.

Stimulus-response models

One class of microscopic models are stimulus-response models motivated by the large amount of empirical data collected from the comprehensive field experiments carried out by General Motors Group. Response of a driver towards the precedent vehicle is represented in these models(Gerlough and Huber, 1975).

The most basic stimulus-response model is the linear car following model which models the acceleration or deceleration rate $\ddot{x}_n(t+T)$ after reaction time T. It is proportional to stimulus, as shown in Equation 2.3.

$$\ddot{x}_n(t+T) = \lambda[\dot{x}_{n-1}(t) - \dot{x}_n(t)] \tag{2.3}$$

where λ is the sensitivity constant and $\dot{x}_n(t) - \dot{x}_{n+1}(t)$ is the relative speed which serves as the stimulus.

Safety-distance model

The safety-distance model is one of the first models established in vehicle-following theory. Pipes (1953) developed the model based on the safety distance regulation suggested by Californian Motor Vehicle Code which is as follows:

> "A good rule for following another vehicle at a safe distance is to allow yourself at least the length of a car between your vehicle and the vehicle ahead of every ten miles per hour of speed at which you are travelling"

Pipes (1953) implemented the minimum safety distance in a vehicle-following model with consideration of the minimum safety distance. Specified terms related to driver's reaction time and braking distance are also included in Kometani and Sasaki (1961).

The vehicle-following theory based on the minimum safety distance can be the expressed by Equation 2.4.

$$x_{n-1} - x_n = d + h^M v_n + l_{n-1} \tag{2.4}$$

where h^M is the minimum time headway, l_{n-1} is the length of the leading vehicle n and d stands for the distance between two following vehicles at standstill. $h^M v_n$ is the minimum safety distance.

Microscopic simulation of bus-traffic interaction

Most studies on modelling and simulating interaction between public transport and road traffic are based on microscopic models. Silva (2001) concluded that an effective microscopic platform to capture traffic interaction should satisfy three basic requirements:

1. Appropriate car-following models
2. Explicit representation of public vehicles and road traffic
3. Realistic model of lane changing behaviour

Various microscopic bus-traffic simulation platforms have been proposed such as NETSIM (Sibley, 1985), MIXNETSIM (Hossain and McDonald, 1998), HUTSIM (Kosonen, 1999), SIGSIM (Silcock, 1993) and VISSIM(Fellendorf, 1994), which have been proposed with all three requirements satisfied. Microscopic simulation takes different input variables which include 1) drivers' response towards their leading vehicles in the same line and adjacent vehicles in other lanes; 2) vehicle types such as cars and trucks; 3) vehicle operations such as stop, acceleration and deceleration (Fellendorf, 1994). Some simulators also consider pedestrians (Kosonen, 1999) and on-street parking(Silcock, 1993) in order to study their impact on traffic behaviour.

Microscopic simulation to represent bus-traffic interaction is advantageous in that it can capture extremely detailed behaviour of vehicle operations and road design. Since microscopic simulation tracks behaviours of individual vehicle and drivers' reaction, bus-traffic interaction can be modelled directly based on responses of bus drivers or private vehicle drivers. However, microscopic vehicle interaction does not consider mode-specific characteristics of buses, such as bus dwelling to embark and disembark passengers (Silva, 2001). Due to the large number of parameters to calibrate in microscopic simulation, it can be prohibitively difficult and expensive to apply it in an integrated urban transport network for evaluating bus service performance and control strategies of different bus routes at different times.

2.2.2 Macroscopic models

This section starts from a review of macroscopic variables and their numerical relationships represented by the fundamental diagrams. It is followed by a review of macroscopic traffic flow models, numerical solutions to solve these models, and simulations based on macroscopic models.

Macroscopic variables

Macroscopic models assume traffic as a continuum flow and explore the temporal and spatial dynamics of traffic flow. Individual vehicles are not identified by macroscopic models which differentiate them from microscopic models. Vehicles are modelled in an aggregated approach characterized by three macroscopic variables which are traffic density, flow and speed in which:

- Flow measures the number of vehicles per unit time.
- Density measures the number of vehicles per unit length of road.
- Speed measures the distance per unit time.

Figure 2.2 shows vehicle trajectories travelling through a time-space plane. Each line represents the trajectory of an individual vehicle. Consider region A as a time-space region with space length Δx, and time length Δt and a cumulative number of N vehicles travel through this area.

Since macroscopic models assume the traffic to be a continuum flow, which indicates that the N value is continuous. Based on the N value, Leutzbach (1988) developed Equation 2.5 and Equation 2.6 to calculate instantaneous traffic flow and density.

$$q(x,t) = \lim_{\Delta t \to 0} \frac{N(x, t+\Delta t) - N(x,t)}{\Delta t} \tag{2.5}$$

$$\rho(x,t) = \lim_{\Delta x \to 0} \frac{N(x+\Delta x, t) - N(x,t)}{\Delta x} \tag{2.6}$$

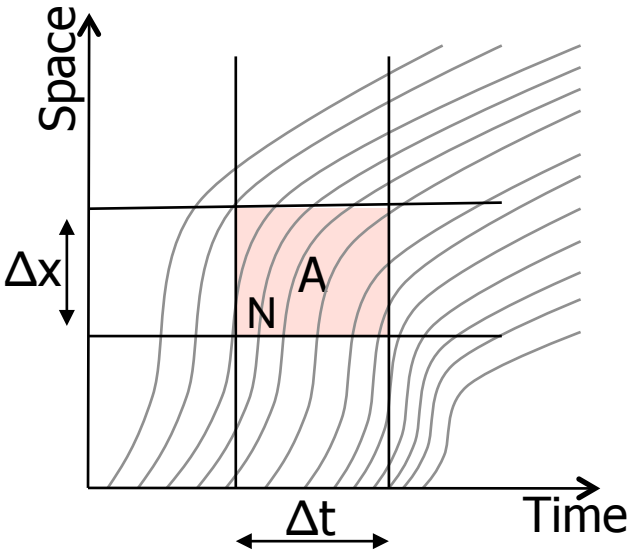

FIGURE 2.2: Demonstration of macroscopic variables in time-space plane

Based on Equation 2.5 and 2.5, the relationship between traffic flow and density can be identified as:

$$q(x,t) = \rho(x,t)v(x,t) \tag{2.7}$$

where the instantaneous speed $v(x,t)$ is the space mean speed. It equals to the harmonic mean of the distribution of traffic speed over time.

Reciprocals of these variables have different physical interpretations and can also be used to represent traffic states. Reciprocal variables are summarized in Table 2.1.

TABLE 2.1: Reciprocals of macroscopic variables

Variable	Reciprocal	Measurement
Spacing	reciprocal of density	the average distance between two successive vehicles
Headway	reciprocal of flow	average time between two successive vehicles passing a fixed point
Pacing	reciprocal of speed	time spent per unit length of road

Depending on specific research questions, researchers represent traffic conditions with different pairs of macroscopic variables such as speed and density (Heydecker and Addison, 2011), spacing and speed (van Wageningen-Kessels *et al.*, 2009, 2010; Yuan *et al.*, 2012; van Wageningen-Kessels *et al.*, 2013) and speed and flow (Li, 2008).

Fundamental diagrams

The fundamental diagram is the quantified relationship between different macroscopic traffic flow variables. Kuhne (2011) claimed that Greenshields *et al.* (1935) is arguably the founder of the traffic flow theory by establishing an observed model of traffic flow movement at a time-space point. Greenshields *et al.* (1935) proposed a linear fundamental relationship which shows decrease of traffic flow speed with the increase of traffic flow density. The associated quadratic fundamental diagram indicates that when the road is fully congested, vehicles stop moving.

Since Greenshield's work, many researchers have proposed various forms of fundamental diagrams. Underwood (1961) presented a speed-density relationship which works well in free-flow conditions. Greenberg (1959) presented the formulation of a concave speed-density relationship which is advantageous in its simplicity in application deployment and accuracy in high-density traffic approximation. Nevertheless, the speed in Greenberg's model is boundless as density approaches zero which is not realistic in practice. Edie (1961) developed a mixed speed-density model which combines the advantage of Underwood (1961) in modelling free-flow traffic condition and the advantage of Greenberg (1959) in modelling congested traffic condition.

Among various fundamental diagrams, the triangular density-flow relationship proposed by Newell (1993) is frequently used in traffic modelling and management for its simplicity and convenience.

The triangular fundamental diagram is shown in Figure 2.3 and the numerical relationship is expressed by Equation 2.8,

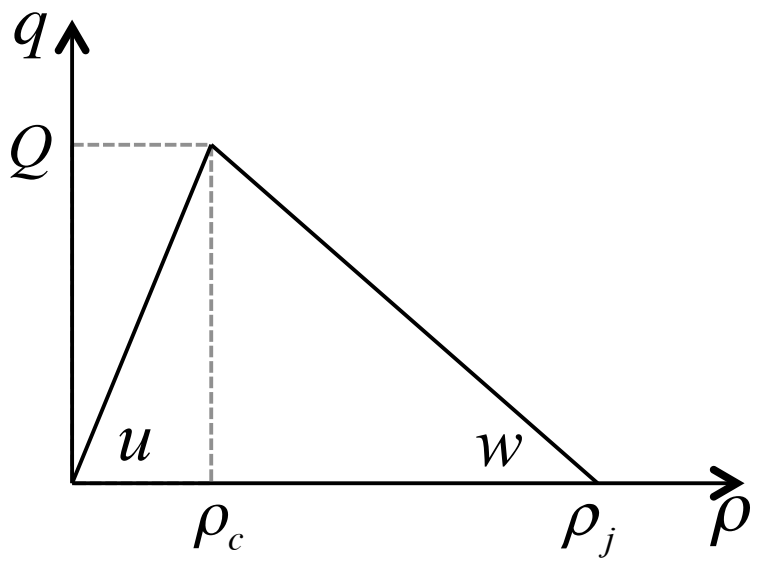

FIGURE 2.3: The triangular fundamental diagram

$$q = \begin{cases} u\rho & (0 \leq \rho \leq \rho_c) \\ w(\rho_j - \rho) & (\rho_c \leq \rho \leq \rho_j) \end{cases} \tag{2.8}$$

where ρ_c refers to the critical density at which traffic flow level reaches the maximum level, u is free flow speed and w is backward wave speed. Q and ρ_j are two critical parameters in the fundamental diagram which define transport link capacity. Q is the maximum traffic flow which can travel through a transport link and ρ_j is the maximum density of vehicles which can be held by a transport link in full congestion.

Based on the classical studies above, Carey and Bowers (2012) presented a comprehensive review and suggested that essential properties of fundamental diagrams should include free flow speed, jam density, wave speeds, and among others. Further study on specifications of fundamental diagrams is referred to by Chow *et al.* (2015) which validates their performances for dynamic modelling purposes with empirical data.

First-order traffic flow model

Lighthill and Whitham (1955) and Richards (1956) originally developed a kinematic wave model of macroscopic traffic flow, known as the LWR model, which

treats traffic stream as compressible one-dimensional flow like fluid. The LWR model is one of the most widely accepted traffic flow models due to its capability to represent physical traffic behaviours such as the formulation of traffic queue and spillover[1]. The LWR model has been broadly applied in traffic modelling and control in both motorways (Newell, 1993) and urban networks (Geroliminis and Daganzo, 2008).

LWR model establishes the numerical relationship between traffic flow q and traffic density ρ. The first-order LWR model is also called LWR partial differential equation (PDE). LWR PDE calculates traffic macroscopic variables such as flow and density based on scalar hyperbolic conservation law as defined by Equation 2.9. Equation 2.9 is the conservation law in LWR model which shows the mass balance of vehicles in motorway without any external traffic flow.

$$\frac{\partial q}{\partial x} + \frac{\partial \rho}{\partial t} = 0 \tag{2.9}$$

where x and t are spacial and temporal parameters. Furthermore, q can be expressed by Equation 2.10:

$$q = \Phi(\rho, x, t) \tag{2.10}$$

where Φ is the fundamental diagram which determines traffic flow q based on density ρ, location x and time t.

By taking the full-range of fundamental diagrams into account, the LWR model has the advantage of capturing various macroscopic traffic features such as development of traffic congestion, propagation of shockwaves[2], formation and dissipation

[1]Spillovers occur when growing queues at the downstream signal block the arrivals from the upstream signal, and vehicles cannot depart even though the signal phase is green.

[2]Shockwaves are transition zones between two traffic states (e.g. between free flow and congestion) that move through a traffic environment like a propagating wave.

of traffic queues. Traffic waves or shockwaves are discontinuities in traffic densities. Traffic wave trajectories in a time-space plane are determined by shockwave speeds which can be derived from the LWR model.

However, the LWR model is also limited in reproducing some complicated traffic phenomena such as capacity drop and hysteresis (Li *et al.*, 2012). Hall and Agyemang-Duah (1991) defined the capacity drop as the "reduction of maximum flow rates when a queue forms". From a macroscopic perspective, the hysteresis phenomena means that there is a higher traffic flow during traffic congestion onset compared to during traffic congestion offset for the same traffic density (Geroliminis and Sun, 2011).

In order to solve the LWR model numerically, several discretised computational algorithms have been proposed. The most popular solution method is arguably the cell transmission method by Daganzo (1994) based on Godunov's scheme by Godunov (1959).

Cell Transmission Method

CTM works on predefined space-time grids with a triangular fundamental diagram. The entire road network is discretised into a collection of sections or 'cells'. Traffic outflows and density of each cell are updated at each time interval. The detailed algorithm of CTM is described in Chapter 3 where CTM is implemented to compare its performance with the proposed simulation platform.

Since Daganzo (1994), CTM has been applied in a number of studies ranging from freeways as in Gomes and Horowitz (2006) and Chow *et al.* (2008), and to urban networks as in Ziliaskopoulos (2000), Lo and Szeto (2002) and Chow *et al.* (2010).

Despite its popularity, Daganzo (2006) and Mazare *et al.* (2011) claimed that a weakness of CTM is producing errors at discontinuity (i.e. shock) in the solution just like other first-order Godunov's schemes (LeVeque, 1992). The flow and density profiles are smeared in regions near the discontinuities (i.e. 'shocks') and this feature is termed as 'viscosity' by LeVeque (1992) (LeVeque, 1992).

Moreover, the space-time discretization under CTM is limited by the Courant-Friedrichs-Lewy (CFL) condition (Courant *et al.*, 1928) which requires the length of each 'cell' to be smaller or equal to traffic free flow speed times the time step size. This is to ensure the numerical stability and non-negativity of traffic quantities by constraining traffic from not travelling further than the length of the cell in one simulation time step.

It is also revealed that CTM, as a Godunov scheme, is ineffective in modelling a moving bottleneck, such as congestion caused by slow moving buses in an urban network (Lebacque *et al.*, 1998).

Variational Method

Daganzo (2005*a*) proposed a variational formulation of kinematic waves as a simplified form of the LWR model. Daganzo (2005*b*) formulated the kinematic wave theory in a way that traffic is treated as fluid in a continuous function of time t and space x represented by $N(x,t)$. $N(x,t)$ is the cumulative traffic flow at a particular point in time-space plane, which denotes the cumulative traffic flow. N is a function of time t and space x. Use N_t to denote $\frac{\partial N}{\partial t}$ which is traffic flow and N_x to denote $\frac{\partial N}{\partial x}$ which is traffic density. Therefore, Equation 2.10 can be transformed into Equation 2.11 which satisfies the Hamilton-Jacobi-Bellman equation.

$$N_t = \Phi(-N_x, x, t) \tag{2.11}$$

where the subscript stands for partial derivatives of N over the subscripted parameter.

The basic concept of the variational method is illustrated in Figure 2.4. Given that the N value at B is known, the N value at point P can be calculated by working out the minimum operational rule expressed by Equation 2.12.

$$N_p = \min\{N_B + \Delta N_{\overline{BP}}\} \forall \overline{BP} \in P_p \tag{2.12}$$

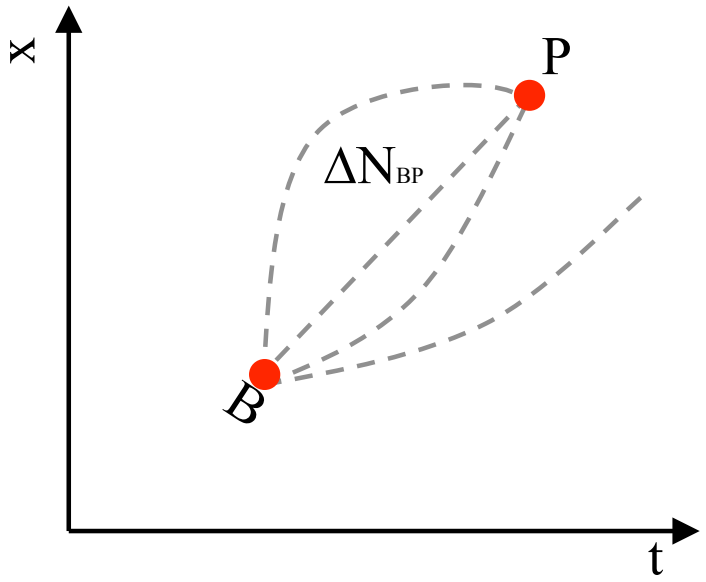

FIGURE 2.4: Basic concept of the variational method

where $\overline{BP}$ refers to space-time paths from B to P as represented by the grey dash lines in Figure 2.4, Pp is the set of all direct wave paths $\overline{BP}$ from B to P. N_B is the N value at the start boundary B of the path and $\Delta N_{\overline{BP}}$ is the predicted change in cumulative traffic flow along the wave path $\overline{BP}$ which can be solved by the method of characteristics. Continuity of this solution was demonstrated in Newell (1993) together with a tedious calculation process to identify the unique and correct N at every point in space-time.

Based on Newell (1993), Daganzo (2005*a*) and Daganzo (2006) rigorously proved the posedness, continuity and stability of the variational formulation. Daganzo (2005*b*) further proposed a solution method based on dynamic programming algorithm to calculate N values.

Given the initial and boundary conditions, Equation 2.11 can be solved by dynamic programming with any concave fundamental diagrams with unprecedented accuracy (Daganzo and Laval, 2005; Daganzo, 2005*b*, 2006).

A cost function Θ is introduced by Daganzo (2005*b*) to calculate the term $\Delta N_{\overline{BP}}$ in Equation 2.12. The analytical concept of the cost function is illustrated in Figure

2.5. The physical meaning of Θ is the maximum rate at which traffic can pass an observer moving at wave speed $W(x,t)$ at location x and time t.

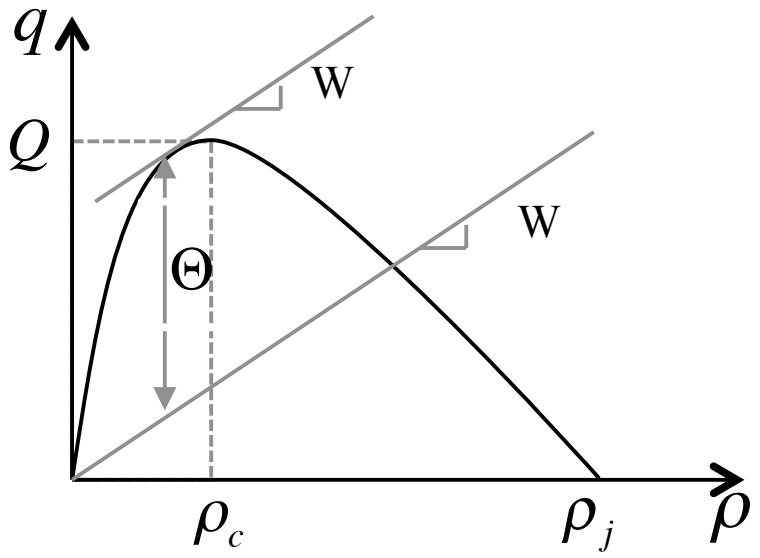

FIGURE 2.5: Concept of cost function in the variational method

Research in variational formulation of kinematic wave models has been extended to other coordinate systems at theoretical level. Leclercq *et al.* (2007) formulated the variational method in Lagrangian coordinates. The Lagrangian variational principle can be extended to simulate moving bottlenecks and self-similar highways. Laval and Leclercq (2013) further applied the variational theory to 3-dimensional traffic surface and developed solutions to each of the three 2-dimensional representations of traffic flow which are $N(x,t)$, $T(n,x)$ and $X(t,n)$.

The variational method has been researched to estimate traffic conditions or represent complicated traffic phenomena in motorway or simplified urban networks. Daganzo and Laval (2005) modelled moving bottlenecks on the motorway with the variational method. It was assumed that moving bottleneck trajectories and the associated escaping rates are exogenously defined. Additional nodes representing moving bottlenecks are added to the predefined computational grid and calculated as shortcuts. Mehran *et al.* (2012) applied the variational theory to estimate vehicle trajectories and journey time in a single-lane arterial with the support of empirical data from fixed and probe sensors. Their proposed data fusion approach reconstructs vehicle trajectories in affine conditions. The process

to estimate vehicle trajectories requires complex calibration due to vehicle entering and exiting from the midblock. It is time-consuming and inefficient to be applied to a large-scale or multi-lane transport network. Mehran and Kuwahara (2013) extended their research to fulfil real-time estimation of traffic conditions in signalized junctions.

The variational method can also be potentially applied for urban traffic control. With the same idea of cost function as used in the variational method, Han *et al.* (2013*a*) proposed a link-based approach for adaptive traffic signal control which calls for less binary variables compared to the CTM-based approach. However, results generated by this event-based approach have errors in urban networks application due to ignoring internal boundary conditions. It also cannot deploy space-dependent or time-dependent fundamental diagrams which are common in complex urban networks. Moreover, this control approach does not consider downstream blockage. When spill over builds up in the network, extra green time assigned to upstream links can be wasteful since downstream links are blocked.

Macroscopic simulation of bus-traffic interaction

Compared to microscopic simulators, there are far fewer macroscopic simulators to represent interaction of buses and the surrounding traffic. Available microscopic simulators are based on a static framework which cannot fully address dynamic traffic conditions and bus operations. Valencia (2012) developed a macroscopic model to capture the bus-traffic interaction at bus stops which is based on formulae suggested in the US Highway Capacity Manual. This research assumes that buses travel at a constant commercial speed regardless of road traffic conditions and only focuses on impact from bus control on road traffic. Gu *et al.* (2013) developed an analytical framework based on the LWR model to represent interaction between bus' dwelling at a single bus stop with the rest of road traffic before an isolated intersection. Bus-traffic interaction over multiple stops in a dynamic environment remains unknown.

TRANSYT is a macroscopic simulation platfrom which is capable of representing public vehicles, such as buses, from the rest of the road traffic. In the latest

version of TRANSYT 15, buses are modelled on a bus lane as separate traffic stream. Bus cruising speed and dwell time at bus stops are exogenously defined which are independent of the prevailing road traffic conditions (TRL, 2014). This assumption is not necessarily practical since bus dwell time and transit time also depends on bus control strategies and the surrounding traffic, especially in an integrated multi-modal system.

2.3 Bus system

2.3.1 Performance indicators

Passenger perceptions about good bus service performance are closely related to high efficiency and strong reliability which can be quantified by indicators such as short travel time, short waiting time, easy access to bus service, high punctuality and regularity (Koenig, 1980; Murray and Wu, 2003; Hensher *et al.*, 2003; Gardner *et al.*, 2009). Public transport performance affects the passenger decision-making process and route-planning outcome (Bates *et al.*, 2001; Nam *et al.*, 2005; Noland and Polak, 2002). A reliable bus service can attract more passengers and meet their satisfaction (Boyle, 2006; Hensher *et al.*, 2003; Hollander, 2006). If more people take public vehicles which are more efficient in terms of the number of carried passengers per unit of road space, the total traffic demand for the transport network can be relieved through the modal shift.

Among all performance indicators, bus service reliability has been recognized as the most important one by many researchers and interpreted with various concepts (Benn, 1995). In previous studies, reliability indicators include deviation of journey times (Chen *et al.*, 2003; Perk *et al.*, 2008), discrepancy between actual bus arrival times and pre-defined times (Bates *et al.*, 2001) and deviation of headways (Janos and Furth, 2002). As a broad concept, bus reliability covers two main aspects of bus service which are punctuality and regularity. Punctuality measures adherence of bus arrival times to time tables. Regularity measures deviation of

bus headways or journey times. Welding (1957) showed that the average passenger waiting time T^W for buses at one bus stop can be expressed by Equation 2.13.

$$T^W = \frac{\bar{h}}{2} + \frac{\sigma^2(h)}{2\bar{h}} \tag{2.13}$$

where $\bar{h}$ is average bus headway and $\sigma(h)$ is the standard deviation of bus headways. Equation 2.13 shows that passenger waiting time increases as bus service becomes more irregular.

Bus service regularity can be further identified at different levels. At route level, Chen *et al.* (2003) and Perk *et al.* (2008) found that passengers value small journey time deviation more than short journey time duration. At stop level, bus regularity is represented by headway maintenance. Bates *et al.* (2001) and Perk *et al.* (2008) found that the evenly distributed bus headways are associated with minimized passenger waiting time at bus stops. This finding can also be numerically inferred from Equation 2.13. For a high-frequency bus service, Welding (1957) and Hundenski (1998) showed that headway maintenance is more important than schedule adherence since headway regularity directly determines passenger waiting time.

A bus system, especially in an urban transport network, experiences perturbations of a relatively high level. As referred to by Strathman *et al.* (2000), Woodhull (1987) categorised these perturbations as endogenous and exogenous. Endogenous perturbations arise within the bus transit system such as passenger loading, route configurations, bus schedule and driver operation. Exogenous perturbations are related to the external environment where buses are located, such as their surrounding traffic conditions, road accidents, signalised junctions, and so on. Schramm *et al.* (2010) ranked the impact of various perturbations on bus service unreliability and concluded that road traffic conditions between bus stops and passenger boarding at bus stops are closely related to bus service reliability.

A bus system without any control strategy is inherently unreliable. A small perturbation can inevitably cause headway and schedule deviation which reduces service

regularity and punctuality. The root cause of this instability is the positive correlation between total passenger boarding time and the length of bus headway (Newell and Potts, 1964). If two buses are running at a shorter headway, there are fewer passengers for the following bus to pick up compared to the leading bus. Thus the following bus dwells for a shorter time at the bus stop, departs earlier than the schedule and further catches up with its leading bus.

The worst outcome of uncontrolled bus system is bus bunching with multiple buses arriving at one stop at the same time as illustrated by Figure 2.6. Thus, headways between bunched buses are zero and headways between bunched and unbunched buses are extended. This leads to strong headway deviations which increase the average passenger waiting time as indicated by Equation 2.13. Bus bunching arises as the result of headway deviation amplified through time and space. Even in an ideal scenario with constant headway and equal distance between bus stops, any cruising time perturbation can lead to bus bunching (Newell and Potts, 1964).

FIGURE 2.6: Bus bunching in London bus transit system (27/11/2012)

Overall, bus bunching and irregular bus service negatively affect travellers and operators. Travellers need to allocate extra time waiting at the stop to ensure finishing the journey before the appointed time. Passengers left stranded in a

station due to bus bunching in other stations have to wait a longer time for public transport service. Passengers on board of buses experience journey time with greater uncertainty. Public transport operators might have to be assigned a longer layover time to ensure bus service availability.

2.3.2 Bus control

Various bus control strategies have been proposed and implemented to reduce bus journey time delay, improve bus service regularity and punctuality. Some control strategies are passive strategies which do not require real time traffic information and are usually developed based on historical traffic statistics. Active priority control strategies are based on real-time traffic information collected from sensors via telecommunication technology. Sensors are usually installed in public vehicles and urban transport infrastructure. For example, TfL have installed SCOOT, iBus and Automatic Vehicle Location (AVL) systems in the London transport networks and bus transit systems to collect real-time traffic information in order to make timely and reliable control decisions.

Bus priority strategies

A popular bus priority strategy is to set up separate bus lanes to assign more priority to buses if there is enough space in the road. Chow (2013) summarised that there are two types of bus lanes: contra-flow lanes and with-flow lanes. Buses in contra-flow lanes are separated from the rest of road traffic and do not interact with them. With-flow lanes are usually located next to road kerbs and extend all the way to a stop line or to a certain distance before the stop line. Buses in with-flow lanes interact actively with private vehicles.

Bus priority assignment can also be realised from traffic signal coordination. Passive signal control strategies determine signal timings based on traffic statistics in the road. Buses can be considered during a signal timing plan optimization process in terms of their higher passenger occupancy and distinct travel characteristics compared to the rest of road traffic (Chow, 2013). For bus passenger occupancy,

an objective function with importance weights on mean passenger occupancy can be used for calculating signal timings. Since bus occupancy tends to be higher than that of private vehicles, road priority can be assigned to the transport approach where buses are located. Buses also differentiate from other road traffic because they need to dwell to have passengers board and alight. Traffic signal timings can be designed to consider this travel behaviour in order to reduce bus delay (Robertson , 1974).

Active signal priority strategies are applied by adjusting traffic control signals to assign priority to public vehicles as they approach transport intersections. If a public vehicle arrives at a junction at the end of a green light phase with the right of way, an extension strategy can be applied to increase the length of the green light to allow the public vehicle to travel through the junction during the current signal cycle. This strategy requires the exact timing for the end of the green light and vehicle's arrival time to match. Despite its relatively low chance of being deployed, the extension strategy is usually effective to eliminate long delays of public vehicles if it can be appropriately applied. If a bus arrives at a junction during a signal stage without the right of way, two other active priority strategies can be applied to assign priority back to the public vehicle. The hurry-call strategy shortens the signal stage in the current signal cycle based on the minimum safety value. The recall strategy reduces the current signal stage first, and then replaces the reduced amount of time by the signal stage which assigns buses the right of way. Compared to the hurry-call strategy, the recall strategy gives buses more priority and causes more disruption to road traffic due to the change of signal sequence.

Impact of transit signal priority strategies have been studied analytically(Heydecker, 1984) or numerically (Chin *et al.*, 1992). Additional rules have been proposed to limit the frequency of deploying active priority strategies or to compensate for the vehicles whose right of way is reduced(Vincent *et al.*, 1978; Allsop, 1977; Heydecker, 1983*b*).

Bus holding strategies

Bus holding strategies aim at improving bus service regularity by holding buses at control points. Other control strategies with similar objectives include stop skipping, short running, and deadheading among others (Koffman, 1978; Turnquist, 1982; Wilson *et al.*, 1992; Ceder and Stern, 1981; Delle Site and Filippi, 1998). Stop skipping, also known as expressing, allows a bus to skip bus stops in order to shorten its journey time and reduce headway with its leading bus. Short running terminates buses before they reach the final destinations. Deadheading is similar to stop skipping in terms of skipping bus stops; however, deadheading empties buses and all passengers need to alight before buses move forward. However, Strathman *et al.* (2000) pointed out that bus skipping, short running and deadheading are usually considered less desirable than bus holding strategies because they cause passengers to alight for bus transferring and leave passengers waiting at stops stranded for a bus service.

In early studies, bus holding strategies are developed with a single control point or a few widely spaced control points (Osuna and Newell, 1972; Barnett and Kleitman, 1973; Barnett, 1974; Bly and Jackson, 1974; Hickman, 2001; Zhao *et al.*, 2006). With the objective of minimizing passenger waiting time, Osuna and Newell (1972) were among the first researchers to propose holding buses at one control point with the case of one stop with two buses. Barnett and Kleitman (1973) extended Osuna and Newell (1972) to explore the efficiency control point location with one bus and several stops. Barnett (1974) explored the effectiveness of a single control point with different bus departure patterns at the bus route entrance. Bly and Jackson (1974) researched into maintaining bus headway at the target value through a single control point. Hickman (2001) formulated a stochastic model to determine the optimal length of holding time at a control point to regulate bus service. Zhao *et al.* (2006) identified the optimal slack time to minimize passengers' expected waiting time. Daganzo (2009) pointed out that a bus holding strategy based on one or few control points cannot adequately address bus service instability or a bus bunching problem, especially for a bus service with high frequency and long distance.

Recent bus holding strategies are developed with dynamic bus holding times based on real-time bus headways. Compared to previous bus holding strategies, these holding strategies are applied at multiple control points which are usually bus stops (Daganzo, 2009; Daganzo and Pilachowski, 2011; Bartholdi III and Eisenstein, 2012; Delgado *et al.*, 2012). Daganzo (2009) proposed a headway-based control strategy (forward holding strategy) which aims at bus headway deviation. This dynamic bus strategy was established with inputs of expected passenger demand for a public bus service and forward bus headway. Daganzo and Pilachowski (2011) proposed a two-way bus holding strategy which improved the forward holding control strategy by considering bus-to-bus operation with both forward headway and backward bus headway. Bartholdi III and Eisenstein (2012) developed a simplified control strategy called backward holding strategy which only considers backward bus headway. With consideration of boarding limit, Delgado *et al.* (2012) proposed an optimised bus holding control with the objective of minimizing passengers' total journey time.

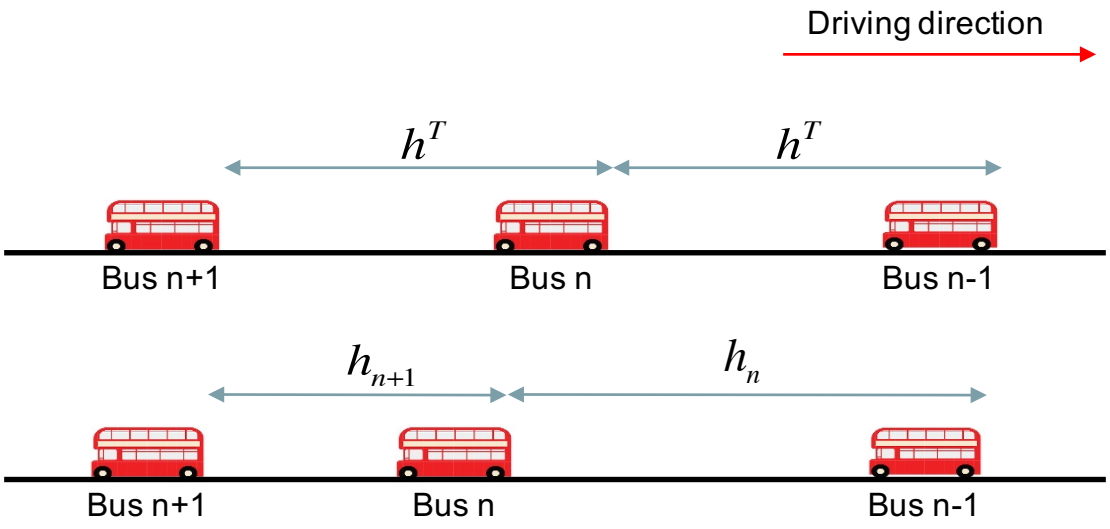

FIGURE 2.7: Illustration of bus headways

To further understand different bus headway-based holding strategies, Figure 2.7 presents headways of bus $n-1$,n and $n+1$. In an ideal scenario where buses operate with high regularity, bus headways are maintained as h^T. If bus headways become uneven as $h_{n+1} < h^T$ and $h_n > h^T$, the forward holding strategy aims

at reducing h_n; the backward holding strategy aims at extending h_{n+1} and the two-way holding strategy strikes a balance between h_n and h_{n+1}.

2.4 Discussion

2.4.1 Research gap

Based on the review of traffic flow models and bus transit control in previous sections, several academic challenges have been identified in terms of estimating road traffic conditions, understanding bus holding impact and improving bus service reliability.

First, there is not a simulation platform which is both simple and effective to estimate road traffic conditions and represent bus-traffic interaction. Although microscopic simulation can incorporate a sufficient number of vehicle and transport infrastructure details, it is difficult to be calibrated and applied to model real-world transport networks. For macroscopic models, CTM-based simulation has been widely used by academia and industry; however, several disadvantages have been identified with CTM:

1. CTM produces numerical errors at discontinuities of solutions. The flow and density profiles are smeared in regions near the discontinuities and this feature is termed as 'numerical viscosity' (LeVeque, 1992).

2. CTM cannot effectively capture a moving bottleneck which is a common phenomenon in an urban network due to slow moving vehicles including buses. Lebacque *et al.* (1998) attempted to incorporate bus movement as a moving bottleneck in an urban transport system based on CTM; however, it requires the assumption of homogeneity in each road segment divided by buses which is rarely satisfied in practice.

3. Application of CTM in estimating urban traffic is limited because it has to satisfy Courant-Friedrichs-Lewy (CFL) condition. CFL condition requires

CTM time step size Δt to be set such that $\Delta t \leq \min_i \frac{\Delta x_i}{v_i}$, where $\min_i \frac{\Delta x_i}{v_i}$ refers to the smallest ratio of cell length to the associated free–flow speed along the section(Courant *et al.*, 1928). CFL condition ensures the numerical stability and non-negativity of traffic quantities by preventing traffic from travelling further than the length of the cell in one simulation time step. It also constrains the application of CTM in limited urban networks.

Second, the effectiveness of dynamic headway-based bus holding strategies given traffic conditions remains unknown, and their impact on the surrounding traffic of buses is missing from available literature. Lack of bus control evaluation is due to the difficulty of implementing these dynamic holding strategies in an actual transport system which can be cost-prohibitive and time-inefficient. Toledo *et al.* (2010) developed an event-based mesoscopic simulation platform called MezzoBus to evaluate bus service operations. Based on the MezzoBus platform, Cats *et al.* (2012) assessed bus service reliability under different bus holding strategies from passengers' and bus operators' perspectives. However, this event-based simulation platform is incapable of incorporating internal boundary conditions such as traffic incidents and temporal lane shut-down which makes it inadequate to model a dynamic transport system.

Third, there is not an effective service reliability improvement strategy which is responsive to road traffic conditions and efficient in bus commercial speed. Diab and El-Geneidy (2013) found that most current bus service improvement strategies aim at improving transit priority rather than service reliability. Moreover, some transit priority control can even increase service variability since overall bus route mobility is improved and buses operate with more consistent commercial speeds. Available reliability improvement strategies either cancel service at certain stops or compromise bus commercial speed (Strathman *et al.*, 2000). The headway-based holding strategies assume a predefined slack time so that buses are always held at each control point (Daganzo, 2009; Bartholdi III and Eisenstein, 2012; Daganzo and Pilachowski, 2011). Reliability improvement strategies also consider buses as a separate traffic flow without any interaction with their surrounding traffic;

however, road traffic conditions directly affect bus cruising time between stops which significantly contributes to bus service reliability (Schramm *et al.*, 2010).

2.4.2 Research motivation

Based on the literature review and identified research gaps, the proposed PhD research framework focuses on 3 aspects:

- Establish a macroscopic simulation platform based on the variational formulation of LWR model to estimate road traffic conditions and represent bus-traffic interaction
- Evaluate and compare dynamic headway-based bus holding strategies in terms of their effectiveness under different traffic conditions and their impact on the road traffic
- Develop a more effective bus service improvement strategy which responds to road traffic dynamics and maintains bus system efficiency

Law *et al.* (2015) proposed a comprehensive framework system study which exhaustively states three experiment-based methods which include experiments with the real-world system, experiments with physical models of the system and experiments with mathematical models of the system. The thought process to identify the proposed research direction of establishing a macroscopic simulation platform based on the variational formulation of the LWR model to study the transport system is presented in Figure 2.8. It presents the research process to identify the proposed research direction and framework. It extends the framework proposed by Law *et al.* (2015) by incorporating findings from literature review in this chapter. Figure 2.8 illustrates the process from the research question of understanding the transport system where public transits operate to the research objective to develop a macroscopic simulation platform which evaluates service improvement strategies. The green arrow represents the choice made at each level which is

driven by academic motivation and practical consideration. How these choices are made is discussed below.

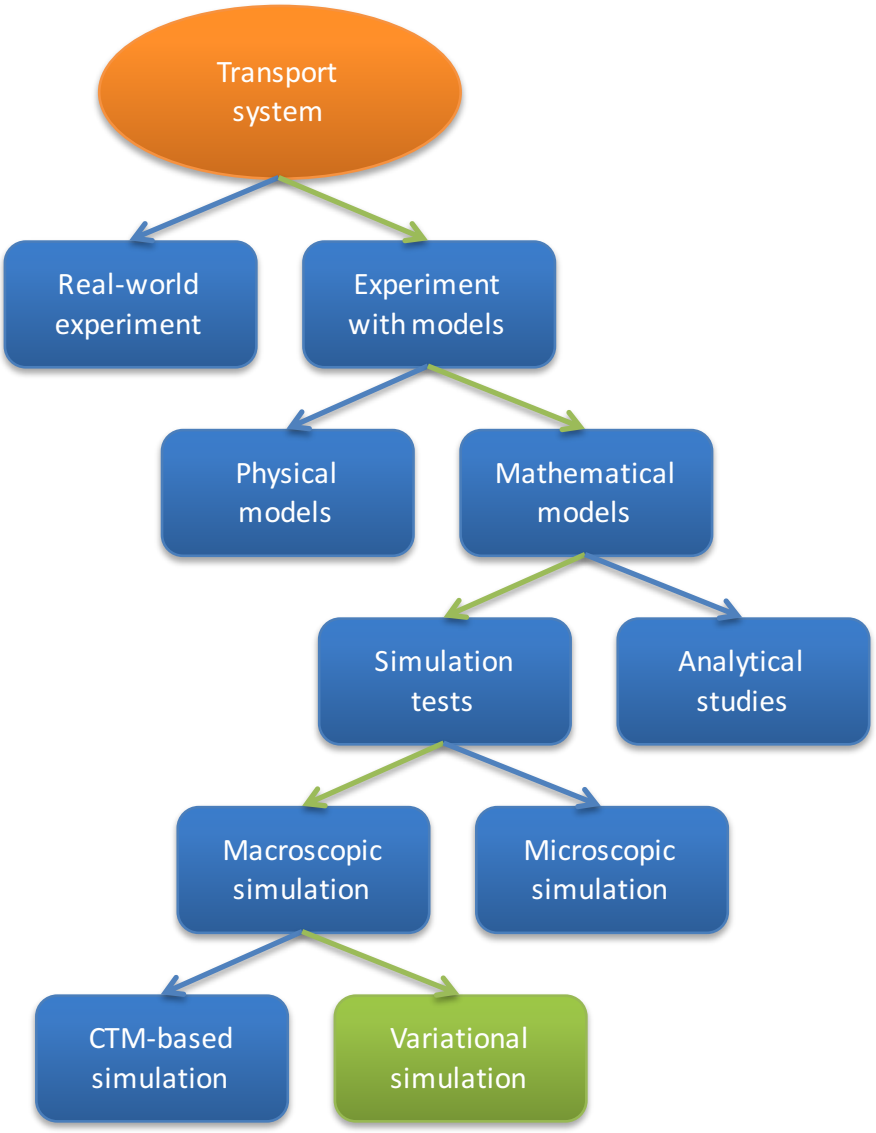

FIGURE 2.8: Thought process to identify the proposed research framework and direction, adapted from Law *et al.* (2015)

Why simulation-based experiment?

Experiments with the actual transport system are the most straightforward method to understand local traffic conditions or evaluate bus control strategies (Chow, 2007). However, this method can be cost-prohibitive and time-consuming with a complicated implementation and observation process which often makes a real-world experiment infeasible (Heydecker, 1983*a*). An analytical study deploys simplified mathematical representations of the transport system. However, analytical

models have limited parameters and may not be effective to estimate dynamic urban transport dynamics.

The complexity and effectiveness of a simulation-based experiment approach are between the two approaches outlined above. Compared to analytical models, simulation can better represent a dynamic system with more parameters deployed. Its computational load can be mitigated by advanced computing technology. Compared to real-world experiments, simulation is relatively convenient to deploy and simple to exclude the impact of unrelated variables.

Why macroscopic simulations?

The decision is reached after comparing advantages and disadvantages of macroscopic and microscopic models.

Microscopic simulations can effectively perform field tests with actual data, validate specific transport design and detailed parameters. However, it is more difficult to implement and calibrate microscopic simulations in real-world cases than macroscopic simulations since they require far too many parameters (Bellomo and Dogbe, 2011).

By comparison. macroscopic models can be conveniently deployed and validated with large amounts of available data. These input macroscopic data can be accessible through existing sensing systems installed in the transport networks such as SCOOT and Automatic Vehicle Localization (AVL). By deploying, calibrating and validating macroscopic models, policy makers can gain further insights into the underlying physical relationships and causality of different variables.

Why variational method?

It has been decided to focus on the variational method over CTM as the future research direction because of its advantages to incorporate generic fundamental diagrams, represent traffic bottlenecks more effectively and estimate traffic conditions more accurately. The proposed study will develop a simulation platform of an integrated urban transport system based on the variational method which has

not been solved by other researchers. There are two challenges to overcome in this regard:

1. The existing variational method is mainly focused on motorways or transport corridors. In order to develop a comprehensive urban transport simulator, it is necessary to develop an effective transport node model to combine variational corridor models together.

2. Most research on the variational method is focused on theoretical development which leaves the application of the variational method in practice rarely touched. The proposed variational simulator will be implemented with urban traffic signal control to estimate urban traffic condition and predict urban transport journey times. This serves as the foundation to evaluate bus schedule management policies in an urban network.

Why headway-based holding strategies?

A great many researchers have proposed various bus holding strategies (Cats *et al.*, 2012; Daganzo, 2009; Daganzo and Pilachowski, 2011; Bartholdi III and Eisenstein, 2012). However, a systematic and comprehensive evaluation on the impacts of bus holding strategies has been missing in both theoretical and empirical research. This PhD study is thus of research value to fill this gap in the research field of bus holding strategies.

Compared to other reliability improvement strategies such as stop skipping, short running and dead heading, bus holding strategies are preferred by operating agencies as they avoid having passengers get off at unplanned stops for transfer or keeping them wait for the next bus. Although bus holding is usually applied in isolated bus stops or separate bus lanes, not all bus systems are operated independent of other road traffic due to spatial constraints such as buses in Lisbon (Silva, 2001; Danaher, 2010). Building separate bus lanes and bus stops can cost a significant amount of time and money. This research is thus of practical value to policy makers by providing quantitative insights into bus holding strategy advantages and disadvantages in their specific transport systems.

Moreover, current bus holding strategies are difficult to implement partly due to the fact that on-board passengers get annoyed upon knowing they are held at bus stops (Bellinger, 2011). This research aims at mitigating this challenge by holding buses in a more discreet way by leveraging traffic signal adjustment. Bus holding strategies can become easier for passengers to accept and operators to apply. However, since buses and other road traffic are both subject to traffic signal control, it is thus important to understand the comprehensive impact of bus holding strategies on both buses and their surrounding traffic.

Headway-based holding strategies are selected rather than schedule-based holding strategies because bus headway reliability is generally considered more important than schedule adherence as identified by Welding (1957), Hundenski (1998) and Balcombe *et al.* (2004). For bus routes of high frequencies in an urban network, their schedules are usually ignored by passengers. They focus on bus headways which directly determine their waiting time for the next bus.

Recent research focuses on developing dynamic headway-based holding strategies which take advantage of real-time bus information enabled by advanced information technology. For example, TfL has deployed the iBus system which tracks bus location through onboard global positioning system (GPS). Development of innovative dynamic bus holding strategies can improve utilization of the existing information technology system and develop more efficient bus reliability improvement strategies.

Chapter 3

Modelling urban traffic dynamics

3.1 Introduction

This chapter presents the development of a macroscopic simulation platform based upon the variational formulation of LWR model. The established simulation platform can be used to estimate traffic conditions of multi-modal urban traffic flows and interactions between buses and their surrounding traffic. This chapter is organised as follows: Section 3.2 outlines research motivation and research gaps. Section 3.3 documents the methodology to develop the proposed macroscopic transport network simulation framework. Section 3.4 presents a range of numerical experiments that aim to compare the characteristics of CTM and the variational method over different applications. Section 3.5 presents the case study with traffic data collected from Tottenham Court Road in Central London, UK. Finally, Section 3.6 presents some concluding remarks.

3.2 Background

Understanding the characteristics of urban congestion is a prerequisite for modelling multimodal traffic dynamics in an urban transport system. An accurate estimation of traffic conditions is the base to derive effective transport policies

and management plans. A previous study reveals that 25%-30% of observed congestion in Central London could be reduced by effective traffic control (Chow *et al.*, 2014).

Due to the complexity of urban traffic dynamics and the lack of relevant data, there has not been much research conducted in urban streets compared to research in motorways. However, recent increasing availability of data from different sources provided by advanced information technology has enabled researchers to carry out more comprehensive research on urban network traffic modelling.

Among all traffic models proposed in the literature, the kinematic wave model remains one of the most widely accepted ones due to its ability to capture realistic traffic behaviour such as spillover and propagation of shockwaves with parsimonious mathematical structure as discussed in Section 2.2.2.

The popular cell transmission method (CTM) calculates numerical values of the LWR model. Daganzo (1994) proposed the CTM based on first-order discretization schemes by Godunov (1959). CTM has been applied broadly in both motorways (Gomes and Horowitz, 2006; Chow *et al.*, 2008) and urban streets (Ziliaskopoulos, 2000; Lo and Szeto, 2002; Chow *et al.*, 2010). However, CTM produces error at discontinuity (i.e. shock) in the solution (Daganzo, 2006; Mazare *et al.*, 2011), and CTM is not effective in modelling bottlenecks caused by stationary or slow-moving vehicles like trucks or buses (Lebacque *et al.*, 1998; Mazare *et al.*, 2011). Therefore, a more accurate and effective numerical method is needed to solve the LWR model.

Daganzo (2005*a*) and Daganzo (2005*b*) proposed an alternative LWR model solution which is known as the variational method. The variational method integrates Equations 2.9 and 2.10 into a Hamilton-Jacobi-Bellman (HJB) equation. Following this, Daganzo (2005*b*) shows that the LWR model can then be solved by dynamic programming (see Equation 3.17) with any concave fundamental diagram Φ under this variational formulation. The variational method shows significant improvement on solution accuracy with respect to the analytical solution over the

traditional CTM (Daganzo and Menendez, 2005). Stationary and moving bottlenecks such as buses or trucks can also be modelled by the variational method (Daganzo and Menendez, 2005; Mazare *et al.*, 2011).

Most previous studies on the variational formation of kinematic waves are either theoretical analysis or applications on motorways; there are few studies on multimodal urban streets. The study fills this gap by presenting a variational-based network modelling framework which considers various aspects in an urban area including traffic signals, slow-moving buses, and dispersion of platoons. Performance of the variational method is compared with the established CTM over a range of scenarios and a case in Central London.

3.3 Dynamic network model

The dynamic network model consists of a node component and a link component.

3.3.1 Node model

Node m has I_m incoming links and J_m outgoing links. Following Nie *et al.* (2008), Chow *et al.* (2010), and others, a split matrix $\boldsymbol{\eta}_k = [\eta_{ij}(t)]$, which has a dimension of $(I_m \times J_m)$, is defined for the node m and updated regularly (e.g. every 15-min) over interval t based on field observations. The element $\eta_{ij}(t)$ in the split matrix $\boldsymbol{\eta}_t$ specifies the proportion of traffic on each incoming link i, where $i = 1, 2, ..., I_m$, that is heading to each outgoing link j, where $j = 1, 2, ..., J_m$, through node m at time t. Principle of conservation requires that

$$\sum_{j=1}^{J_m} \eta_{ij}(t) = 1, \tag{3.1}$$

for all $i = 1, 2, ..., I_m$. The split ratios $\boldsymbol{\eta}_t$ may also be determined endogenously by traffic conditions in the network through a dynamic traffic assignment model (Lo

and Szeto, 2002; Heydecker and Addison, 2005; Chow, 2009). However, detailed discussion of a dynamic traffic assignment model is beyond the scope of the present paper.

Without consideration of excessive blocking (i.e. traffic can be freely flowing through a node without restraint due to downstream queue), the traffic flow $q_{ij}(t)$ at time t flowing from incoming link i to outgoing link j is determined as:

$$q_{ij}(t) = \eta_{ij}(t) q_i^S(t), \tag{3.2}$$

where $q_i^S(t)$ is total traffic flow on link i wanting to be sent out through node m at time t.

If the node is controlled by a traffic signal, the signalling effect can be captured by associating a binary variable $\gamma_{ij}(t)$ with the term on the right-hand-side in Equation 3.3 (Chow *et al.*, 2010), i.e.

$$q_{ij}(t) = \eta_{ij}(t) q_i^S(t) \gamma_{ij}(t), \tag{3.3}$$

for a signal-controlled node, in which:

$$\gamma_{ij}(t) = \begin{cases} 1, & \text{if movement from } i \text{ to } j \text{ is given a green signal} \\ 0, & \text{if movement from } i \text{ to } j \text{ is given a red signal} \end{cases} \tag{3.4}$$

The formulation Equation 3.4 works for both fixed-time plans (which operate according to a predefined timing plan) and responsive controllers which operate based on real-time vehicle actuations (Chow *et al.*, 2010).

Moreover, the corresponding total traffic flow $q_j^R(t)$ through node m which can be received by link j will be

$$q_j^R(t) = \sum_{i=1}^{I_m} q_{ij}(t). \tag{3.5}$$

Nie *et al.* (2008) and Zhang *et al.* (2013)) suggested that formulations Equation 3.3 and Equation 3.5 can be extended to capture excessive blockage through considering the available space at the downstream. Let $Q_j(t)$ be the maximum flow that can be accommodated by link j at time t. This $Q_j(t)$ can be estimated by various link traffic models (see Section 3.3.2) while for now it is assumed to be known. Nie *et al.* (2008) proposed to adjust the flow $q_{ij}(t)$ in Equation 3.3 as

$$\hat{q}_{ij}(t) = \frac{\min(\eta_j(t), Q_j(t))}{\eta_j(t)} q_{ij}(t), \tag{3.6}$$

It is noted that if $q_j^R(t) \leq Q_j(t)$, which implies there is enough capacity on link j to accommodate the incoming traffic, then Equation 3.6 will produce an identical estimate of $q_{ij}(t)$ as Equation 3.3. If $q_j^R(t) > Q_j(t)$ (i.e. excessive blockage occurs), Equation 3.6 states that contributions $q_{ij}(t)$ from all links i should be reduced by a common factor $\dfrac{Q_j(t)}{q_j^R(t)}$. This guarantees the predefined split ratio matrix $\boldsymbol{\eta}$ remains unchanged. Following the adjustment by Equation 3.6, the $q_i^S(t)$ needs to be adjusted accordingly as

$$\hat{q^S}_i(t) = \sum_{j=1}^{J_m} \hat{q}_{ij}(t), \tag{3.7}$$

where $\hat{q^S}_i(t) \leq q_i^S(t)$.

3.3.2 Link model

The link model describes the dynamic propagation of traffic along the link. The point queue model, which is also known as the bottleneck model or deterministic queueing model, is one of the simplest representations of link traffic propagation (Zhang *et al.*, 2013; Vickrey, 1969; Chow, 2009). The model considers each link

to consist of two parts: a freely flowing part with a flow-invariant travel time combined with a queue of traffic at its downstream end being discharged with a maximum rate. The traffic queue is considered to be stacking up vertically and hence takes no physical space of the road. Recent studies show that this point-queue model can be equally applied to the variational method (Han *et al.*, 2013*b*,*c*) which will be discussed in detail in the following sections. Nevertheless, ignoring the spatial effect of traffic can lead to ill-representation of physical behaviour as shown by a number of previous studies (Szeto and Lo, 2006; Zhang *et al.*, 2013). Considering plausibility, this study will use the LWR model and the following sections will present the two solution schemes adopted here: cell transmission and variational methods.

Cell transmission method

Under CTM, the entire road network is discretised into a collection of sections or 'cells' as shown in Figure 3.1 in which the cells are numbered from upstream i, to downstream $i+1$.

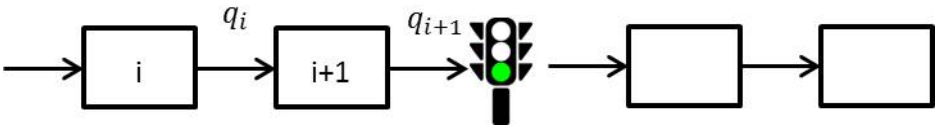

FIGURE 3.1: Cell representation of a signal-controlled link

Given the traffic flow $q_i(t)$ travelling from each cell i to cell $i+1$ from time t to time $t+1$, the state equation on the corresponding density ρ_i can be derived from conservation law as Equation 3.8.

$$\rho_i(t+1) = \rho_i(t) + \frac{\Delta t}{x_i}\left[q_{i+1}(t) - q_i(t)\right], \tag{3.8}$$

where Δt and x_i are respectively the lengths of the simulation time step and cell i. Equation 3.8 can indeed be regarded as a discrete version of Equation 2.9. The flow $q_i(t)$ between each pair of cells $(i, i-1)$ is related to the associated densities (ρ_i, ρ_{i-1}) through a triangular fundamental diagram as shown by Figure 2.3 at each cell. The triangular fundamental diagram is consistent with the one proposed by

Newell (1993) as reviewed in Section 2.2.2. Each cell i is associated with a capacity Q_i which specifies the maximum flow that can be discharged from that cell, and a jam density $\rho_{j,i}$ which is the maximum traffic density that can be stored in the cell. When there is no congestion, traffic moves through cell i at a free flow speed, u_i. The quantity w_i specifies the backward propagation speed of congestion along cell i. The density in cell i associated with the capacity flow is known as the critical density $\rho_{c,i}$.

With this piecewise linear specification, the outflow $q_i(t)$ from cell i is determined from the traffic densities ρ_i and ρ_{i-1} as

$$q_{i-1}(\Delta t) = \min\left\{v\rho_{i-1}(\Delta t), Q_i, Q_{i-1}, w\left[\rho_{j,i} - \rho_i(\Delta t)\right]\right\}, \tag{3.9}$$

which can be viewed as a mathematical expression of the triangular flow-density relationship depicted in Figure 2.3. The outflow function Equation 3.9 is due to the assumption of the triangular fundamental diagram shown in Figure 2.3. As shown in Daganzo (1997), Laval (2004), Szeto (2008), Jin *et al.* (2009), Jabari and Liu (2012), and others, the outflow function can be generalized as

$$q_{i-1}(\Delta t) = \min\left\{q_i^R(\Delta t), q_{i-1}^S(\Delta t)\right\}, \tag{3.10}$$

where $q_{i-1}^S(\Delta t)$ and $q_i^R(\Delta t)$ are regarded as the traffic flow to send from link $i-1$ and the traffic flow to receive into link i. The sending and receiving traffic flow represent respectively the traffic demand for advancing from upstream $i-1$ to downstream i, and the supply at the downstream $i-1$ for receiving incoming traffic from the upstream i. The general form shown in Equation 3.10 allows the use of different forms of fundamental diagrams in addition to the triangular ones.

Lo (1999) showed that CTM can model the traffic signal effect at cell i by formulating the associated capacity term Q_i as a binary time-varying variable as Equation 3.11:

$$Q_i(t) = \begin{cases} Q, & t \in \mathbb{G} \\ 0, & t \in \mathbb{R} \end{cases} \tag{3.11}$$

where $\mathbb{G}$ and $\mathbb{R}$ represent the green and red phases respectively (Lo, 1999). For fixed-time signals, they operate according to a predefined timing plan while responsive controllers operate based on real-time vehicle actuations.

A number of implementation algorithms to develop a CTM-based simulation platform are available in the literature for solving CTM. Readers are referred to Kurzhanskiy *et al.* (2009) for a detailed description of CTM implementation for general networks.

Variational method

The variational method can be dated back to the seminal work by Newell (1993) which proposes a simplified version of kinematic wave model and expresses the solutions in terms of cumulative count of traffic $N(x,t)$ at x and t (Newell, 1993), where by definition

$$\frac{\partial N}{\partial t}\Big|_{(x,t)} = q(x,t), \tag{3.12}$$

$$-\frac{\partial N}{\partial x}\Big|_{(x,t)} = \rho(x,t). \tag{3.13}$$

Newell (1993) showed that cumulative traffic that passes by a location at a particular time can be determined by its upstream and downstream boundary conditions by simple translations of cumulative curves. This simplified kinematic wave theory has been applied to develop efficient network loading models (Yperman, 2007; Balijepallia *et al.*, 2013*b*), a sensitivity analysis of traffic control (Chow and Lo, 2007), and urban traffic optimisation (Han *et al.*, 2013*a*). Daganzo (2005*a*) and Daganzo (2005*b*) proposed a numerical scheme using a dynamic programming scheme for solving the LWR model based upon Newell's work which is now known as the

variational method (Daganzo, 2005*a*,*b*). By inputting Equation 3.12 and 3.13 into the Equation 2.10 of the LWR model, it can be derived that:

$$\frac{\partial N}{\partial t}\Big|_{(x,t)} = \Phi\left[-\frac{\partial N}{\partial x}\Big|_{(x,t)}\right], \tag{3.14}$$

Equation 3.14 is recognised as a Hamilton-Jacobi-Bellman equation where the fundamental diagram Φ is regarded as the Hamiltonian function. Given the initial and boundary conditions, it is shown that this equation 3.14 can be solved by dynamic programming with concave fundamental diagrams with unprecedented accuracy and efficiency (Daganzo, 2005*b*). To solve this variational formulation, Daganzo (2005*a*) introduces the following cost function in wave speed $W(x,t) = \frac{\partial q}{\partial \rho}\Big|_{(x,t)}$ over (x,t) as:

$$\Theta(u,x,t) = \sup_{\rho}(\Phi(\rho,x,t) - W(x,t)\rho). \tag{3.15}$$

This cost function Θ is recognised as a Legendre-Fenchel transformation of the fundamental diagram Φ (Daganzo, 2006; Mazare *et al.*, 2011). The function Θ can be physically interpreted as the maximum rate at which traffic can pass an observer moving with wave speed W at location x and time t.

Given a set of N values at the boundary $\mathbb{B}$, the HJB Equation 3.14 can be solved with the cost function Equation 3.15 by applying the minimum operating rule:

$$N(x,t) = \min_{\mathbb{B}}\left\{N_{\mathbb{B}}(x_{\mathbb{B}},t_{\mathbb{B}}) + (t-t_{\mathbb{B}})\Theta\left(\frac{x-x_{\mathbb{B}}}{t-t_{\mathbb{B}}}\right)\right\}, \tag{3.16}$$

where $N_{\mathbb{B}}$ is the set of known values of N given at $(x_{\mathbb{B}},t_{\mathbb{B}})$ on boundary $\mathbb{B}$ (Daganzo, 2005*b*; Laval and Leclercq, 2013). Equation 3.16 is known as the Lax-Hopf formula (Mazare *et al.*, 2011), and it can be solved by a number of effective and high quality solution algorithms including the event-based grid-free algorithm that does not require predefinition of a computational space-time grid (Mazare *et al.*, 2011). A

disadvantage of the event-based algorithm is that it cannot incorporate space-time dependent fundamental diagrams and hence it is inconvenient for modelling local and temporary events such as traffic lights and incidents. Applying the principle of optimality in dynamic programming (DP), Daganzo (2005*b*) presented a forward DP-based method for solving Equation 3.16 (Daganzo, 2005*b*). The DP-formulation can be written for a general concave fundamental diagram over a discrete space-time grid as:

$$N(x,t) = \min_{u \in \mathbb{W}} \{N(x - W\Delta t, t - \Delta t) + \Delta t \Theta(w)\}, \tag{3.17}$$

where $\mathbb{W}$ is the set of all possible wave speeds in the fundamental diagram Φ. Unlike Godunov schemes and CTM, the spatial interval Δx is endogenously determined from the time step Δt through the term '$W\Delta t$' with the set of shockwave speeds $W \in \mathbb{W}$.

Consider a simple case where Φ is triangular as the one depicted in Figure 2.3 in which the wave speed $W = \dfrac{x - x_{\mathbb{B}}}{t - t_{\mathbb{B}}}$ can only take two possible values: u (free flow speed) and w (backward wave speed), the cost function Θ becomes:

$$\Theta(u,x,t) = \begin{cases} 0, & \text{if } W = u \\ w\rho_j, & \text{if } W = w \end{cases} \tag{3.18}$$

for all (x,t). Equation 3.17 can then be reduced to:

$$N(x,t) = \min\{N(x - u\Delta t, t - \Delta t), N(x - w\Delta t, t - \Delta t) + \rho_j w \Delta t\}, \tag{3.19}$$

which is consistent with the theory presented in Newell (1993). It is shown that, unlike CTM, the solution derived from Equation 3.19 with triangular Φ is exact.

The effect of traffic lights at a specific location x^* or moving bottlenecks (e.g. slowing buses) can be captured in Equation 3.17 through introducing 'shortcuts'

(Daganzo, 2005*b*). A traffic light at x^* can be modelled by introducing the following revised cost function $\Theta^*(0, x^*, t)$ associated with wave speed $W = 0$ at x^*:

$$\Theta^*(0, x^*, t) = \begin{cases} Q, & t \in \mathbb{G} \\ 0, & t \in \mathbb{R} \end{cases} \tag{3.20}$$

The idea of cost function Equation 3.20 is indeed the same as Equation 3.11 which regulates the capacity flow at x^* according to a predefined timing plan. To simulate the effect of a moving bottleneck M, which can be a slow moving bus or truck on the road, with a trajectory $x = M(t)$ over time t, one can introduce the following shortcut:

$$\Theta^*(u, x, t) = \begin{cases} \Theta_M(t), & \text{if } x = M(t), W = \frac{dM}{dt}, \\ \Theta(W, x, t), & \text{otherwise,} \end{cases} \tag{3.21}$$

where $0 \leq \Theta_M(t) \leq \Theta(\frac{dM}{dt})$, and $\Theta_M(t)$ physically represents the maximum passing rate of traffic that can pass through the moving bottleneck M.

3.3.3 Numerical implementation

The proposed simulation platform can be viewed as a combination of input variables, the algorithm based on variational theory and outputs. Figure 3.2 illustrates these different components.

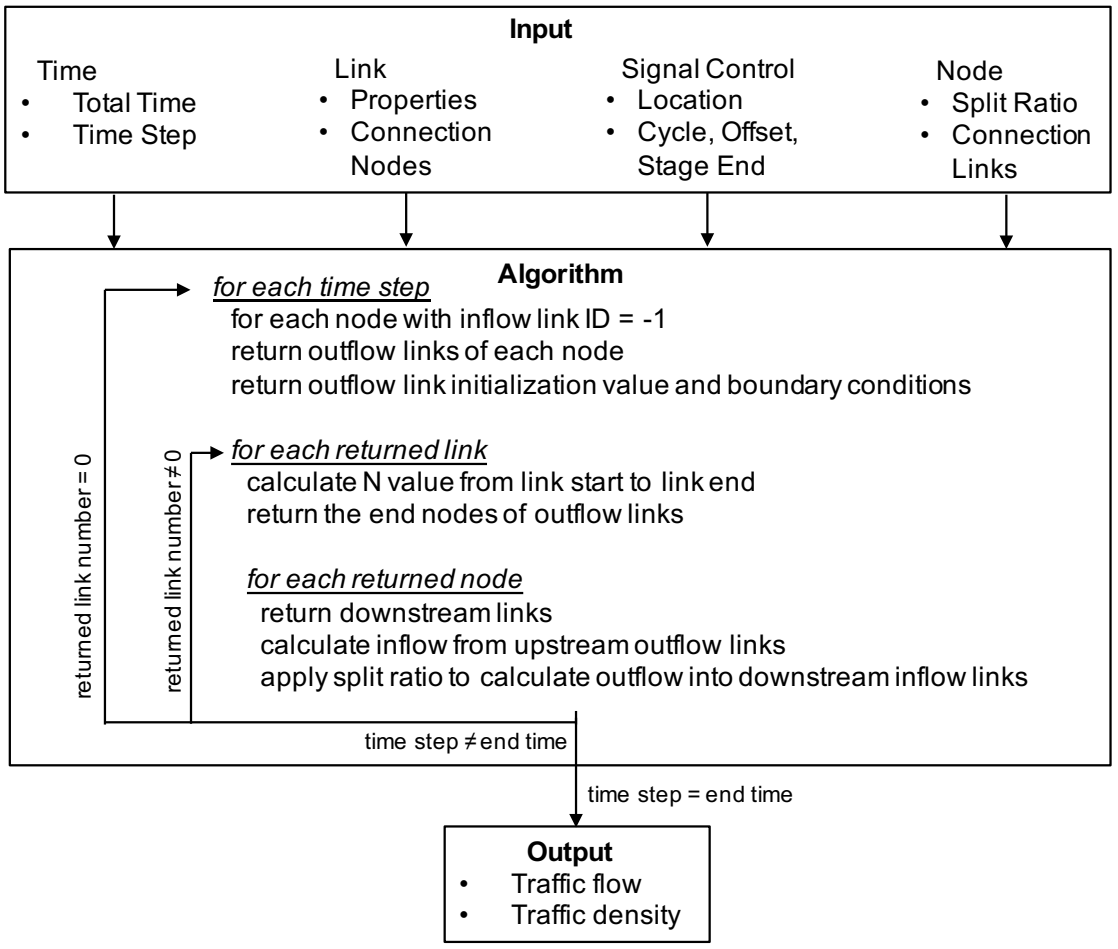

FIGURE 3.2: Components of the proposed simulation platform

The method to implement the variational method in the proposed simulation platform is documented as below:

Step 0: Initialization

0.1 Set total time T, traffic demand profile $d(t)$ and time step Δt

0.2 Set transport link parameters regarding their lengths, saturation flow, jam density, flow speeds, and connected nodes.

0.3 Set transport node parameters regarding their connected transport links, split ratio. Traffic signal timing needs to be defined for signalised transport nodes.

Step 1: Calculation of cumulative traffic flow $N(x,t)$

1.1 Set the boundary condition $N(0, t_{\mathbb{B}})$ and initialize transport links $N(x_{\mathbb{B}}, 0)$. While $t \leq T$, iteratively perform Step 1.2

1.2 Calculate $N(x, t)$ from the start to the end of the transport route iteratively based on Equation 3.17 at time t. Set $t := t + \Delta t$

Step 2: Calculation of traffic flow and density

2.1 Calculate traffic flow $q(x, t)$ based on $q(x, t) = \frac{N(x,t+\Delta t)-N(x,t)}{\Delta t}$

2.2 Calculate traffic flow $q(x, t)$ based on $\rho(x, t) = \frac{N(x-\Delta x,t)-N(x,t)}{\Delta x}$

3.4 Numerical examples

This section presents some numerical experiments comparing traffic characteristics produced by the two numerical methods. In Section 3.4.1, 3.4.2 and 3.4.3, a link which is 0.5-mile with a traffic light located in the middle of it is constructed. The transport route is illustrated in Figure 3.3.

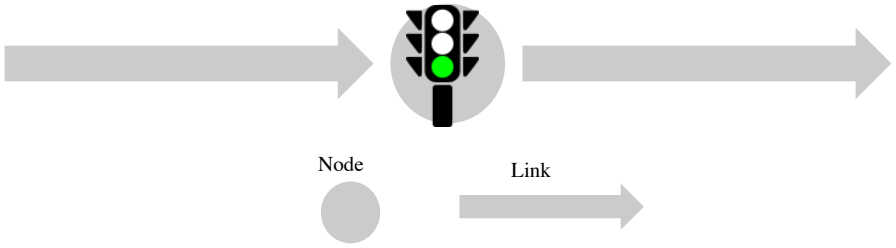

FIGURE 3.3: Network of the numerical case

A triangular fundamental diagram (Figure 3.4a) is adopted by this research with which the speed of traffic under free-flow, v, is 30 (mph) for all densities $\rho < \rho_c$. The triangular fundamental diagram is frequently used by other researchers for its simplicity to represent actual traffic conditions (Daganzo, 1995; Chow *et al.*, 2015). The traffic is loaded into the link at saturation flow, Q, which is 1800 vehicles per hour (vph). The reason for using such a high loading rate is to magnify the features of the numerical methods. The jam density ρ_c is set to be 240 vehicles per mile

(vpm). The critical density ρ_c is $\frac{1800}{30} = 60$ vpm. The parameter w, which is the speed of the backward-propagating congestion, is taken as 10 mph for all $\rho > \rho_c$.

Figure 3.4b, c and d show a set of fundamental diagrams with multi-segmented free-flow portions. An application of such construction is to generate a different degree of dispersion of vehicle platoons or rarefaction waves (Geroliminis and Skabardonis, 2005). All fundamental diagrams shown in the figure have the same capacity ($Q = 1800$ vph), critical density ($\rho_c = 30$ vpm), and jam density ($\rho_j = 240$ vpm). The difference between the fundamental diagrams lies in the free-flow portion of various waves speeds. Different wave speeds are associated with certain traffic density ranges limited by critical densities.

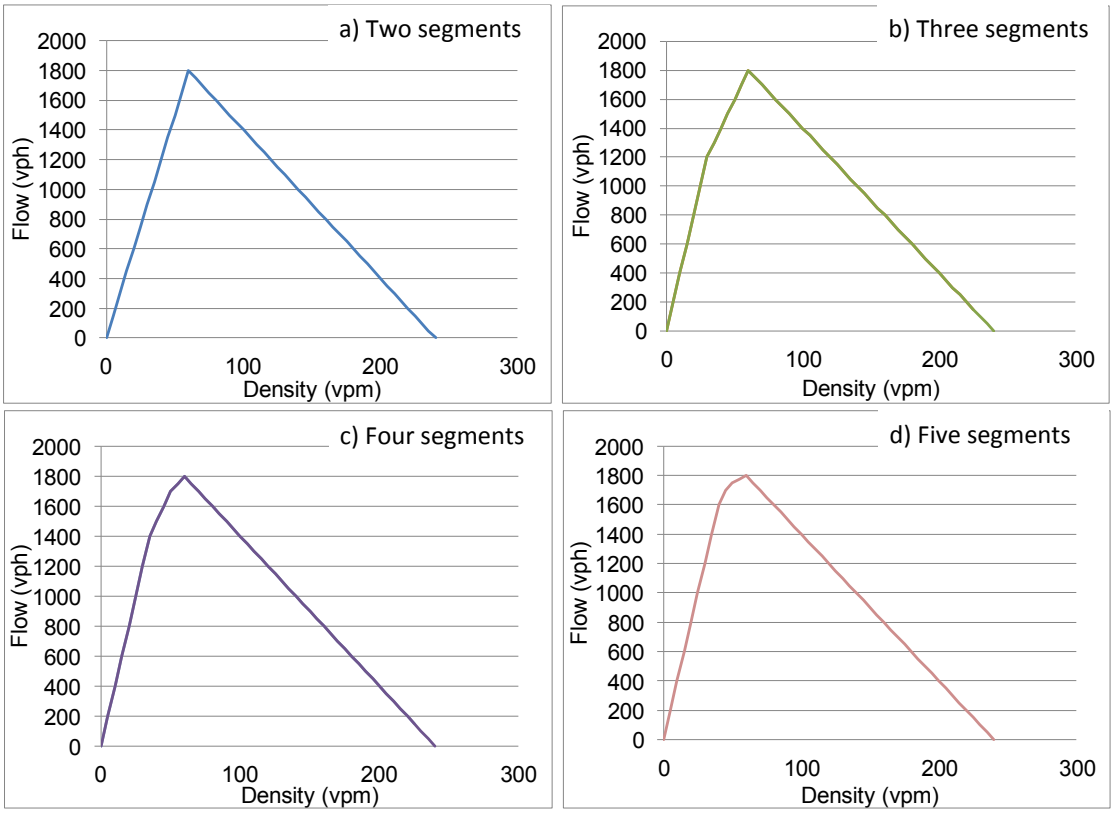

FIGURE 3.4: Fundamental diagrams with different numbers of segments

The red and green durations of the traffic light are set to be 30 sec and 30 sec respectively. During the green period, traffic is discharged at Q and 0 (vph) during the red period. Consequently a queue is developed and propagates backward to the upstream end during the red phase.

3.4.1 Viscosity at shocks

Figures 3.5 and 3.6 show the density maps generated respectively by CTM and variational method over time t. The horizontal axis is time and vertical axis is space. For the variational method, the density maps are derived from the cumulative flow $N(x,t)$ as $\rho(x,t) = -\frac{\Delta N}{\Delta x}\Big|_{(x,t)}$ over (x,t). The simulation time step Δt for both methods is set to be one second. Under CTM, the road section is discretised into 28 cells which gives a spatial discretization Δx to be 0.01786 mile. The space-time discretization is set such that the CFL condition is satisfied for all fundamental diagrams (see Section 3..3.2 for details) adopted in the study. To maintain consistency, the density map under variational method are generated with the same spatial granularity. It is also worth noting that the computational complexity of both methods is the same with the same space-time discretization and fundamental diagrams adopted. The computational time of both methods are both linear in the number of time steps and number of locations considered. For each time and location point, both methods solve a minimisation problem (Equation 3.10 for CTM; Equation 3.17 for variational method). The only difference is that CTM solves for flows and densities while variational method solves for cumulative flows.

Figure 3.5a shows that transition between blue and red becomes more blurred at the location closer to the upstream boundary. On the other hand, Figure 3.6a shows that the transition between blue and red remains constant throughout the whole transport link. As the underlying LWR model assumes that the change of different traffic densities can be achieved instantly without going through any transition. Thus, transitional densities between different equilibrium traffic densities are numerical errors produced by the underlying numerical solutions. From Figure 3.5a and Figure 3.6a, it is clear that numerical error (known as viscosity) arises along the density discontinuities under CTM, while the variational method is able to produce exact answers.

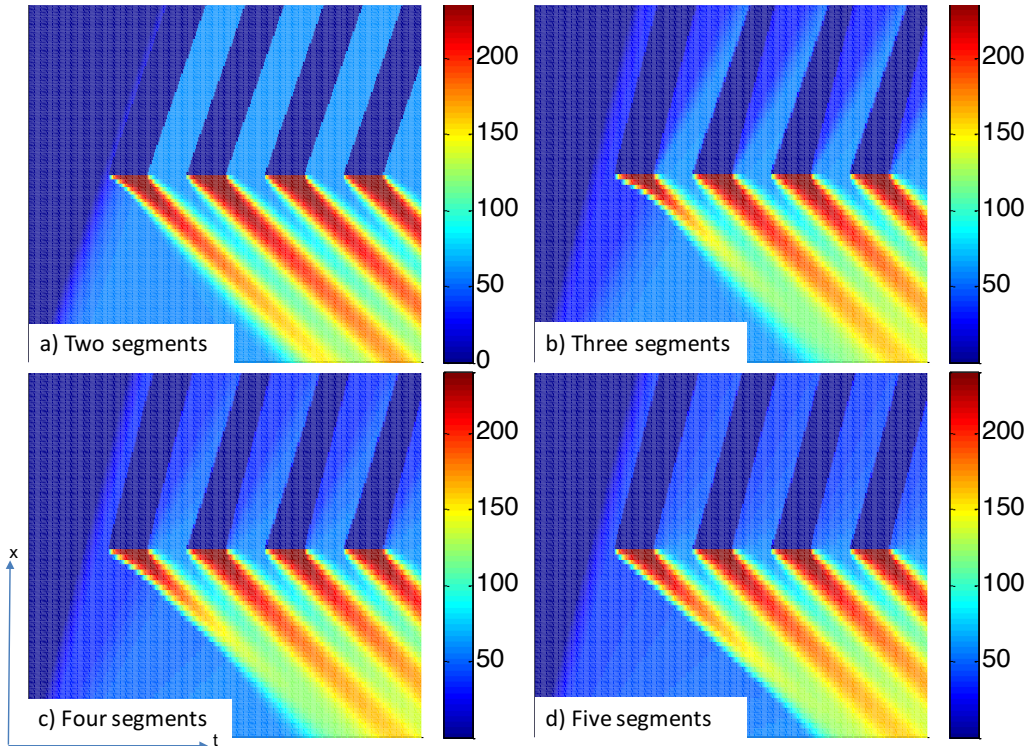

FIGURE 3.5: Density maps (in: vpm) generated by CTM with different fundamental diagram specifications

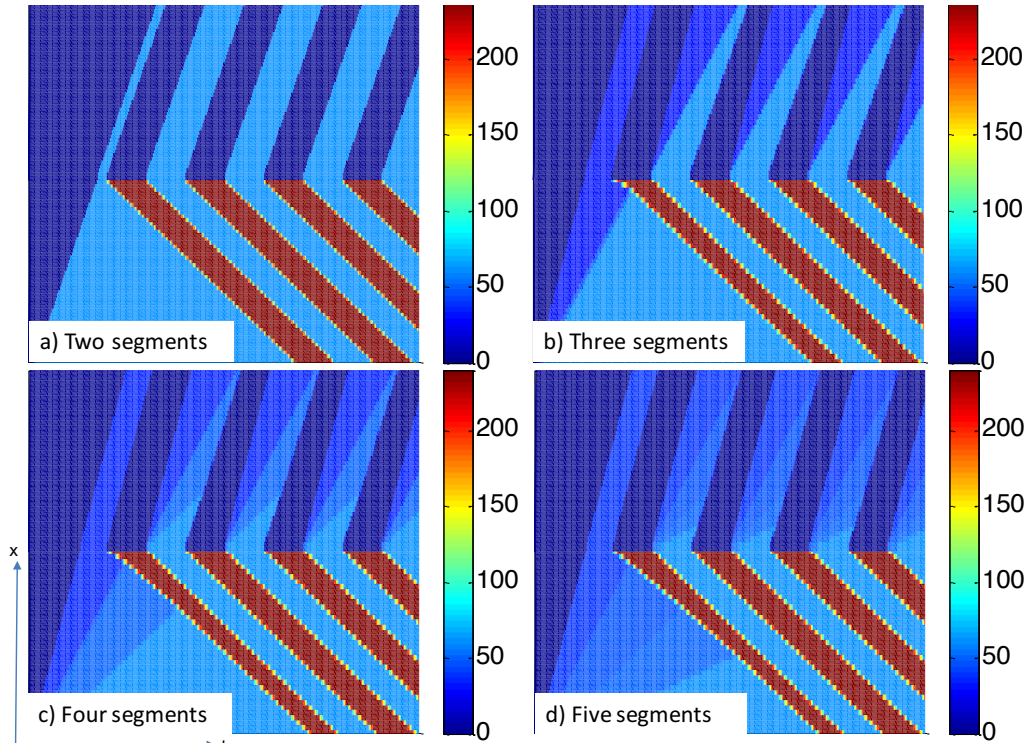

FIGURE 3.6: Density maps (in: vpm) generated by variational method with different fundamental diagram specifications

It should be emphasized that the space-time discretizations used for both methods in the numerical examples are the same. The differences observed in Figures 3.5 and 3.6 are due to the solution methods themselves rather than the underlying discretization scheme. LeVeque (1992) suggested that the numerical error observed in CTM due to viscosity can be reduced by using finer space-time resolution (LeVeque, 1992). Of course, it is known that improving numerical accuracy through refining resolution will have to come at the expense of computational effort. However, it is shown that the variational method with a triangular fundamental is indeed error-free as suggested by Daganzo and Menendez (2005) and Daganzo (2006) regardless of the space-time discretization used. Error will only arise in variational method when a more complicated fundamental diagram instead of a triangular one is used (Daganzo and Menendez, 2005).

3.4.2 Platoon dispersion

TABLE 3.1: Summary of different FD specifications

Case	**Wave speed (mph)**	**Cost rate (vph)**	**Critical density [1] (vpm)**
Triangular FD	[30 -10]	0; 2400	0;60;240
FD of 3 segments	[40 20 -10]	[0 600 2400]	0;30;60;240
FD of 4 segments	[40 20 10 -10]	[0 700 1200 2400]	0;35;50;60;240
FD of 5 segments	[40 20 10 5 -10]	[0 800 1250 1500 2400]	0;40;45;50;60;240

Table 3.1 presents values of different parameters used in the tested fundamental diagrams. It is noted these fundamental diagrams are all concave and hence they are all implementable under the variational framework. Table 3.1 shows the difference between the fundamental diagrams lies in the free-flow portion: the two-segment (triangular) fundamental diagram (Figure 3.4a) has a free-flow portion with constant free-flow speed ($v = 30$ mph) for all densities $\rho \in [0, 60]$ vpm; the three-segment fundamental diagram (Figure 3.4b) has a higher free-flow speed (v_1

[1] The term critical density here is different from the traditional one used in triangle FD which divides forward wave speed and backward speed. The critical density here refers to the density which divides two different wave speeds.

= 40 mph) for densities $\rho \in [0, 30]$ vpm and a lower free-flow speed ($v_2 = 20$ mph) for densities $\rho \in [30, 60]$ vpm to reflect a reduction in speed when the traffic state approaches the capacity; the four-segment fundamental diagram (Figure 3.4c) has three free-flow speeds $v_1 = 40$ mph, $v_2 = 20$ mph, and $v_3 = 10$ mph for densities $\rho \in [0, 35]$ vpm, $\rho \in [35, 50]$ vpm, and $\rho \in [50, 60]$ vpm respectively; the five-segment fundamental diagram (Figure 3.4d) has four free-flow speeds $v_1 = 40$ mph, $v_2 = 20$ mph, $v_3 = 10$ mph, and $v_4 = 5$ mph for densities $\rho \in [0, 40]$ vpm, $\rho \in [40, 45]$ vpm, $\rho \in [45, 50]$ vpm, and $\rho \in [50, 60]$ vpm respectively. The shock wave speed w is -10 mph in all cases.

Since multiple forward wave speeds can result in traffic platoon dispersion, density maps generated with 3-segment, 4-segment and 5-segment fundamental diagrams should show the change of traffic densities as traffic is discharged with green light. Equation 3.19 shows the theoretical formula used by the variational theory to calculate the minimum N value associated with different forward wave speeds. The proposed variational simulation platform implements this equation by calculating all the potential N value of each time-space node and selecting the minimum one as the result.

Figures 3.5 and 3.6 show the density maps generated by CTM and the variational simulation with different fundamental diagrams. Exact solutions are obtained for all these piecewise fundamental diagrams from the variational method which supports the theoretical analysis in previous studies (Daganzo and Menendez, 2005; Mazare *et al.*, 2011). With the multi-segmented free-flow part, portions of discharging traffic with different proceeding speeds and densities are generated. In addition to being used as a representation of the platoon dispersion phenomenon, this also gives further flexibility to the model for capturing traffic characteristics in the real world. Compared with the variational method, the density maps generated by CTM are distorted due to the errors arising along the discontinuity between traffic states. Hence, the variational formulation is considered as a better numerical method for computing traffic dynamics with non-triangular fundamental diagrams than CTM.

To gain further insight, Figure 3.7 shows the discharging flow profiles estimated by the four fundamental diagrams in Figure 3.4 under the variational framework. The flow profiles are taken at a location $x_1 = 0.1$-mile downstream of the stopline. It is noted that the total traffic volumes under the flow profiles are all equal to 15 vehicles and hence traffic is conserved.

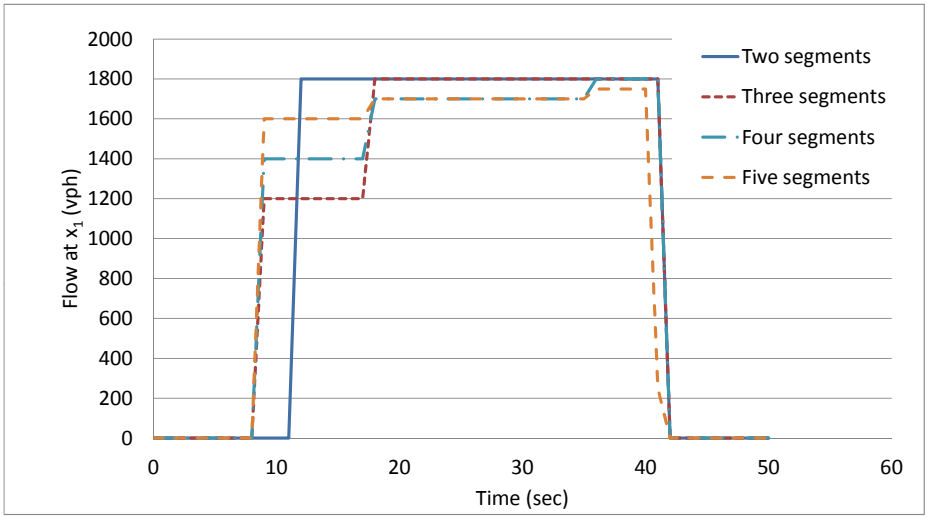

FIGURE 3.7: Outflow profiles generated with different fundamental diagram specifications

The traffic signal turns green at time $t = 0$ in the figure. Since flow profiles can be derived for other fundamental diagrams in Figure 3.4 following the corresponding specifications of the fundamental diagrams, solutions of arrival times associated with different traffic platoons were calculated and presented in Table 3.2.

TABLE 3.2: Analytical solutions of platoon arrival times

Case	**Platoon arrival time (sec)**
Triangular FD	12(1st)
FD of 3 segments	9(1st); 18(2nd)
FD of 4 segments	9(1st); 18(2nd); 36(3rd)
FD of 5 segments	9(1st); 18(2nd); 36(3rd);72(4th)

Analytical results agree with the numerical solutions generated by the proposed framework. Numerical results show that the discharged traffic takes 12 sec (=0.1/(30/3600)) to reach x_1 where all traffic is considered to be proceeding with a common forward speed 30 mph under the triangular (two-segment) fundamental diagram. For the

three-segmented fundamental diagram with two portion free-flow parts, the discharged traffic will reach x_1 in two packets. The first packet reaches x_1 at time $t = 9$ sec (=0.1/(40/3600)) at speed 40 (mph) and flow 1200 (vph) (=40 (mph) $\times$ 30 (vpm)) as specified in the fundamental diagram. The second packet reaches x_1 at $t = 18$ sec (=0.1/(20/3600)) at speed 20 (mph) and flow 1800 (vph).

With the variational formulation, high quality solutions are obtainable even with the multi-segmented fundamental diagrams as shown in Figure 3.6. Thus, it becomes easier to capture the sophisticated but important feature of the platoon dispersion phenomenon that cannot be modelled by triangular fundamental diagrams.

A final note is that the wave-front tracking algorithms proposed by Wong and Wong (2002) and Henn (2005) can also cope with platoon dispersion in a similar way as used in the variational method. Nevertheless, as also noted by Mazare *et al.* (2011), the wave-front tracking algorithm is an event-based method which increases its computational complexity which is difficult to analyse. The algorithm becomes especially complicated when dealing with fundamental diagrams that have many segments, let alone the continuous fundamental diagrams. The variational method herein does not have such a problem as it is implemented through a time-based approach.

3.4.3 Error Analysis

Figure 3.6 shows the density map generated by the proposed simulation platform which contains a transitioning zone from free flow region (represented by the blue area) to the congested region (represented by the red area), or the other way around. A zoom-in view of a transitioning zone in Figure 3.6a with a time range 72 sec to 162 sec and a space range 0.33 km to 0.39 km is depicted in Figure 3.8. Cells highlighted with colours other than blue and red form the transitioning zone Figure 3.8.

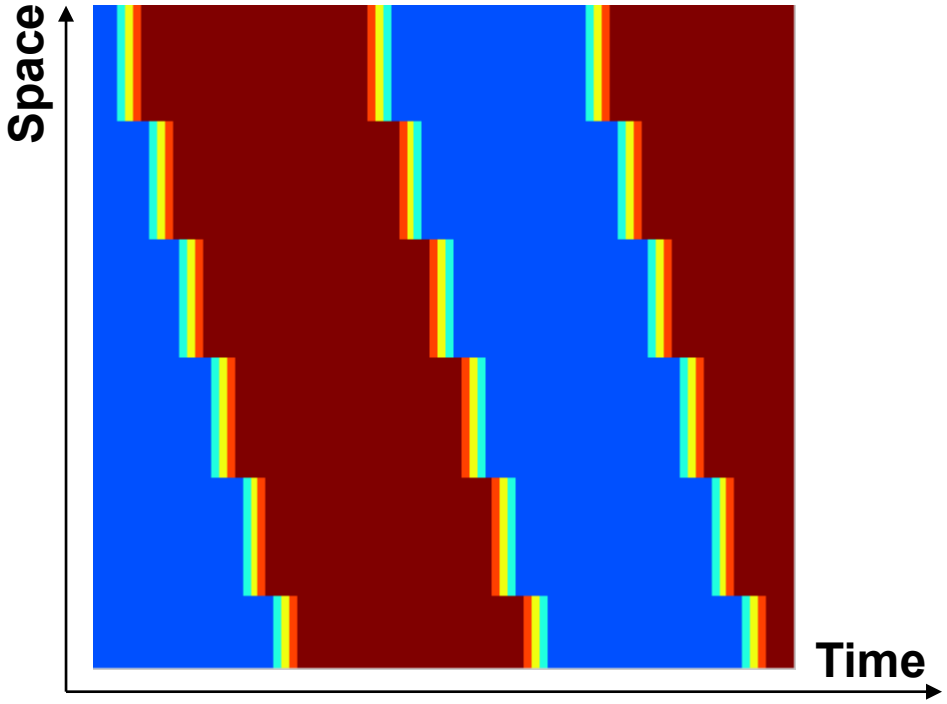

FIGURE 3.8: The transitioning zone from free flow state to congestion

The transitioning zone demonstrates bounded numerical errors associated with results generated by the variational method. Figure 3.8 shows that the error is bounded within 3 cells. These bounded errors are caused by the fact that computational grids of the variational method are not aligned in parallel with the shock wave propagation directions.

To understand the development of this transitioning zone, it is necessary to investigate the calculation of N value in the space-time plane along the path of backward shock wave propagation directions, as shown by Figure 3.9.

In Figure 3.9, points A and B are placed on the propagation path of backward shock wave which is represented by the white line. Computational grids adopted by the variational method are a vertical spatial grid and a horizontal temporal grid. Since the wave propagation direction is along the line AB, it is not in parallel with either the vertical or the horizontal direction. The wave propagation path intersects with the computational grids and divides the 4 cells between point A and B into 2 parts: the part underneath the shock wave in free-flow condition and the part above the shock wave in congested condition. As the proposed variational

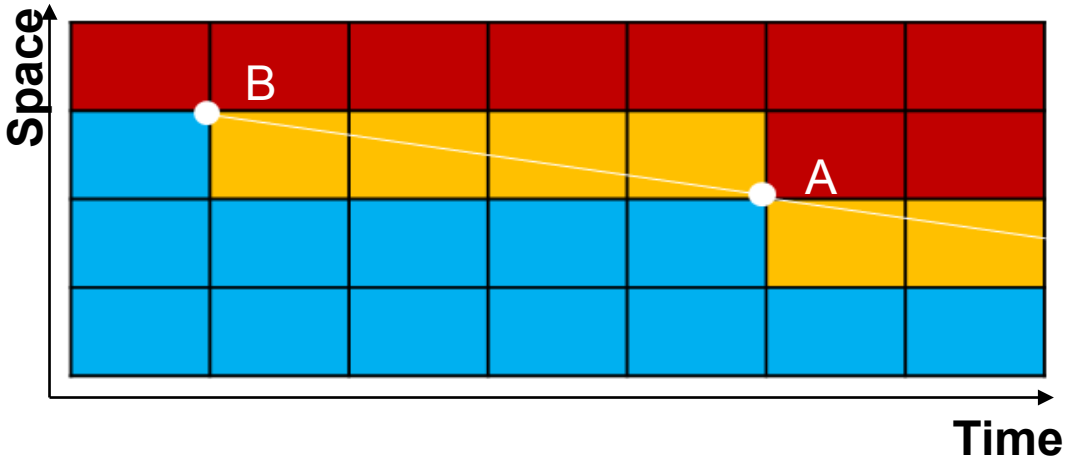

FIGURE 3.9: Formation of the transitioning zone

method assumes the density between points is evenly distributed in time and space, a transitioning zone is generated.

It should be noted that density errors represented by the transitioning zone only exist in the density maps, which are the secondary results generated by the proposed variational simulation platform. The primary result of the variational method is N value. Therefore, accuracy here can be measured by the discrepancy between simulation output N value and its analytical result. The lower the discrepancy, the higher the accuracy.

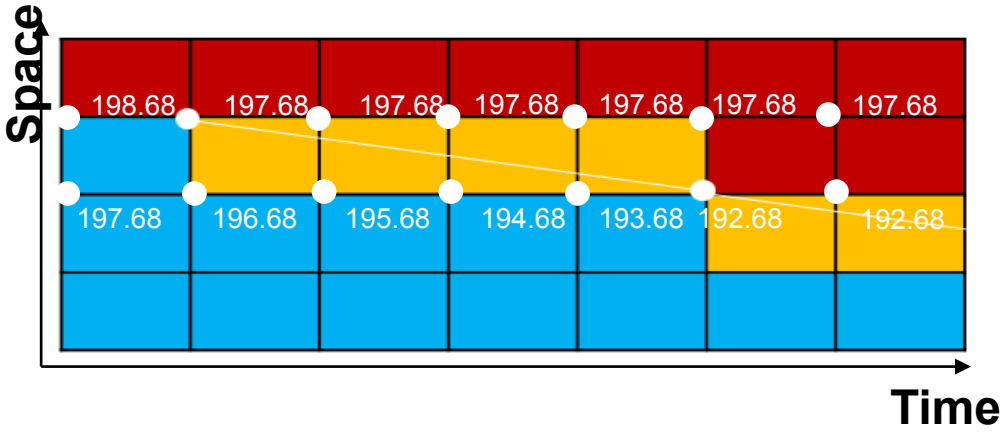

FIGURE 3.10: N value [in: veh] at the points in the transitioning zone

Figure 3.10 shows the N value of each point in the transitioning zone. The calculated flow from the transitioning points below the shock waves is 3600 vph

and the calculated flow of points above the shock wave is 0. This result is accurate with no discrepancy between simulation output and theoretical analysis.

3.4.4 Bus-traffic interaction

In this section, the performance of CTM and variational method on modelling moving bottlenecks is compared. Here the hypothetical arterial is 1-unit long and 4-lane wide with saturation flow 7200 vph, jam density 480 vpm, free-flow speed 30 mph, and backward congestion propagation speed -30 mph. Overview of the road section where buses and traffic interact with each other is illustrated in Figure 3.11.The fundamental diagram here is assumed to be triangular. Traffic is being loaded into the arterial at saturation flow 7200 vph. Suppose now a bus enters the arterial at location $x = 0.3$ unit and time $t = 0.01$ (hr). The bus proceeds with a speed 15 mph and it stops at a bus stop at $x = 0.6$ and $t = 0.03$ (hr). The bus dwells at the stop for 2 minutes (0.033 hr), then moves on at the previous speed and leaves the arterial at $x = 0.9$ at $t = 0.08$ (hr). The maximum passing rate (relative to the bus) of traffic around the bus is considered to be 5400 vph (3 lanes out of 4) when the bus dwells at the bus stop and 2700 vph when the bus moves at a slower speed relative to the surrounding traffic.

An analytical solution can be derived for this simple example as described in Newell (1998). Numerically, the effect of this slow-moving bus can be captured in the variational framework by adjusting the cost formulation Equation 3.21. For CTM, the method adopted is presented in Lebacque *et al.* (1998). To the best of our knowledge, Lebacque *et al.* (1998) still remains one of the very few documentations of modelling slow-moving buses on a kinematic wave platform. With CTM, the movement of a bus over time and space is represented by a first-order kinematic law (i.e. distance travelled equals to integration of speed over time) and hence the simulator can track which cell the bus is in at each time step. The effect of the moving bottleneck induced by the bus is captured as follows: whenever the bus is proceeding more slowly than its surrounding traffic in the

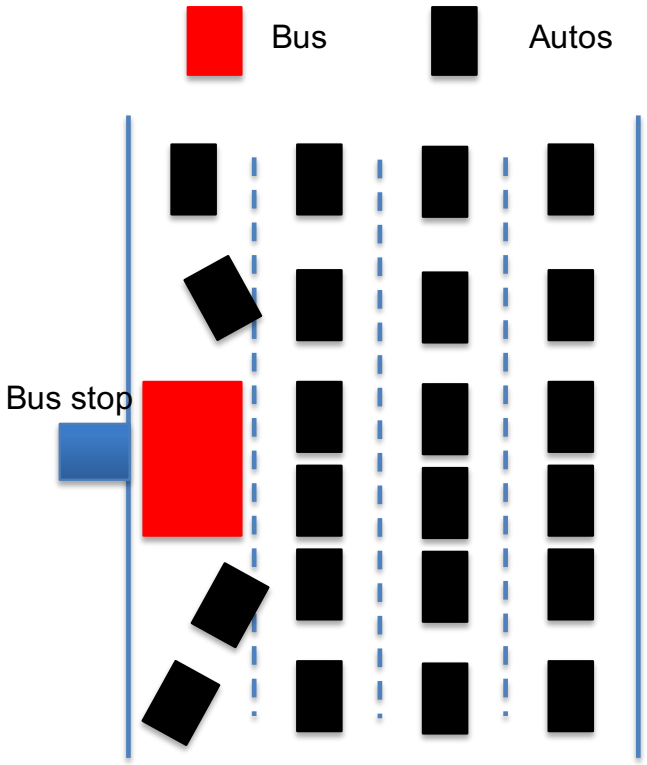

FIGURE 3.11: Illustration of bus-traffic interaction

cell, the speed of 'all' traffic (no matter whether they are in front of or behind the bus) in the cell will be reduced to the speed of the bus.

Figure 3.12 shows the analytical result with associated transition of traffic states along the fundamental diagram.

Figures 3.13 and 3.14 respectively show the numerical result generated by variational method and CTM in which the arrowed solid line represents the trajectory of the bus on the space-time plane.

Points A, B, C, and D in the figures respectively represent the events of the bus entering the arterial, arriving at the bus stop, leaving the bus stop, and leaving the arterial. Region '1' refers to the traffic state $\rho = 240$ (vpm) and $q = 7200$ (vph) before the bus enters the arterial. Region '2' is the traffic passing the slow-moving bus which is $\rho = 180$ (vpm) and $q = 5400$ (vph) as specified. Region '3' is the traffic queued behind the bus while it is moving. The slope of the dotted line joining '2' and '3' in Figure 3.12 is the speed of the moving bus which is 15 mph. Hence the flow and density at '3' can be derived from geometry as 6300 vph

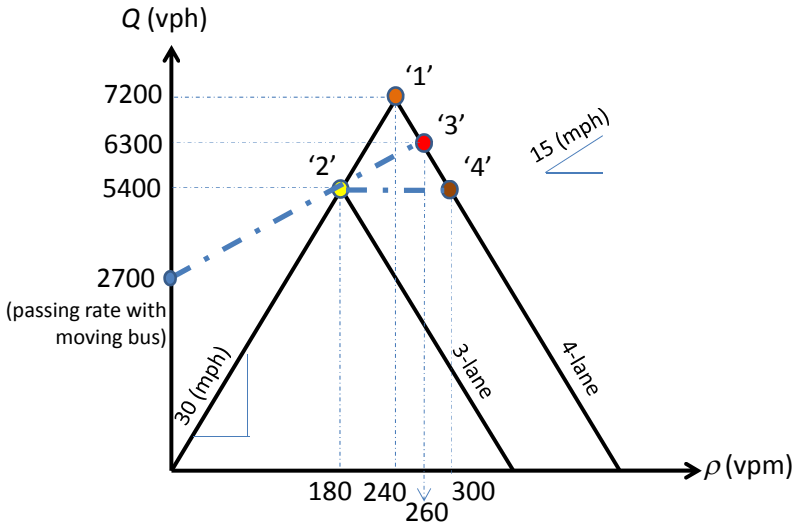

FIGURE 3.12: Transition of traffic states associated with the slow-moving bus

and 270 vpm respectively. Region '4' is the traffic state behind the bus when it is stopped. Region '4' has a flow value of 5400 vph and density 300 vpm. Similar results can be derived from CTM as shown in Figure 3.14 while the dotted line pattern formed in Region '3' in Figure 3.14 is recognised as erroneous due to the uniform assumption (i.e. all traffic in the cell affected by the presence of the bus in the same way) adopted under CTM as discussed in Lebacque *et al.* (1998). Here it shows that variational method provides a more accurate solution with respect to the the analytical model when dealing with traffic bottlenecks (e.g. buses).

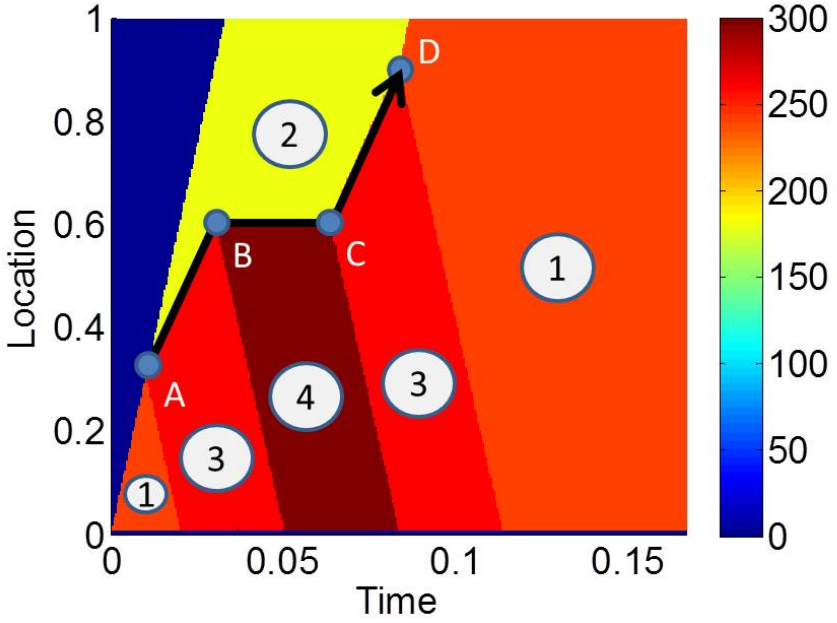

FIGURE 3.13: Simulation of impact of a slow-moving bus under variational method

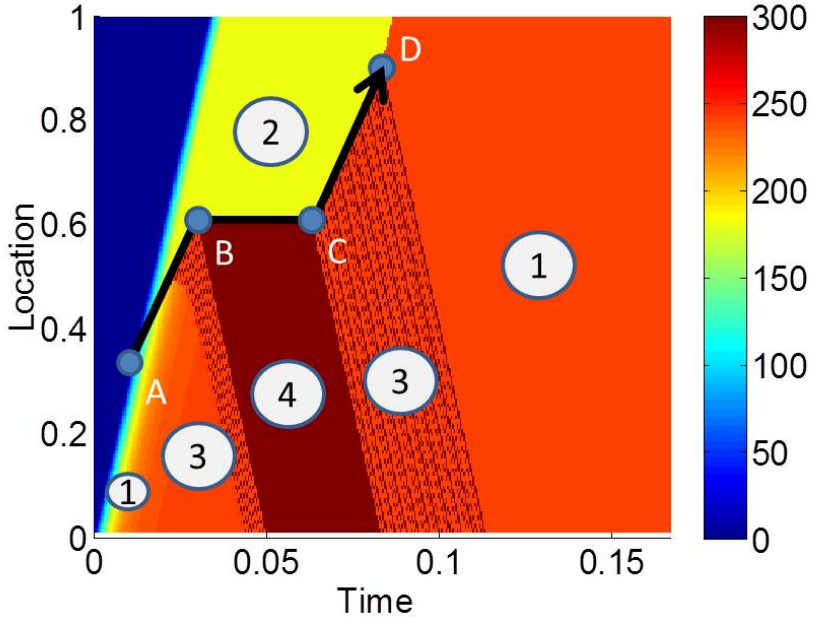

FIGURE 3.14: Simulation of impact of a slow-moving bus under CTM representation

3.5 Real-world application

This research applies the proposed variational simulation platform to a real world scenario with a 0.9-mile long section of Tottenham Court Road (TCR) in Central London, UK (Figure 3.15).

FIGURE 3.15: Tottenham Court Road (TCR), London, UK (1:10000)

The road section consists of two lanes and seven signal-controlled intersections. The traffic signals are operated under the SCOOT Urban Traffic Control system in which the cycle time, offsets, and green splits are adjustable according to real time traffic detection. Five of them: Bayley Street (N02/056), Goodge Street (N02/058), Torrington Place (N02/062), University Street (N02/060), and Grafton

Way (N02/059), are equipped with loop detectors at which available information includes volumes and signal timings. The indices in the bracket are IDs of the junctions used under the SCOOT system. There are another two signal-controlled intersections: Howland Street and Store Street (marked by two triangles in the figure) at which there is no detection.

3.5.1 Traffic data

Traffic data used in this study include journey time estimates derived from the London Congestion Analysis Project (LCAP) system, which is an application of automatic vehicle identification (AVI) technique. Traffic flow and concentration measures are also available through collection from loop detectors in the city of London which are operated under the SCOOT urban traffic control system. The data were collected on 5 June 2013 (Wednesday). Journey times and loop detector data are used as simulation input and benchmark for calibrating and validating the proposed traffic models.

Automatic vehicle identification

A number of transport policies in London, including the congestion charge and low emission zone schemes, are enforced by using the Automatic Number Plate Recognition (ANPR) technology. The plate numbers of vehicles passing the ANPR cameras are recognized and recorded along with the corresponding times, which are used to decide whether the vehicles detected have paid the charge. The journey times of vehicles between two ANPR camera sites are then estimated by matching the license plate numbers. The journey times are processed and stored in 5-min averages. The journey time data can be used to derive various performance metrics such as speeds, journey time reliability, and impacts of major events including strikes (Tsapakis *et al.*, 2012) and the Olympics (Chow *et al.*, 2014). This enables the road operator to calculate the benefits and costs associated with different policies or control plans to improve the day-to-day operation of the network. Nevertheless, it is noted that various errors may arise in matching the license plate

numbers due to various reasons such as misreading of license plates, vehicles stopping en-route, and vehicles taking an unusual long route between the two camera locations (Robinson and Polak, 2006). Consequently, a set of data filtering and processing rules is adopted to improve the journey time estimation. For example, the overtaking rules described in Robinson and Polak (2006) are used to eliminate the data noise caused by camera errors and delivery vehicles stopping along the route. Information from the Driver and Vehicle Licensing Agency (DVLA) is used to eliminate the data related to unauthorized vehicles on the bus lanes. On some occasions, data may be missing over some time intervals due to no sample (e.g. no vehicles can be matched during the time interval) or failure of the hardware system. A range of patching algorithms will be used to impute the missing data in those circumstances.

Urban loop detectors

There are about 3,000 intersections in the city of London operating under the SCOOT Urban Traffic Control system (Siemens, 2012). The intersections are equipped with loop detectors which measure the incoming flow and occupancy of traffic and hence derive optimal timing strategies in real-time. For performance measure purposes, measured traffic quantities including flows and occupancies are stored and processed in archived SCOOT dataset. The dataset also records signal timings used, excessive queues detected, and journey times estimated. These data and statistics are stored in different 'messages' in the SCOOT dataset and different messages record different traffic characteristics and estimates (Siemens, 2012). The SCOOT dataset provides the following information of demand and signal timings through its 'M13' and 'M29' messages (Siemens, 2012):

1. **Flow counts** - flow counts are recorded once a signal cycle at each SCOOT detector station in the M29 messages. The cycle time in the TCR area is 88-sec and hence the unit of these flow counts will be vehicles per 88 seconds (veh/88-sec).

2. **Signal timings (green durations)** - SCOOT M13 messages provide the durations of green phases. The green durations are time-varying and derived

from the SCOOT optimiser in real time.

3.5.2 Building traffic models

In addition to demands, signal timings, and split ratios as stated in the previous section, it is necessary to determine the fundamental diagram of each link in order to complete the specification of the traffic models. The key parameters here are wave speeds, saturation flows, critical and jam densities.

Saturation flow

The SCOOT detector data are processed and stored in averages over a signal cycle which makes it impossible to identify the true values of saturation flow with these cyclic averages. This research estimates the saturation flow by assuming the maximum cyclic flow value observed on an approach will be equal to $(\frac{g}{g+r}Q)$, where g and r are respectively the effective green and red durations allocated to that approach over a cycle, and Q is the saturation flow which is an unknown. In traffic engineering, this $(\frac{g}{g+r}Q)$ is regarded as the signal-controlled capacity of the approach. It is noted that both g and r are records of real-time operations. However, both g and r are not constant due to the adaptive nature of SCOOT controller and hence the average values of them are used to calibrate the traffic model. The sum of them $(g + r)$ gives the total cycle time c which is 88-sec in the TCR network. Consequently, the saturation flow s on each approach can be derived accordingly.

Table 3.3 summarises the measured maximum flows (in [vph per lane]) in one cycle and average $(\frac{g}{g+r})$ ratios allocated to TCR during the study period at the four intermediate detector stations (N02/058, N02/062, N02/060, and N02/059). The table also shows the corresponding estimated saturation flows Q.

To further investigate the reliability of the saturation flow estimation, a sensitivity analysis on the corresponding overall journey time and flow estimates produced

TABLE 3.3: Estimation of saturation flows on Tottenham Court Road

	N02/058	N02/062	N02/060	N02/059
Max. flow (vph per lane)	655	675	634	695
g/(g+r)	0.42	0.43	0.41	0.43
Saturation flow (vph per lane)	1554	1572	1555	1620

by the model with respect to different choices of s values is conducted. As an example, Figure 3.16 shows the sensitivity of journey time and flow estimation error with respect to the saturation flow s at Junction Goodge Street (N02/058) over a range of values from 1400 vph/lane to 1800 vph/lane.

The errors are quantified in terms of mean absolute percentage error (MAPE). The MAPE of journey times e_{T^J} estimates is calculated with respect to the observed values as Equation 3.22.

$$e_{T^J} = \frac{1}{T}\sum_{t=0}^{T}\left|\frac{\hat{T}^J(t) - T^J(t)}{T^J(t)}\right|, \tag{3.22}$$

where $\hat{T}^J(t)$ and $T^J(t)$ are respectively the estimated and measured journey times at time interval t within the time horizon T.

It is shown that a saturation flow of around 1550 vph/lane will give the lowest error for journey time and flow estimations. This 1550 vph/lane indeed is consistent with the number obtained in Table 3.3.

Similar results are observed at the other three junctions and hence it suggests using the controlled capacity $\frac{g}{g+r}Q$ which is a reasonably reliable way to estimate saturation flows with the coarse data. Finally, it is worth noting that the estimated values in Table 3.3 appear to be less than the nominal value 1800 vph per lane. This is estimated to be due to the narrow streets, high volumes of turning traffic, and pedestrian crossing in the area.

Jam density

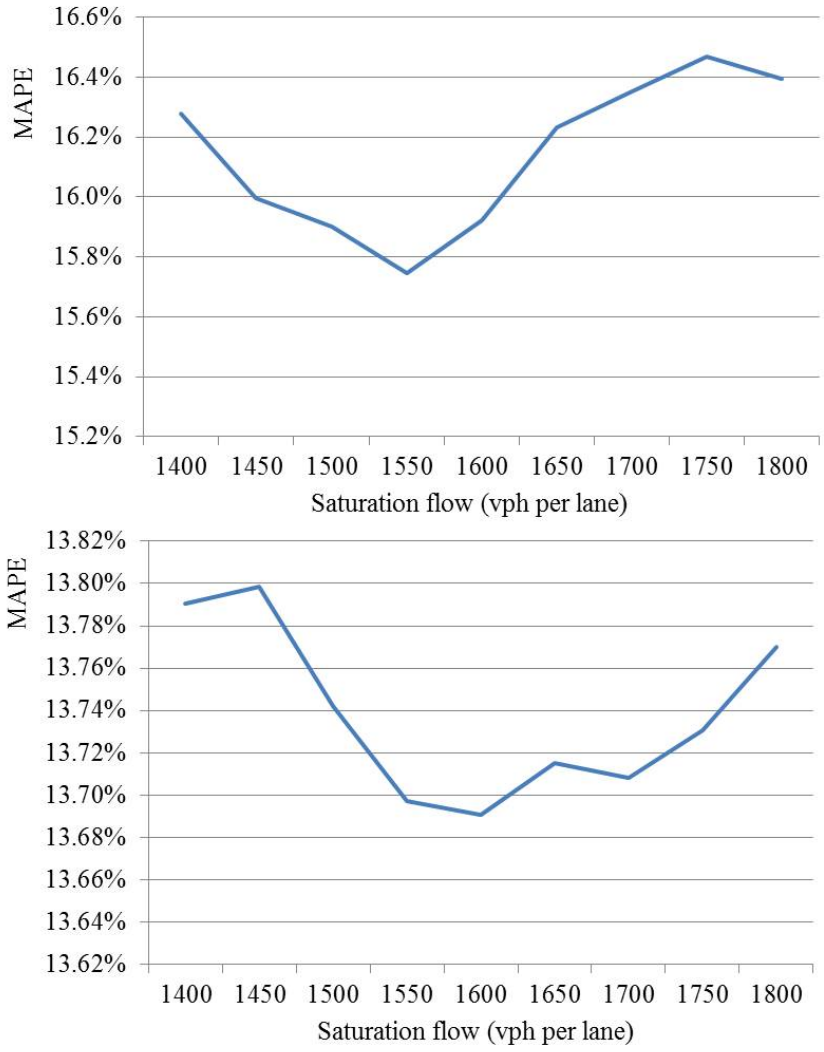

FIGURE 3.16: Sensitivity analysis of estimation errors with respect to choice of saturation flow (at Goodge Street)

The SCOOT dataset does not provide a reliable estimate of jam density which is relatively more difficult to collect than traffic flow data in practice. To facilitate the calibration process, here a nominal value 225 vpm per lane is adopted. The value 225 vpm falls in the nominal jam density range between 180 and 250 vpm per lane as suggested by May (1990) and Nanda (1993).

Wave speeds

Given the saturation flows and jam densities, the main objective of calibration now is to determine the wave speeds $\mathbb{U}$ with which the fundamental diagrams can be specified accordingly.

The wave speeds are determined such that the discrepancies between the journey times along TCR derived from the traffic models and those measured from the on-site ANPR system are minimised. For CTM, the journey times are derived by using the frozen field method (Chow *et al.*, 2010). After running a CTM simulation, one can obtain the traffic speed matrix $v_i(t) = \frac{q_i(t)}{\rho_i(t)}$ over all cells i and times t. A virtual infinitesimal probe can then be 'released' at the upstream end of the route over a set of departure times t^D. Using the basic principle of kinematics, the distance travelled of each of these probes over time can be obtained from integrating the speed $v_i(t)$ over time and space. The probe is said to be exiting the current cell i and entering the subsequent cell $i+1$ at time t_1^D when the distance travelled is greater than or equal to x_i. The travel time of the probe through cell i is then determined as $T_i^J = (t_1^D - t^D)$. Applying the same methodology to other cells and departure times, a travel time profile through the entire route can be derived accordingly. For the variational method, the trajectory of vehicles can be derived as the iso-contours of the N values (Daganzo and Menendez, 2005), which can give the corresponding journey time of each vehicle.

Figure 3.17 shows the MAPE estimated by both CTM and the VM simulation platform with different wave speeds. With the backward wave speed of a triangular FD fixed, numerical tests were carried out iteratively with different free flow wave speeds from 11 mph to 30 mph. The relationship between free flow wave speeds and estimate accuracy follows a similar U-shape pattern for both CTM and VM. The highest accuracy is achieved with an optimal free flow speed in the range between 17 mph to 19 mph. A further iterative line searching process at one decimal place was carried out to identify the optimal free flow wave speed at 17.3 mph.

3.5.3 Results

Estimation of journey times

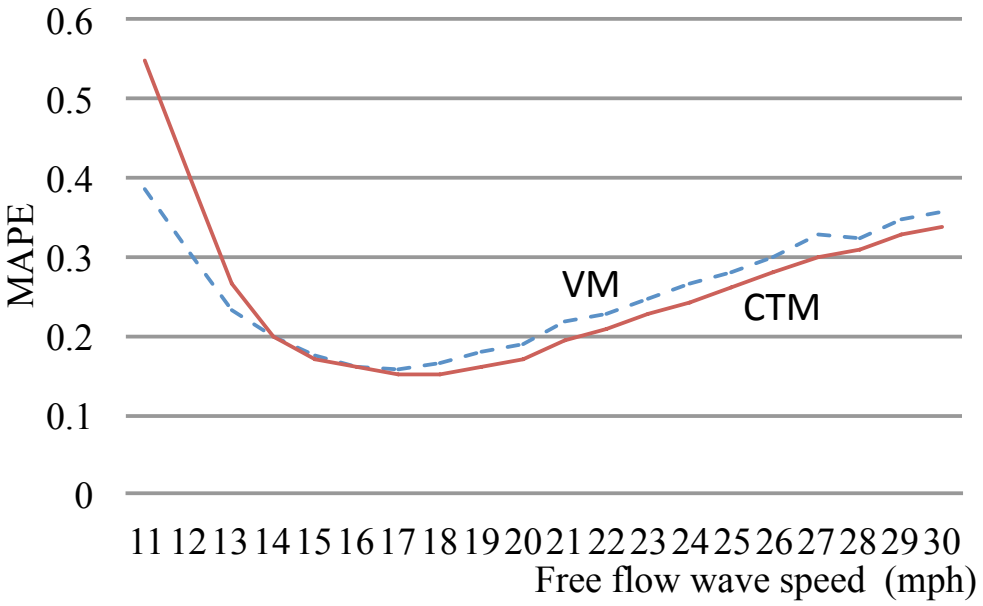

FIGURE 3.17: MAPE of journey time estimates with different wave speeds

After specifying the general form of the fundamental diagrams (i.e. the number of segments and where the fundamental diagrams are segmented), iterative line searches were adopted to estimate the corresponding wave speeds in the fundamental diagrams aiming to minimise the discrepancies between modelled and measured journey times. The results are shown in Figure 3.18. All data were collected on 5 June 2013 (Wednesday) from 12:00 to 15:00.

Figure 3.18a presents estimates produced by models with two-segment fundamental diagrams, and Figure 3.18b presents estimates produced with three-segment fundamental diagrams. In both figures, the dotted lines as 'ANPR' are measured journey times from ANPR system and they are regarded as 'ground truth' here. 'CTM' are journey times estimated by CTM and 'VM' are journey times derived from the VM-simulation.

The proposed variational simulation platform generates more accurate journey time estimation with three-segment fundamental diagrams. With the two-segment fundamental diagrams, both CTM and the VM-simulation have a tendency to underestimate the journey times through neglecting the reduction in speed when traffic approach high values of density. With the three-segment fundamental diagrams, the feature of platoon dispersion can be captured (see Figure 3.7) which

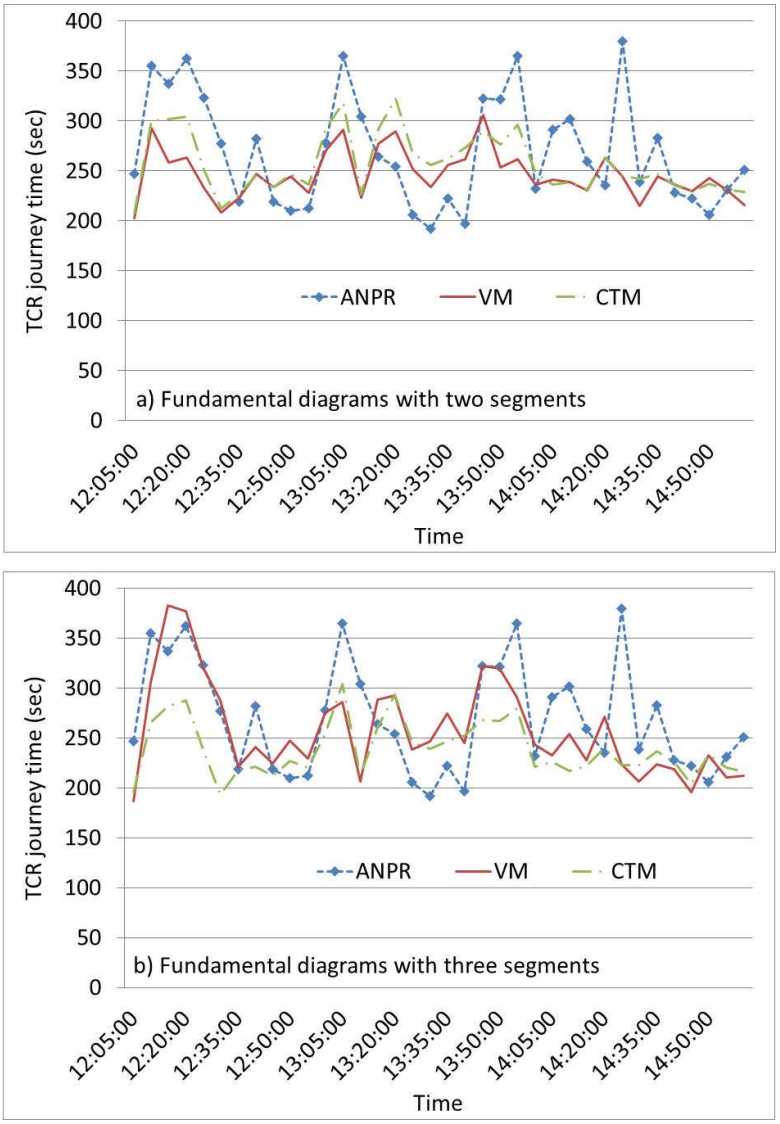

FIGURE 3.18: Comparison of TCR journey times (5 June 2013)

enables traffic proceeding under free-flow at different densities to be associated with different speeds. Consequently, traffic will slow down when the associated density grows toward the critical value under the three-segment fundamental diagram specification. The resultant model fits better with reality and also gives additional flexibility in parameter specification. Hence the model can produce more accurate estimates of journey times with respect to the observed values.

Nevertheless, one should note that there can be other factors contributing to the underestimation of journey times. This includes oversimplification of the junction dynamics, presence of pedestrians, and heterogeneity of traffic (e.g. presence of

slow moving vehicles such as buses, bikes, etc). Incorporating these factors requires more advanced modelling techniques such as detailed node modelling that captures the discrete movements of vehicles at junctions, and multi-class modelling that considers explicitly the heterogeneity of traffic flow. These are beyond the scope of this research and will be studied in future research.

The MAPEs of estimates produced by CTM (2-segment), CTM (3-segment), the VM-simulation (2-segment), and the VM-simulation (3-segment) are presented in Table 3.4.

TABLE 3.4: MAPE of journey time estimate by different methods

Method	FD type	MAPE
CTM	Triangular	15.30%
VM	Triangular	15.20%
CTM	3-Segment	15.60%
VM	3-Segment	13.60%

The differences between the estimates of CTM and the variational method are rather insignificant. Nevertheless, it is interesting to note that the variational method gives a slightly better improvement compared with CTM when a three-segmented fundamental diagram is adopted. It is believed to be caused by the numerical errors in CTM at the density discontinuities are accumulated with the increased overlapping different traffic states when a multi-segment fundamental diagram is adopted.

This research also explores the use of more refined fundamental diagrams, where obtained error rates of around 14% for four-segment and five-segment fundamental diagrams. The error rates are lower than that obtained with three-segment fundamental diagram while they are not significantly better despite the additional computational effort. Hence, it can be concluded that the three-segment fundamental diagrams will be a sufficiently good representation of traffic characteristics in this context.

Estimation of traffic flow

To gain further insight into the performance of the models, Figures 3.19 and 3.20 respectively show the corresponding cyclic flows estimated by CTM and the variational method with three-segment fundamental diagrams at the four detector stations (N02/058, N02/062, N02/060, and N02/059).

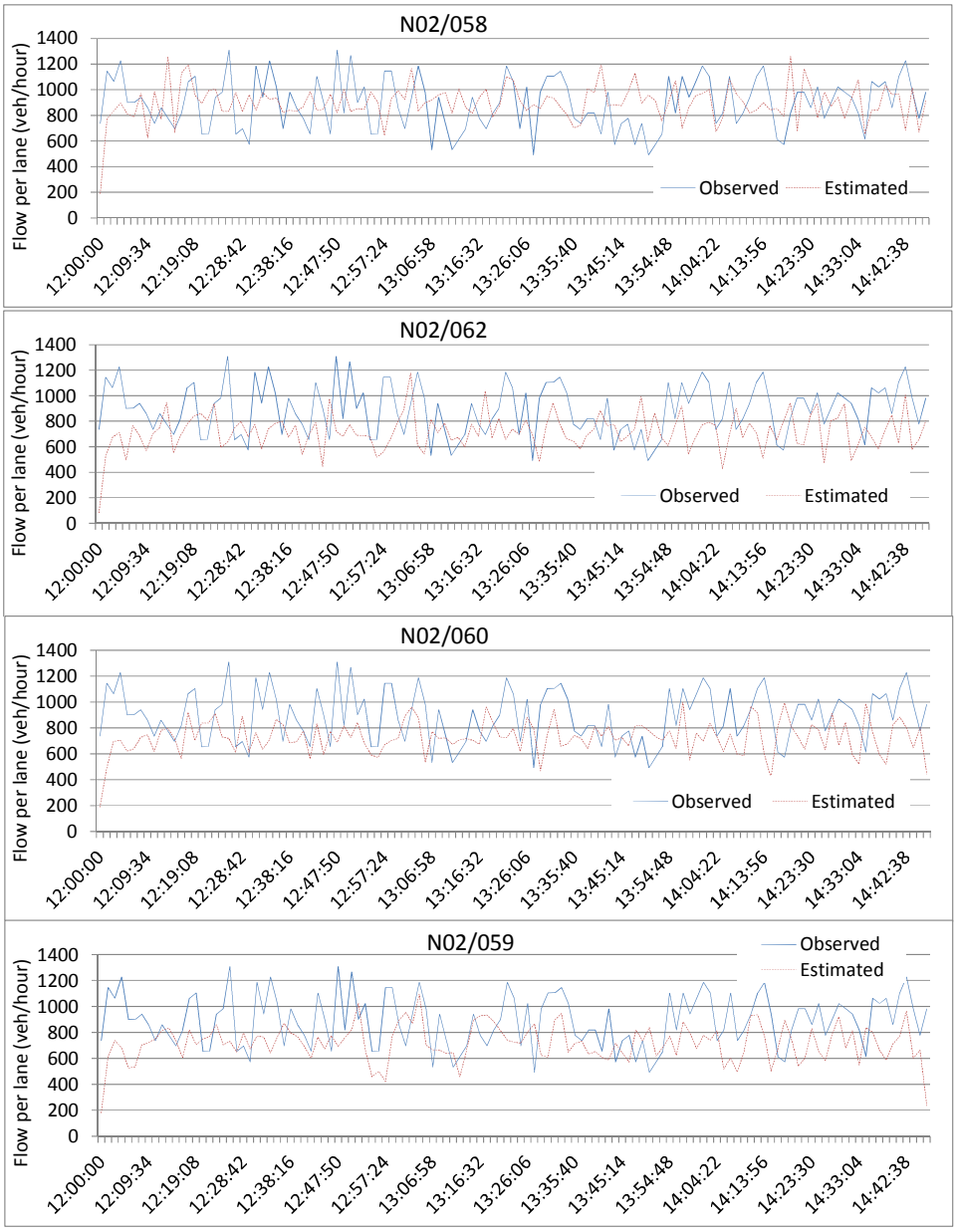

FIGURE 3.19: Flow estimates by CTM with three-segment fundamentals

These estimated flow values are compared against the actual observed values by the detectors. The error rates (in terms of MAPEs) at each station are summarised

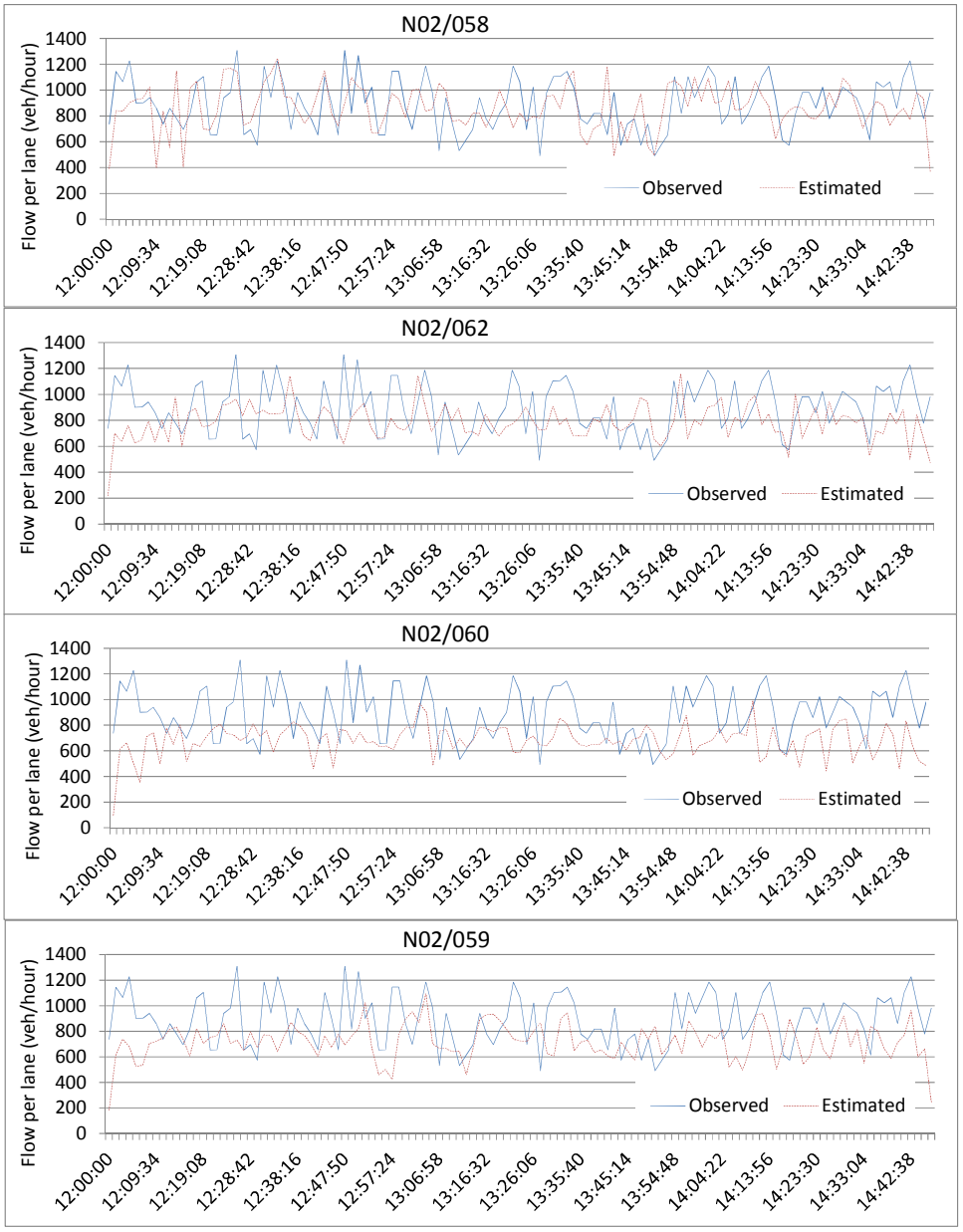

FIGURE 3.20: Flow estimates by variational method with three-segment fundamentals

in Table 3.5 which shows that the flow estimates by CTM and the VM-simulation are close.

The average MAPE of the flow estimates of the variational method is 14.3% while that of CTM is 14.8%. This should not be surprising as the main difference between variational method and CTM is the viscosity in traffic estimates. Nevertheless, when the traffic quantities are aggregated to a reasonably long time scale (say, one

TABLE 3.5: MAPE of flow estimates aggregated in 3 cycles

	N02/058(%)	N02/062(%)	N02/060(%)	N02/059(%)	Average(%)
CTM	10.1%	16.5%	15.7%	16.8%	14.8%
VM	9.5%	17.1%	14.8%	15.8%	14.3%

signal cycle here), the discrepancy due to such viscosity effect will be averaged out and hence the two methods will produce similar results.

Further improvement in flow estimation will require detector data with higher quality and spatio-temporal granularity which are unfortunately not available for the present study. They can be researched for future exploration with this proposed simulation platform. Finally, it is noted that the 'moving bottleneck' is not included herein due to the lack of appropriate data such as bus trajectories and surrounding traffic states. Meanwhile, different authorities are being contacted around the world in order to get required data. It is desirable to report further developments in the future.

3.6 Conclusion

Chapter 3 presents a variational based modelling framework of urban traffic dynamics. This variational method is compared with the traditionally used CTM over a set of hypothetical experiments and a real case in Central London. The numerical experiments suggest that the variational method is easy to implement and able to produce a high-quality solution, in particular for modelling platoon dispersions and moving bottlenecks. The case study with Central London data supports the validity of the variational method for real world applications.

A note to emphasize is that this chapter is not aiming to claim that the variational method is a better 'model' than CTM, as theoretically they both belong to the same model - LWR model. The results are only showing variational method is a more accurate solution method to LWR model than CTM or Godunov which echoes the findings in Daganzo (2005*b*) and Daganzo and Menendez (2005). It

also suggests variational method can be a better implementation than CTM when dealing with platoon dispersions and moving bottlenecks.

One may argue that the smeared solution (i.e. solution with viscosity) produced by CTM and other Godunov schemes may indeed be a better representation of actual traffic. It is agreed that the sharp jump discontinuity is only a feature of the LWR model and is not a real world feature. However, the viscosity is indeed an unexpected characteristic due to the property of the underlying solution method. Indeed the LWR model itself does not explicitly specify such viscosity in its formulation. A good solution method should simply produce a numerical solution as close to the exact or theoretical solution as possible. Whether the numerical solution is a good representation of reality should be a separated question. If one is interested in producing a solution that captures the viscosity, perhaps one should consider revising the model formulation or using a different model rather than LWR.

There have been studies exploring the development of practical estimation and optimisation algorithms based upon the variational method (Mehran *et al.*, 2012; Han *et al.*, 2013*a*). The variational method proves to be a useful and computationally effective tool for estimating and managing urban traffic given its benefits revealed herein and hence should receive more attention in the research community.

Chapter 4

Evaluation of bus holding control

4.1 Introduction

This chapter aims to investigate the impact of road traffic on bus service regularity and evaluate the performance of bus holding strategies under different road traffic conditions in a multi-modal transport system. Bus holding strategies are evaluated from the perspectives of both buses in terms of bus service efficiency and regularity and the road traffic in terms of total traffic delay.

Section 4.2 discusses the research background and research gaps which motivate this study. Section 4.3 presents the development of an integrated simulation platform called VMBus which is used to model bus movement and implement holding strategies. This section also outlines the evaluation metrics used to quantify bus service regularity. Section 4.4 presents various numerical cases to evaluate different bus control strategies under different passenger demands, traffic demands and road traffic characteristics. Section 4.5 validates different holding strategies in simulation experiments based on real-world settings. Section 4.6 concludes this chapter.

4.2 Background

The most important performance indicator of a bus system is arguably bus service regularity which is closely monitored by most transport agencies in order to enhance bus operation performance (Benn, 1995). An improvement in bus service regularity can attract more people to take public transport rather than private vehicles to reduce the traffic demand. An unreliable bus service increases operation costs and undermines fleet efficiency to carry passengers (Lin *et al.*, 2008).

In order to improve bus service regularity, various bus holding strategies have been proposed (Osuna and Newell, 1972; Newell, 1974; Eberlein *et al.*, 2001; Zhao *et al.*, 2006). The main objective of these holding strategies is to eliminate bus bunching problems by holding buses at specific control points, usually bus stops, for a certain amount of time. Bus bunching occurs when multiple buses of the same route number arrive at one stop in close succession. This is an undesirable phenomenon since it decreases bus service regularity and increases passenger waiting time as discussed in Section 2.3.

Section 2.4.1 concludes that there is little research available to systematically evaluate and compare the effectiveness of different bus holding strategies in a multi-modal system where buses and autos share the road space. Moreover, existing studies on evaluating bus holding strategies generally assume buses as a separate traffic flow in a transport system and only focus on impact from the perspective of bus operators and passengers (Bartholdi III and Eisenstein, 2012; Argote *et al.*, 2012; Toledo *et al.*, 2010; Cats *et al.*, 2012).

This research aims to investigate the impact and effectiveness of bus holding strategies in multi-modal systems. Since buses operating in a mixed traffic flow of transits and other road traffic is a common practice in most transport systems, the impact of traffic conditions on the effectiveness of bus holding strategy should be considered and explored for the development of more effective control strategies.

4.3 Development of VMBus platform

4.3.1 Interface of micro buses and macro traffic

VMBus simulation estimates the dynamics of bus movement between stops is expressed as Equation 4.1 and Equation 4.2:

$$t^A_{n,s+1} = t^D_{n,s} + T^C_{n,s+1} \tag{4.1}$$

$$t^D_{n,s} = t^A_{n,s} + T^D_{n,s} \tag{4.2}$$

where $t^A_{n,s+1}$ is the arrival time of bus n at station $s+1$; $t^D_{n,s}$ is the departure time of bus n leaving stop s; $T^C_{n,s+1}$ is bus cruising time from station s to $s+1$; $T^D_{n,s}$ is the dwelling time of bus n at station s.

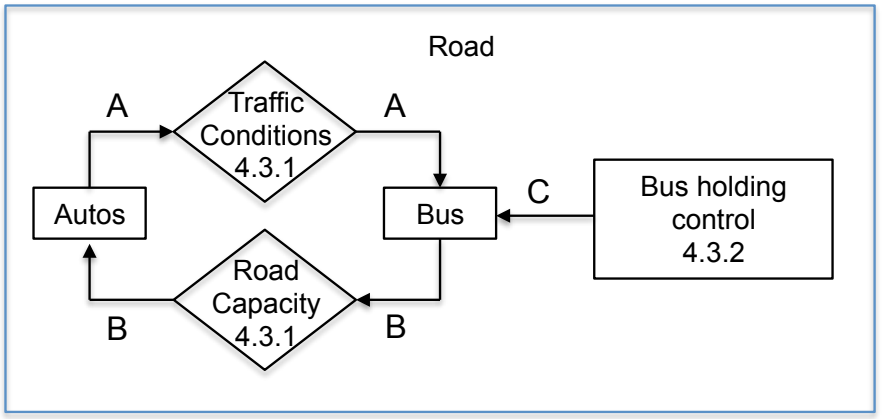

FIGURE 4.1: Bus control in a multi-modal system

Bus journey time and bus dwelling time are closely related to bus-traffic interactions and bus holding strategies. The relationship of bus, road traffic (autos) and bus holding control in a multi-modal system is illustrated in Figure 4.1. Arrow A illustrates the impact of road traffic on buses through affecting road traffic conditions. Arrow B illustrates the impact of buses on road traffic through the change of road capacity. This section focuses on how bus cruising time T^C is estimated by the VMBus simulation platform by capturing bus-traffic interaction represented

by Arrow A and Arrow B in Figure 4.1. Section 4.3.2 presents development of various bus holding strategies and how these holding strategies determine bus dwelling time as represented by Arrow C.

Traffic impact on buses

In order to estimate bus movement in a multi-modal transport link, it is necessary to first identify the movement of traffic flow. VMBus incorporates the simulation platform proposed in Chapter 3 to estimate road traffic conditions based on inputs including traffic demand, urban traffic characteristics and bus-traffic interaction. The primary result of the variational platform is N value, whose derivatives over time t and location x are traffic flow and density as defined by Equation 3.12 and 3.13. Given the value of traffic flow and density in a time-space plane, the traffic flow speed can be further derived based on Equation 4.3.

$$v(x,t) = \frac{\frac{\partial N}{\partial t}\Big|_{(x,t)}}{-\frac{\partial N}{\partial x}\Big|_{(x,t)}} \tag{4.3}$$

It is assumed that buses move with traffic flow when they cruise between stops. Thus bus cruising speed equals to traffic flow speed. This assumption suggests that bus operators are in perfect compliance with bus control strategies and will not adjust bus speeds as they drive. This assumption is necessary and appropriate because it allows us to focus on the impact of road traffic conditions on holding strategy performance without perturbations caused by human factors which were identified to affect bus control efficiency (Abkowitz and Tozzi, 1987; Hill, 2003).

With bus speed equal to traffic speed as estimated by Equation 4.3, bus departure time and bus routes exogenously defined, bus trajectories can be updated with increment of bus speed multiplied by time step size.

Bus impact on traffic

Bus dwelling at stops can reduce road capacity which further affects road traffic conditions. The reduced road capacity, referred to as the bottleneck capacity or

passing rate, can be captured by restricting the maximum number of vehicles to overtake a dwelling bus. VMBus modifies the road capacity x^* by adjusting the cost function defined by Equation 3.18. The following revised cost function $\Theta^*(0, x^*, t)$ associated with wave speed $u = 0$ at x^* is introduced:

$$\Theta^*(0, x^*, t) = \begin{cases} q_M, & t \in \mathbb{M} \\ q_B, & t \in \mathbb{D} \end{cases} \tag{4.4}$$

during time $\mathbb{M}$ when buses move with the traffic flow, the capacity of the road is q_M; during the time $\mathbb{D}$ when buses dwell at a stop, road capacity is reduced to q_B. q_B is determined by various factors, such as reduced transport lanes due to bus dwelling in line with the traffic flow, and interruption of road traffic due to passengers crossing the road.

4.3.2 Implementation of bus holding strategies

Classical bus holding strategies are developed with the objective of regulating bus headways. Bus headway $h_{n,s}$ can be calculated as the arrival time difference between bus n and its forward bus $n-1$ as Equation 4.5.

$$h_{n,s} = t^A_{n,s} - t^A_{n-1,s} \tag{4.5}$$

Figure 4.2 presents trajectories of three buses $n-1$, n and $n+1$ cruising from start to stop s, dwelling at stop s, departing from stop s and cruising to the next stop. All buses enter into the route with an equal headway h^T. By the time buses arrive at stop s, their headways become $h_{n,s}$ and $h_{n+1,s}$. After bus loading time and holding time are applied at stop s, bus headways upon departure from the stop become $\tilde{h}_{n,s}$ and $\tilde{h}_{n+1,s}$. The notation $\tilde{}$ is used to denote the bus headway after bus holding time is applied.

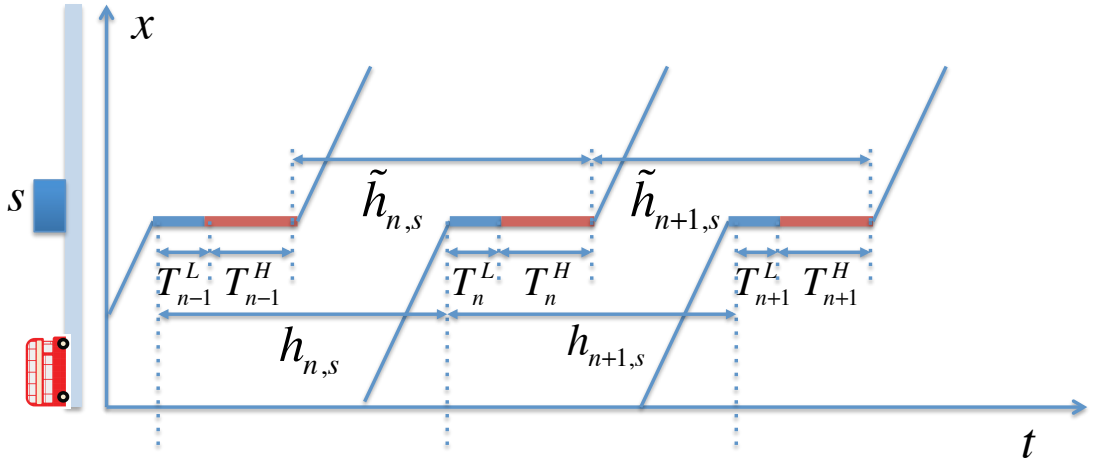

FIGURE 4.2: Bus control in a multi-modal system

The time-space paradigm of Figure 4.2 shows numerical relationship between $\tilde{h}_{n,s}$ and $h_{n,s}$ which is expressed by Equation 4.6:

$$\begin{aligned} \tilde{h}_{n,s} &= h_{n,s} + T^L_n + T^H_n - T^L_{n-1} - T^H_{n-1} \\ &= h_{n,s} + (T^L_n - T^L_{n-1}) + (T^H_n - T^H_{n-1}) \end{aligned} \tag{4.6}$$

where T^L_n is the loading time for bus n to board and disembark passengers and T^H_n is the holding time applied to buses depending on the adopted holding strategy. Equation 4.6 shows that changes of bus headway at stop s are determined by the loading time difference and the holding time difference of two following buses $n-1$ and n at stop s.

In an ideal scenario without any perturbation and the passenger demand is fixed, the bus headways are maintained constant at the target level h^T. All buses have the same loading time T^L and are held at bus stops for the same amount of time T^S, which is called the slack time. The slack time is used to adjust bus headways when they are deviated from the target headway. If buses operate with even headways equal to the target headways, they will be held at stops for the whole duration of slack times.

Bus dwell time T^D is the sum of loading time T^L and holding time T^H as $T^D = T^L + T^H$. Bus loading time T^L is directly related to the time between departure

of bus $n-1$ and arrival of bus n as Equation 4.7,

$$\begin{aligned} T^L &= \beta(h^T - T^D) \\ &= \beta(h^T - T^L - T^H) \end{aligned} \tag{4.7}$$

where β is a dimensionless parameter calculated by multiplying average passenger arrival rate for bus service and average loading rate per passenger. It measures the increase of bus dwell time at a bus stop due to one unit time increase of its headway with the leading bus.

Intuitively, different bus holding strategies can be visualized by Figure 4.3. Figure 4.3a shows that the forward holding strategy works on the green section of the paradigm. When the headway between bus n and its forward bus $n-1$ runs longer than the target headway, bus n should leave the bus stop earlier to catch up with its forward bus. Figure 4.3b shows that the backward holding strategy works on the red section of the paradigm. When the headway between bus n and its following bus $n+1$ runs shorter than the target headway, bus n should be held at the bus stop for longer time to wait for its following bus. Figure 4.3c shows that the two-way holding strategy works on both the forward and backward buses to balance the red section and the green section.

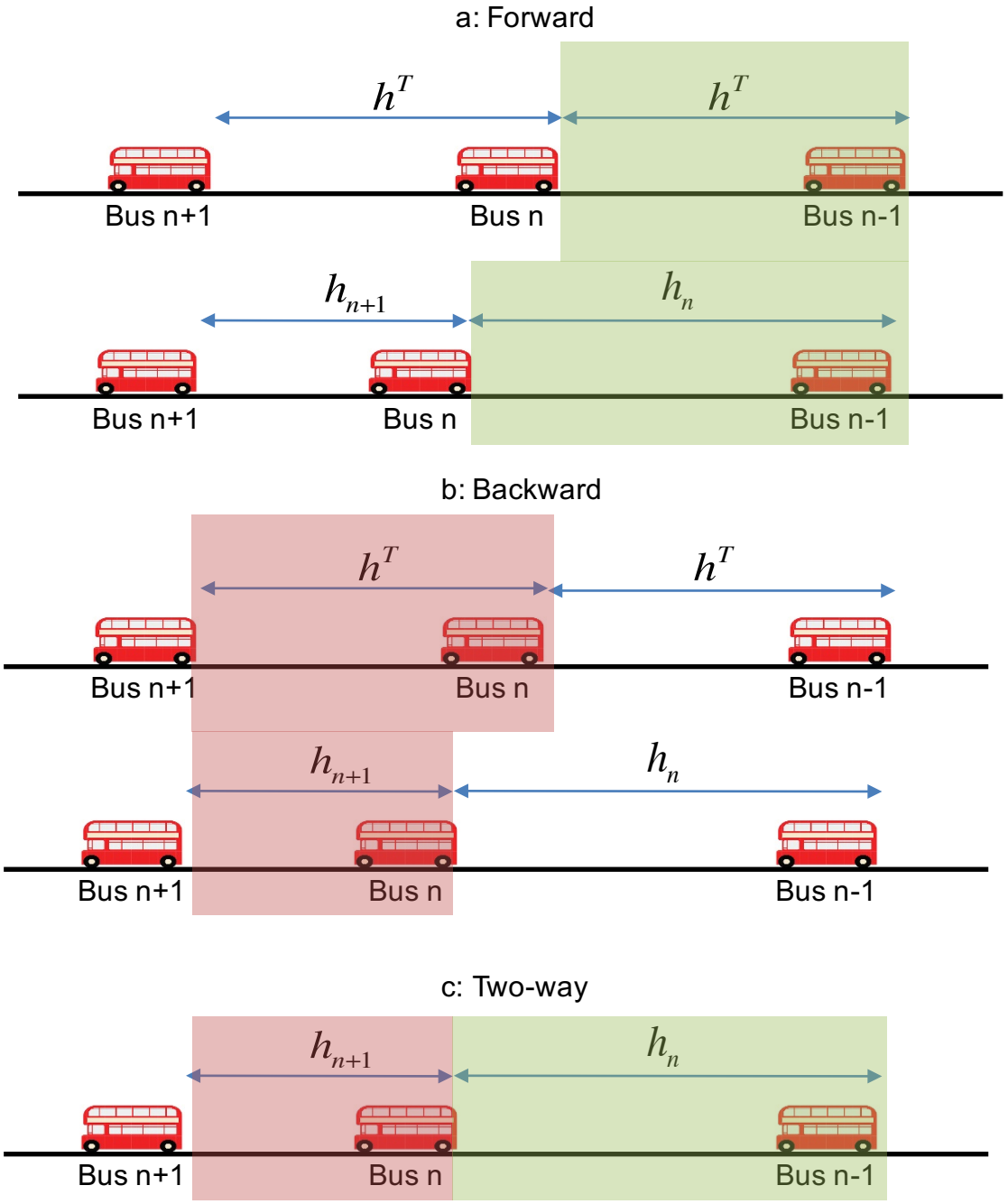

FIGURE 4.3: Illustration of bus control strategies

Forward holding strategy

The forward holding strategy is applied to regulate the bus service when there is a discrepancy ε between bus headway $h_{n,s}$ and the target headway h^T as Equation 4.8.

$$\varepsilon = h_{n,s} - h^T \tag{4.8}$$

Bus headway discrepancy is caused by interruptions along bus routes or at bus stops. It is considered as an exogenous variable here. A detailed discussion of various interruptions is carried out in Section 4.4.1.

Equation 4.7 calculates the bus holding time in the ideal scenario with equal bus headways. Given the new bus headway $h_{n,s}$ with discrepancy as specified by Equation 4.8, Equation 4.9 can be derived which calculates bus loading time in the non-ideal scenario,

$$\begin{aligned} T_n^L &= \beta(h_{n,s} - T_{n-1}^D) \\ &= \beta(h_{n,s} - T^L - T^H) \end{aligned} \tag{4.9}$$

Combining Equation 4.7 and 4.9, bus loading time difference due to their headway discrepancy can be calculated as Equation 4.10,

$$\begin{aligned} T_n^L - T^L &= \beta(h_{n,s} - h^T) \\ &= \beta\varepsilon \end{aligned} \tag{4.10}$$

It is assumed that only bus n is affected and no other buses experience any interruption. Therefore, bus $n-1$ operates as in an ideal scenario with $T_{n-1}^L = T^L$ and $T_{n-1}^H = T^S$. Inserting Equation 4.8 into Equation 4.6 gives Equation 4.11 which shows the bus headway discrepancy $\tilde{h}_{n,s} - h^T$ after bus n is held for time T_n^H,

$$\begin{aligned} \tilde{h}_{n,s} - h^T &= \varepsilon + T_n^L + T_n^H - T_{n-1}^L - T_{n-1}^H \\ &= \varepsilon + T_n^L + T_n^H - T^L - T^S \end{aligned} \tag{4.11}$$

Consider that the applied bus holding time T_n^H reduces headway discrepancy from ε to $(1-\alpha)\varepsilon$ as Equation 4.12,

$$\tilde{h}_{n,s} - h^T = (1-\alpha)\varepsilon, \qquad 0 < \alpha \leq 1 \tag{4.12}$$

where α is regarded as the control parameter to counteract bus headway discrepancy and stabilize bus service. Inserting Equation 4.12 and 4.10 into Equation 4.11 gives the bus holding time which can be expressed as Equation 4.13,

$$T_n^H = T^S - (\alpha + \beta)\varepsilon \tag{4.13}$$

Since Equation 4.13 calculates the amount of time to hold a bus in order to regulate its headway with its forward bus, this control method is called the forward holding strategy. Equation 4.13 is consistent with the forward holding strategy proposed by Daganzo (2009). After the forward holding strategy is applied in Scenario 2, bus headway discrepancy is reduced from ε to $(1-\alpha)\varepsilon$.

Backward holding strategy

The backward holding strategy proposed by Bartholdi III and Eisenstein (2012) with the aim to regulate bus service based on their backward headways. The backward headway is defined as the headway between bus n and its following bus $n+1$. The backward holding strategy is applied when bus n arrives at stop s and its backward headway $h_{n+1,s}$ is different from h^T as Equation 4.14 shows.

$$\varepsilon = h_{n+1,s} - h^T \tag{4.14}$$

After the holding time T_n^L is applied on bus n, updated $\tilde{h}_{n+1,s}$ can be calculated by Equation 4.15,

$$\begin{aligned} \tilde{h}_{n+1,s} &= h_{n+1,s} + T_{n+1}^L + T_{n+1}^H - T_n^L - T_n^H \\ &= h_{n+1,s} + (T_{n+1}^L - T_n^L) + (T_{n+1}^H - T_n^H) \end{aligned} \tag{4.15}$$

The backward control is characterised as a relatively simple holding strategy by not considering passenger demand at a bus stop (Argote *et al.*, 2012; Xuan *et al.*, 2011). Thus bus loading time is deterministic with $T^L_{n+1} = T^L_n$ and $T^L_{n+1} - T^L_n = 0$. Since the following bus of bus $n+1$ has a headway with $h_{n+2,s} = h^T$, bus $n+1$ does not need to be held at stop s and $T^H_{n+1} = T^S$. Consider that the backward holding strategy can reduce bus headway discrepancy from ε to $(1-\alpha)\varepsilon$ with $0 < \alpha \leq 1$. By inserting these equations into Equation 4.15, Equation 4.15 can be reformatted into Equation 4.16,

$$T^H_n = T^S + \alpha\varepsilon \tag{4.16}$$

Equation 4.16 calculates the applied bus holding time T^H_n based on the discrepancy between backward bus headway and the target headway.

When bus n arrives at bus stop s , bus $n+1$ usually has not arrived yet because bus n departs before bus $n+1$ and cruising times of the same bus route are relatively stable for two following buses. It is hence difficult to forecast the backward headway $h_{n+1,s}$ which cannot be physically measured due to the causality relationship. Bartholdi III and Eisenstein (2012) estimated the backward headway based on the distance between bus n and bus $n+1$ divided by an exogenously defined average bus speed. Argote *et al.* (2012) and Xuan *et al.* (2011) used the actual bus headway h_{n+1} associated with the closest upstream bus stop where both bus n and bus $n+1$ have arrived as a proxy for $h_{n+1,s}$. In Bartholdi III and Eisenstein (2012), the dwelling behaviour and traffic signal impact on bus commercial speed is not identified or considered. Therefore, the method to use the average bus speed proposed by Bartholdi III and Eisenstein (2012) is not adopted in this research. The method in Argote *et al.* (2012) and Xuan *et al.* (2011) is applied.

Two-way holding strategy

The two-way bus holding strategy aims at reducing the difference between forward bus headway and backward bus headway $h_{n,s} - h_{n+1,s}$. If $h_{n,s} - h_{n+1,s} > 0$, bus n will be held for a shorter time in order to reduce $h_{n,s}$. If $h_{n,s} - h_{n+1,s} < 0$, bus n

will be held for a longer time in order to increase $h_{n,s}$. Upon implementation of the two-way holding time on bus n, bus headway $h_{n,s}$ will change by $\alpha(h_{n+1,s} - h_{n,s})$. Thus, bus headway after holding time can be expressed as,

$$\tilde{h}_{n,s} = h_{n,s} + \alpha(h_{n+1,s} - h_{n,s}) \tag{4.17}$$

It is also known that $h_n - h_{n+1} = \varepsilon_n - \varepsilon_{n+1}$ as,

$$\begin{aligned} & h_n - h_{n+1} \\ =&(h_n - h^T) - (h_{n+1} - h^T) \\ =&\varepsilon_n - \varepsilon_{n+1} \end{aligned} \tag{4.18}$$

Inserting Equation 4.18 into Equation 4.17 gets Equation 4.19,

$$\tilde{h}_{n,s} = h_{n,s} + \alpha(\varepsilon_{n+1} - \varepsilon_n) \tag{4.19}$$

Equation 4.20 which calculates two-way bus holding time can be derived by inserting Equation 4.19 and 4.18 into Equation 4.6,

$$T_n^H = T^S - (\alpha + \beta)\varepsilon_{n,s} + \alpha\varepsilon_{n+1,s} \tag{4.20}$$

Equation 4.20 analytically shows that the two-way holding time is essentially a combination of forward and backward holding strategies. It can be seen that $-(\alpha+\beta)\varepsilon_{n,s}$ is the element in Equation 4.13 to calculate the forward holding time and $\alpha\varepsilon_{n+1,s}$ is the element to calculate the backward holding time in Equation 4.16.

Daganzo and Pilachowski (2011) proposed Equation 4.20 to calculate the bus holding time under the two-way control. The two-way bus holding strategy is considered as a more flexible control strategy since it can balance both forward and backward bus headways concurrently as bus n arrives at stop s. Thus, the

two-way holding strategy is more effective to improve bus regularity compared to the forward and backward holding strategy given the assumption that bus cruising time is deterministic and bus headways are independent from each other.

4.3.3 Performance indicators

The performance indicators measure bus service regularity with different bus holding strategies on the simulation platform. These indicators can be calculated from direct output of the VMBus platform.

Bus service regularity is measured at both route level and the stop level (Chen *et al.*, 2009). Route-level regularity is measured by journey time deviation. Stop-level regularity is indicated by headway variance. In a metropolitan area with a large demand of passengers and high frequency of buses, stop-level measurement is often used instead of the route-level indicator(Hunter-Zaworski, 2003).

Take $\bar{T^J}$ as the average journey time of all buses and $\bar{h}_s$ as the average headway of all buses at stop s, journey time deviation $\sigma(T^J)$ can be calculated by Equation 4.21 and headway deviation $\sigma(h)$ can be calculated by Equation 4.22,

$$\sigma(T^J) = \sqrt{\sum_{n=1}^{N} \frac{(T_n^J - \bar{T^J})^2}{N-1}} \tag{4.21}$$

$$\sigma(h) = \sqrt{\sum_{n=2}^{N} \frac{(h_{n,s} - \bar{h}_s)^2}{N-1}} \tag{4.22}$$

where T_n^J is the journey time of bus n travelling from start to the end of the route.

In addition to regularity indicators, traffic delay can also be calculated by the VMBus simulation platform to quantify transport system efficiency. Traffic delay is the difference between actual travel time and the travel time under the free-flow traffic condition. It can be calculated based on accumulative traffic inflow curve $N_I(t)$ and accumulative traffic outflow curve $N_O(t)$. With l denoting the distance

between the entrance and exit of a transport link, it takes $\Delta T = l/u$ time for free-flow traffic to travel through the link. By shifting $N_I(t)$ horizontally to the right by ΔT, $N'_I(t)$ can be derived which represents traffic arriving at the link exit without being delayed. The shaded region between $N'_I(t)$ and $N_O(t)$ represents total traffic delay during the time period between t_S and t_E.

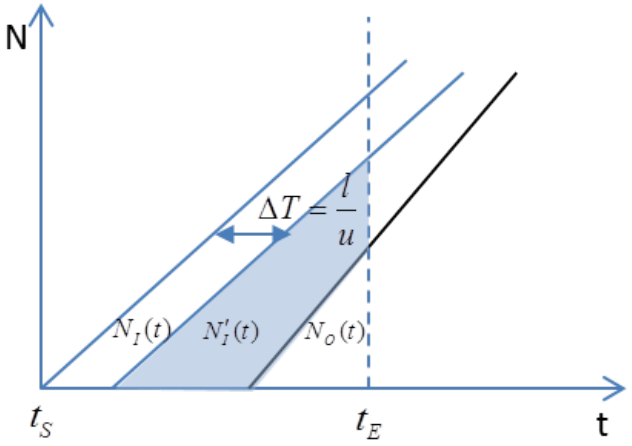

FIGURE 4.4: Representation of traffic delay

Total traffic delay can thus be calculated by Equation 4.23.

$$TD = \int_{t_S}^{t_E} (N'_I(t) - N'_O(t))dt \tag{4.23}$$

Since the primary output of VMBus simulation platform is N, Equation 4.23 can be directly solved with the simulation output. The average traffic delay can be calculated by dividing total traffic delay by the total number of vehicles.

4.3.4 VMBus simulation platform

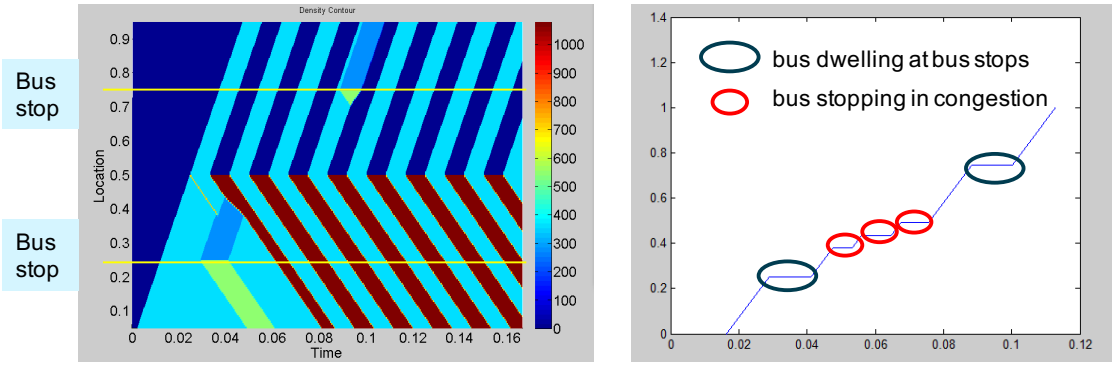

FIGURE 4.5: Sample output of the VMBus simulation platform

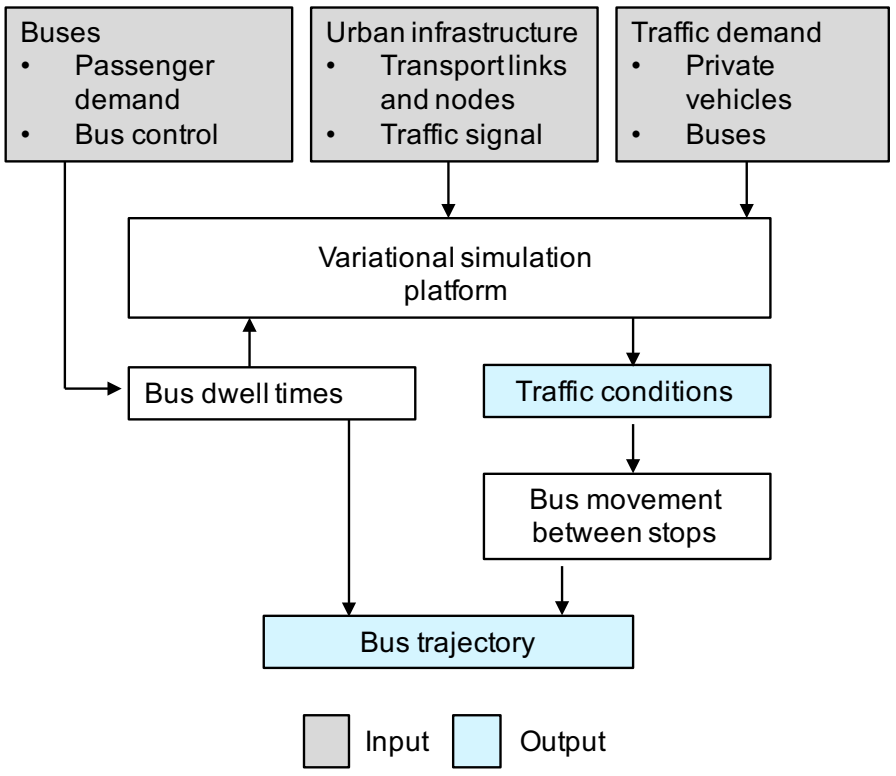

FIGURE 4.6: Components of the VMBus simulation platform

Figure 4.5 presents the sample output of the proposed simulation platform. The time-space density map of a bus route segment composed of two bus stops, one signalized junction and traffic demand at the saturation level. Traffic density distribution in a time-space plane is illustrated on the left side of Figure 4.5. The right side of Figure 4.5 presents the bus trajectory which includes the bus moving among the free-flow traffic, the bus dwelling at bus stops and the bus stopping in

the traffic due to traffic congestion. Bus speed and the associated trajectory are in agreement with an analytical solution worked out based on the LWR model.

Components of the VMBus simulation platform are illustrated in Figure 4.6 which documents details of simulation input, control factors and outputs. Traffic condition and bus trajectory outputs can be used to evaluate the transport system efficiency and bus performance under different bus holding strategies.

4.4 Evaluation of holding strategies

A range of numerical experiments are established and carried out on the VMBus simulation platform to understand and quantify bus service performance in a multi-modal transport system. Outputs from the proposed simulation platforms are studied and explained analytically based on the LWR model, the traffic bottleneck model and findings from other researchers. A detailed comparison with microscopic simulation outputs is not carried out in this research since the proposed simulation platform competes directly with the CTM-based simulation platform, not microscopic ones. Microscopic simulation calls for additional parameters such as predefined drivers' reaction factor which makes the comparison with macroscopic simulation unfair and invalid. Moreover, there is a lack of available commercial microscopic simulators for this research.

Section 4.4.1 presents a sensitivity analysis of the impact of different factors (passenger demand, level of saturation and road traffic characteristics) on bus service regularity and holding strategy effectiveness on improving bus regularity. Section 4.4.2 presents a comprehensive evaluation of the headway-based bus holding strategies in terms of their improvement in bus regularity, impact on bus commercial speed and the overall transport system efficiency.

4.4.1 Sensitivity analysis

This section explores bus regularity under different road traffic conditions and different levels of passenger demand. Passenger demands and road traffic conditions are considered as two major sources that lead to bus service irregularity (Adebisi, 1986; Strathman *et al.*, 2002; Turnquist, 1982; Schramm *et al.*, 2010; Bellinger, 2011). Turnquist (1982), Strathman *et al.* (2002) and Bellinger (2011) found out that highly dynamic passenger demand significantly increases bus headway deviation, especially during peak hours when passenger demand changes abruptly. Schramm *et al.* (2010) showed that bus service irregularity is also closely related to road traffic conditions which is the outcome of road traffic demand and traffic characteristics. Therefore, three major factors are identified to affect bus service regularity which are passenger deviation, road traffic demand and road traffic characteristics.

Different factors affect the bus service in different ways. With the combination of Equation 4.1, 4.2, the dynamics of bus arrival time at a bus stop can be expressed by Equation 4.24.

$$t^A_{n,s+1} = t^A_{n,s} + T^L_{n,s} + T^H_{n,s} + T^C_{n,s+1} \tag{4.24}$$

It can be seen from Equation 4.24 that bus arrival time and hence bus regularity at a bus stop are determined by bus loading time T^L, bus holding time T^H and bus cruising time T^C. Bus loading time T^L depends on passenger demand at the bus stop. Bus holding time T^H depends on the applied bus holding strategies. Bus cruising time T^C depends on the road traffic condition which results from the combination of road traffic demand and urban transport infrastructure.

Passenger demand with spatial deviation means that passenger loads at different bus stops are different. Passenger demand with temporal deviation means that passenger load at the same bus stop varies in time. Fixed traffic demand means that the traffic demand loaded into the bus route is stable in time. Stochastic traffic

TABLE 4.1: Evaluated factors on bus regularity

Passenger demand
• Spatial deviation • Temporal deviation
Traffic demand
• Fixed demand • Stochastic demand • Midblock inflow
Road traffic characteristics
• Passing rate • FD characteristics

demand means that traffic loaded into the bus route varies in time. Midblock inflow means that traffic can enter the bus route not only from the upstream boundary but also from the middle of the bus route. The passing rate is the same as bottleneck capacity. FD characteristics here specifically refers to the shape of deployed fundamental diagrams.

Section 4.4.1 first establishes a base case on the VMBus platform. To analyse the impact of each factor on bus regularity, this section evaluates the effect of passenger demand, traffic volume and transport link characteristics in terms of capacity and fundamental diagrams respectively. Specific factors selected to evaluate are listed specified in Table 4.1.

Test setting

The numerical test establishes a transport network of 2.5 miles in length which comprises 5 links and 4 intersections as shown in Figure 4.7.

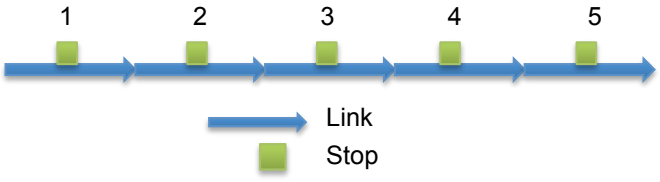

FIGURE 4.7: Configuration of the base case

It is assumed that the links are homogeneous with a common fundamental diagram of a triangular shape as shown in Figure 4.8. There are 2 lanes on the link, of which the saturation flow is $Q = 3600$ vph and the jam density is $\rho_J = 540$ vpm.

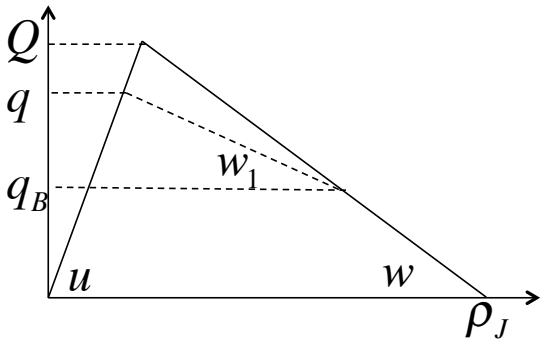

FIGURE 4.8: Fundamental diagram of experiment test

A total of 6 buses enter into the route at an initial headway of 2 minutes and travel from Link 1 to Link 5.

There is one bus stop located in the middle of each link with stop 5 being the terminal. When buses dwell at bus stops, the maximum traffic flow that can pass them is 1800 vph. It is equivalent to one-lane capacity (or $q_B/Q = 50\%$).

In order to understand the impact of each factor, multiple simulations are run with different settings. The consequential bus headway variance is analysed. In the base case, bus cruising time between stops is deterministic and bus loading time at each stop remains constant. This implies no deviation indeed in bus headways. The passenger demand is constant in time and space with $\beta = 0.18$. The traffic demand is fixed with $d/Q = 0.25$ so that bus cruising time between stops is constant at the free-flow level with no congestion on-site.

Passenger demand

Passenger demand deviation leads to unequal loading time for different buses at different bus stops which can further cause bus bunching along the route through affecting the term $T^L_{n,s}$ in Equation 4.24. Passenger demand deviation can be further classified as the spatial deviation or the temporal deviation. The spatial deviation means that passenger demands are different at each bus stop and thus

bus loading time is different among different stops. Temporal deviation means that, at the same bus stop, different passenger volumes vary and thus bus loading time is different for each bus.

With the assumption that passenger loading rate is constant, passenger demand deviation directly determines bus delay parameter β. This section changes the value of β deviation ($\sigma(\beta)$) in different tests while maintaining its mean value $\bar{\beta}$ constant. Other parameters as described in Section 4.4.1 remain unchanged.

Spatial deviation

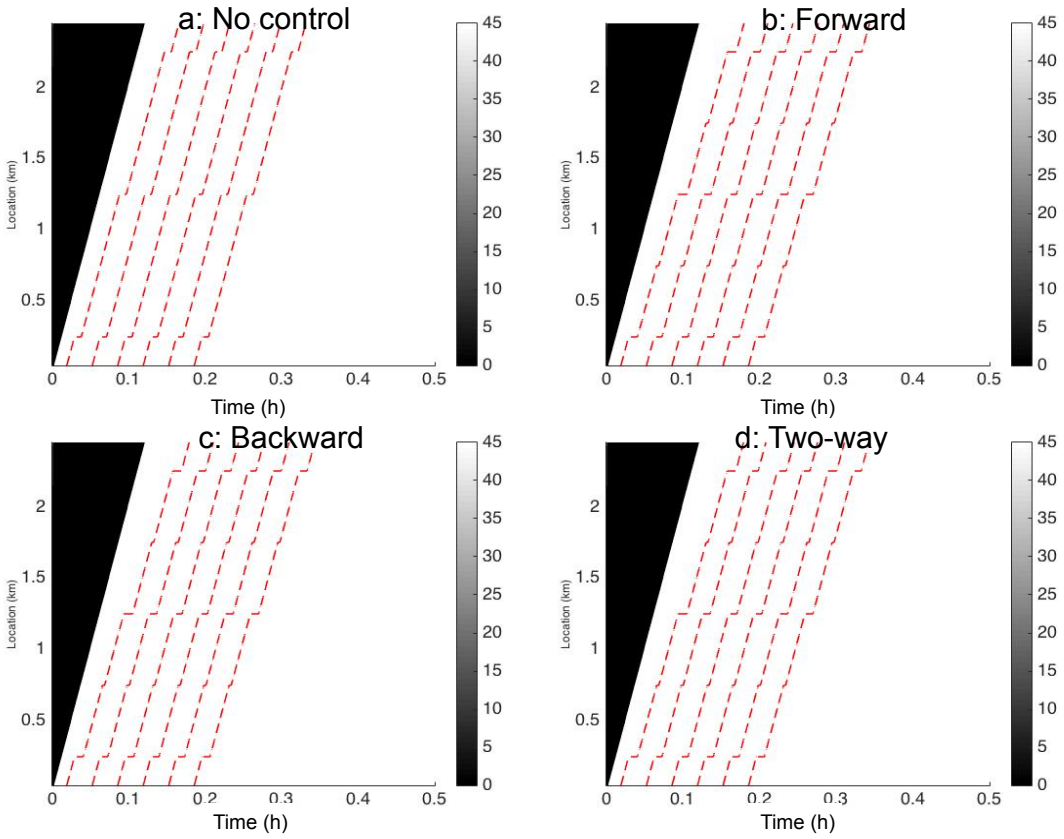

FIGURE 4.9: Bus trajectories with $\sigma(\beta_s)/\bar{\beta}_s = 1$

With the setting of spatial passenger demand deviation, passenger demand is altered at each stop with the total number of arriving passengers in the bus route remaining the same. In this case, $\sigma(\beta_s)/\bar{\beta}_s$ changes from 0 to 100% at 10% increment.

No headway deviation can be identified ($\sigma(h) = 0$) from the numerical output of simulation tests. Figure 4.9 shows bus trajectories in the most extreme case with $\sigma(\beta_s)/\bar{\beta_s} = 1$. Bus loading times at different stops are different due to the β_s changes. Since β_s remains the same for every bus arriving at stop s, all buses arriving at stop s have the same loading time. Without any headway variance, bus loading time is fixed as the slack time. Therefore, bus headway, which is determined by the differences in loading time and holding time as Equation 4.6 suggests, remains constant.

In general, spatial deviation in passenger demand generates a consistent change in loading time and arrival time of all buses which results in zero headway deviation.

Temporal deviation

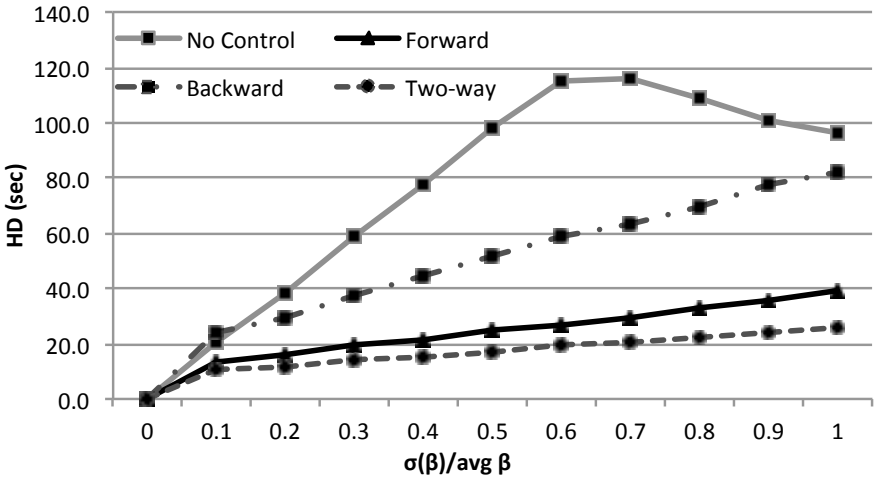

FIGURE 4.10: Bus headway variance with temporal passenger deviation

With temporal passenger demand deviation, $\beta_{n,s}$ changes as different arriving bus stop s. The value of $\sigma(\beta_n)/\bar{\beta_n}$ increases from 0 to 100% with a step size of 10% per test.

Figure 4.10 shows the headway deviation (HD) at stop 4 with different $\sigma(\beta_n)/\bar{\beta_n}$. Stop 4 is selected as it is the last stop for buses to load and disembark passengers before the terminal. Without any control, bus irregularity gets worse as they further travel down the route. Thus, bus headway deviation is the largest at

stop 4 compared to stop 1, 2 and 3. It is easier to identify holding performance difference in terms of improving bus regularity at stop 4.

From Figure 4.10, it can be seen that bus regularity is very sensitive to the temporal deviation of passenger demand. Bus HD equals to 0 when $\sigma(\beta_n)/\bar{\beta_n} = 0$. Without any bus holding strategy, HD increases to around 120 sec when $\sigma(\beta_n)/\bar{\beta_n} = 0.6$ or $\sigma(\beta_n)/\bar{\beta_n} = 0.7$.

It is worth noting that HD does not increase linearly as $\sigma(\beta_n)/\bar{\beta_n}$ grows. Bus HD peaks with $\sigma(\beta_n)/\bar{\beta_n}$ equal to 0.6 and 0.7 when buses become extremely bunched. As $\sigma(\beta_n)/\bar{\beta_n}$ increases higher, buses can overtake their leading buses at a bus stop in a multi-lane road. It helps alleviating the bus bunching phenomenon from the perspective of passengers at the next stop as their waiting time is reduced. This echoes the findings in Schramm *et al.* (2010) which recognize the contributory factory of bus overtaking capability in helping regulate bus service in the extreme case of bus bunching. Figure 4.11 shows bus HD in the no-control scenario without overtaking. It can be seen that bus HD increases monotonically as passenger temporal deviation grows.

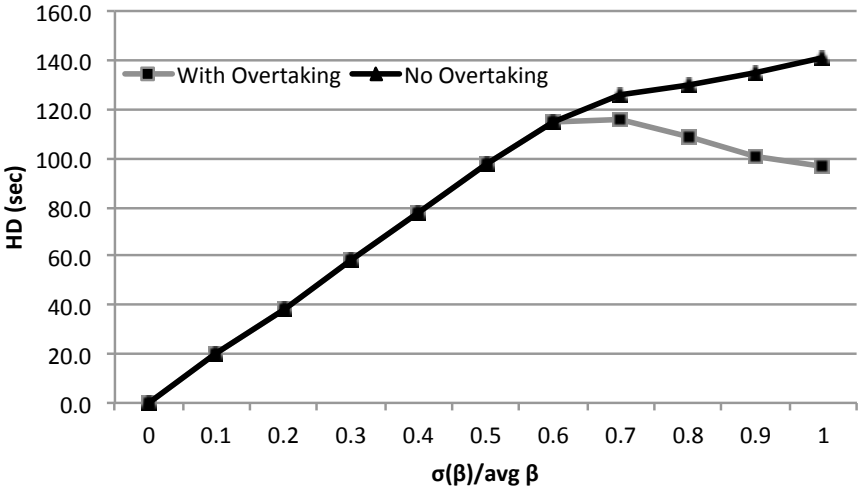

FIGURE 4.11: Bus headway variance with temporal passenger deviation

Bus holding strategy can significantly improve bus service regularity. Buses operated under the two-way control have the lowest HD. The forward control has

lower HD than backward control. Reasons for performance differences of bus holding strategies are further discussed together with other factors at the end of this section.

Degree of saturation

Since buses operate in a mixed flow and interact with the surrounding road traffic, their movement between bus stops depends on prevailing road traffic conditions. Saturation is a measure of traffic demand in terms of the road capacity. In a fully saturated road, the traffic demand equals road capacity. This section evaluates the impact of traffic demand on bus regularity from three aspects: a deterministic demand, a stochastic demand and a midblock turning-in traffic inflow.

Deterministic traffic demand

The base case test is carried out on the VMBus platform with varying traffic demands at fixed levels. Traffic demand is represented by the saturation ratio d/Q which increases from 0 to 100% at 10% increment.

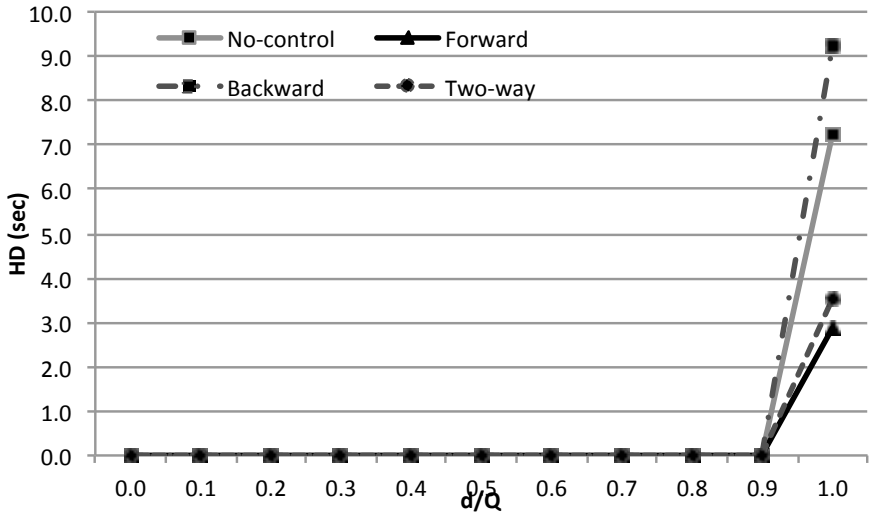

FIGURE 4.12: Bus headway deviation observed at Stop 4 under fixed traffic demands

Figure 4.12 shows HD deviation observed at Stop 4 under different traffic demands. It can be seen that buses operate with high regularity with $d/Q \leq 90\%$. When the road is fully saturated with traffic, bus movement is affected by the road traffic condition and the HD increases to 7.1 sec without any holding strategy.

It is interesting to observe that road traffic starts to affect bus regularity when the saturation is between 90% and 100%. As the saturation degree reaches a certain level, traffic jam formulated downstream of a dwelling bus can affect its following bus as shown in Figure 4.13. Triangles in Figure 4.13 represents time-space regions delayed by the dwelling bus.

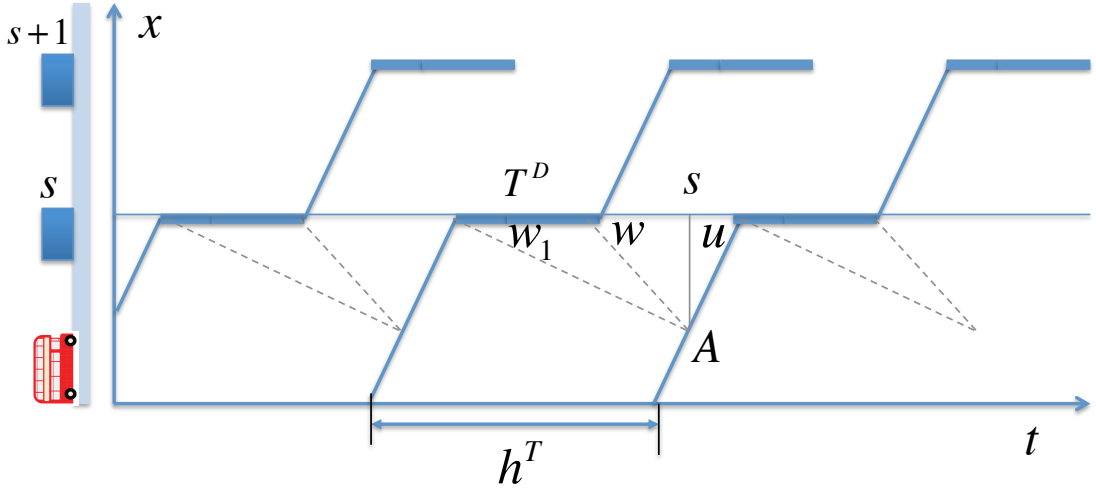

FIGURE 4.13: Traffic congestion region upstream of bus dwelling

The exact saturation ratio at which traffic delay affects bus regularity can be worked out analytically based on the LWR model. The road traffic is characterized by a triangular fundamental diagram as shown by Figure 4.14. If q is larger than q_B, vehicles following the dwelling bus are affected by the bottleneck to slowdown, stop or switch lanes. Characteristics of affected vehicles under the bottleneck impact propagates towards the upstream direction at the wave speed w_1 as show in Figure 4.14.

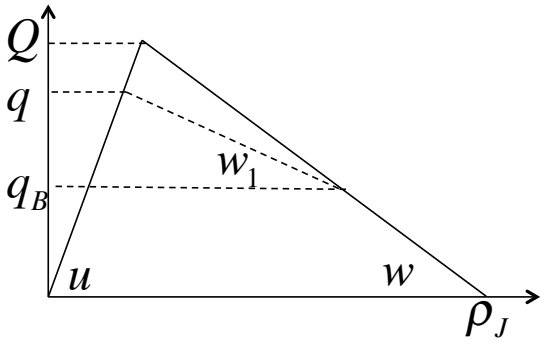

FIGURE 4.14: Base case fundamental diagram

The wave speed w_1 can be calculated by Equation 4.25 based on the triangular geometry presented in Figure 4.14,

$$w_1 = \frac{uw(q - q_B)}{wQ - wq + uQ - uq_B} \tag{4.25}$$

In the base case without any holding strategy, all the buses have holding times of zero and dwelling time $T^D = T^L$. Since $T_n^L = (h - T_{n-1}^D)\beta = (h - T_n^D)\beta$ as Equation 4.7 indicates, it can be derived that,

$$T_n^D = \frac{\beta h}{1 + \beta} \tag{4.26}$$

Denote the distance between point A and stop s as l_{AS}. Based on the paradigm geometry in Figure 4.13, the following two equations can be obtained:

$$\frac{l_{AS}}{w_1} + \frac{l_{AS}}{u} = h^T \tag{4.27}$$

$$\frac{l_{AS}}{w_1} - \frac{l_{AS}}{w} = T^D \tag{4.28}$$

By solving Equation 4.25, 4.26, 4.27 and 4.28, the critical traffic saturation ratio q_c/Q can be calculated by Equation 4.29. In this test, $q_B/Q = 0.5$ and $\beta = 0.18$, thus $q_c/Q \approx 0.92 \in (0.9, 1.0)$.

$$\frac{q_c}{Q} = \frac{1 + q_B\beta/Q}{1 + \beta} \tag{4.29}$$

The forward holding strategy performs better than two-way control with the lowest HD of 2.9 sec. The backward holding strategy has the highest HD of 9.2 sec. Reasons for performance differences of bus holding strategies are further discussed together with other factors at the end of this section.

Stochastic traffic demand

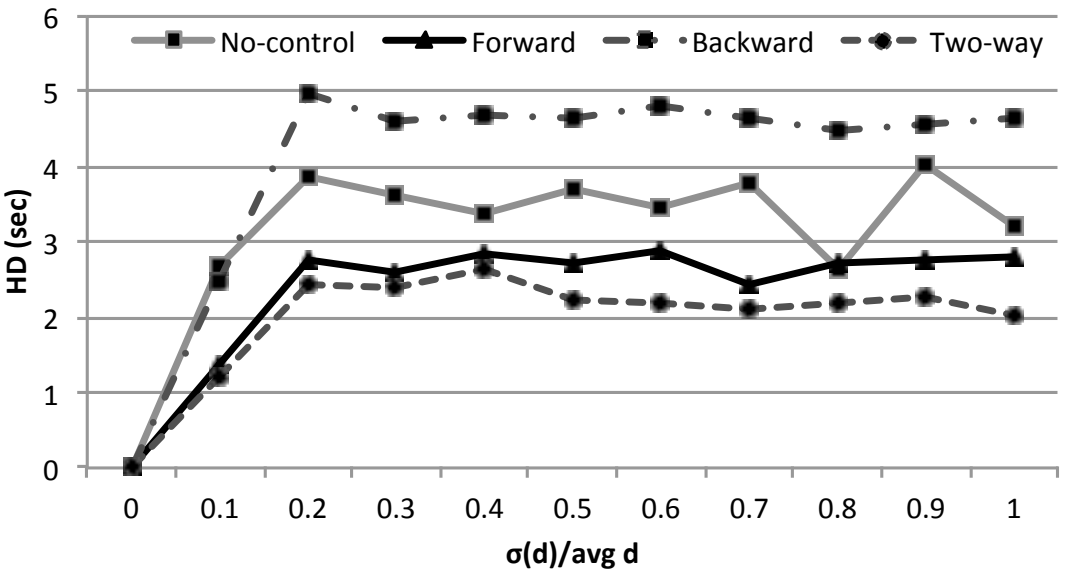

FIGURE 4.15: Bus HD under stochastic traffic demands

Stochastic traffic demands are loaded into the network in order to estimate bus regularity and holding strategy performance under dynamic traffic conditions. Mean traffic demand over the simulation period remains constant with $d = 1800$ (vph) or $d/Q = 50\%$. Standard deviation of traffic demand increases from 0 to 1800 mph with an increment of 180 mph. At each level of traffic demand deviation, the simulation test is run 20 times.

Figure 4.15 presents average bus HDs at Stop 4 of outputs from 20 simulation tests under stochastic traffic demands. It shows that dynamic traffic demand increases bus HD compared to the case of a fixed traffic demand. Bus holding strategies have relatively stable performances in regulating bus service compared to the no-control scenario. Two-way holding strategy has the lowest average HD of 2.25 sec which is 15.4 % lower than the forward holding strategy. The backward holding strategy has the longest HD. Reasons for performance differences of bus holding strategies are further discussed together with other factors at the end of this section.

Midblock traffic inflow

Figure 4.16 shows midblock traffic inflow d_I entering into the bus routes between Link 1 and Link 2. d/Q is maintained at 25% while inflow ratio d_I/Q increases from 0 to 100% at 10% increment.

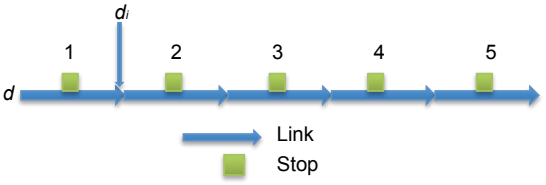

FIGURE 4.16: Configuration of midblock inflow

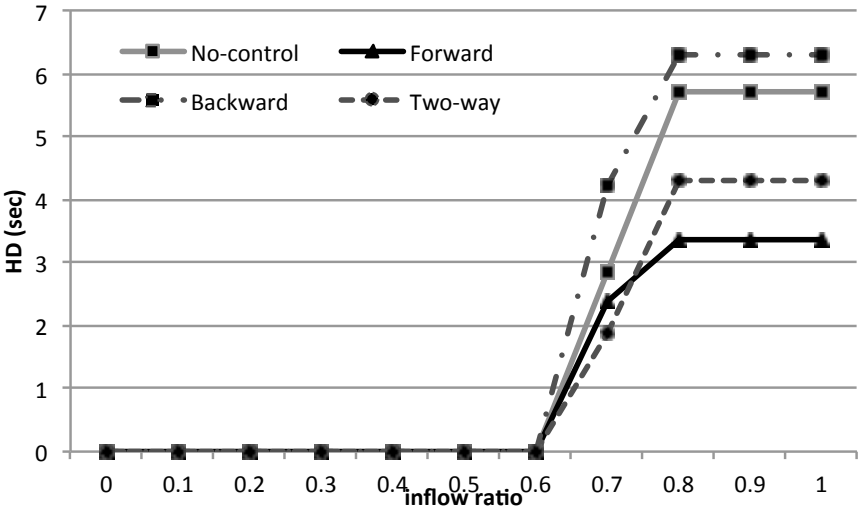

FIGURE 4.17: Bus HD with midblock traffic inflow ratios

Bus HD under different ratio of midblock inflows over saturation flow Q is presented in Figure 4.17. No impact of midblock inflow on bus regularity can be identified with $d_I/Q \leq 60\%$. As d_I/Q increases to 70%, the saturation ratio of combined traffic from the main arterial and the cross street is 95% which is higher than the critical ratio identified by Equation 4.29, which makes the bus service become unstable and bus HD increases. With d_I/Q higher than 75%, the road becomes fully saturated and no more vehicles can enter the main route. Thus,bus HD stabilizes at a relatively high level. The forward holding strategy is better than two-way holding strategy when the road is fully saturated with vehicles. The backward holding strategy is the worst with the highest HD. Reasons for performance differences of bus holding strategies are further discussed together with other factors at the end of this section.

Characteristics of traffic

In addition to the traffic demand, the characteristic of traffic is another factor

that determines road traffic conditions. The characteristic of traffic is expressed in terms of passing rate and FD shapes in this study. The passing rate determines the interaction between buses and their surrounding traffic during bus dwelling at bus stops. The FD shapes determines speeds of traffic flow and degree of dispersion which can affect bus cruising between stops.

passing rate

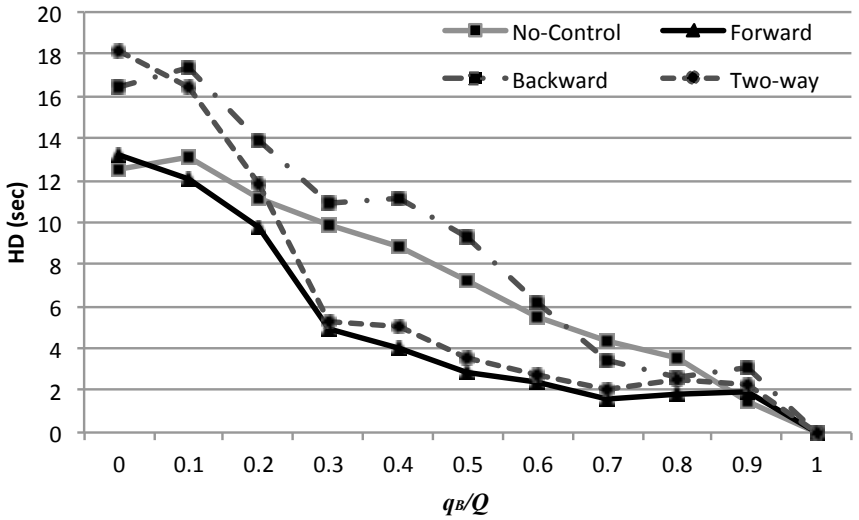

FIGURE 4.18: Bus headway variance with different passing rate

This study uses q_B/Q to measure passing rate levels which increases from 0 to 100% at 10% increment. Figure 4.18 shows bus headway deviation at different levels of passing rates. A decreasing trend can be identified as q_B/Q increases. With a higher q_B/Q, the increasing passing rate can allow more vehicles to overtake buses without being delayed. Thus there is less impact of bus dwelling at the stop on their surrounding traffic compared to low traffic.

The bottleneck is located at the bus stop during the time when buses dwell there. Figure 4.19 illustrates the impact of passing rate on buses and their surrounding traffic. The base case assumes that bus dwelling takes up one-lane space of a two-lane road as shown in Figure 4.19a. In this case, $q_B/Q = 0.5$. In the case with $q_B/Q = 1$, all vehicles can overtake dwelling buses without being delayed. Traffic flow becomes independent of bus loading or holding at bus stops. This scenario is equivalent to bus dwelling at bay stops which segregate them from the mainline

traffic as shown in Figure 4.19b. Bus dwelling at bus stops no longer affects road traffic. In the case of $q_B/Q = 0$, no vehicles can overtake buses. It is equivalent to a single-lane road where buses take up all the road space and vehicles have to queue behind buses as they dwell at bus stops as shown in Figure 4.19c. In this case, bus holding can worsen the road traffic condition and lead to further service irregularity.

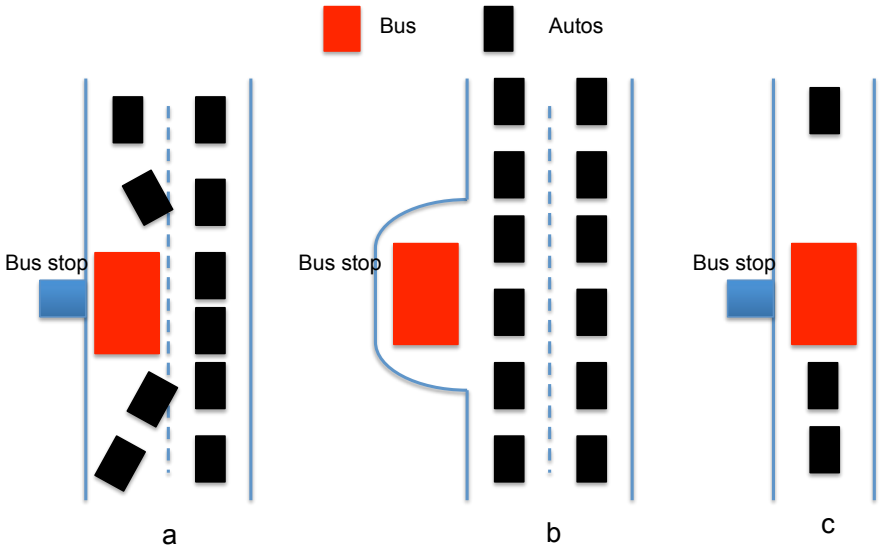

FIGURE 4.19: Impact of different passing rates on buses and surrounding traffic

The forward bus holding strategy is the best to regulate bus service with the lowest average HD of 5.0 sec. It is 21.9% lower than the average HD under the two-way holding strategy. The backward strategy is the worst in terms of bus service regularity. Reasons for performance differences of bus holding strategies are further discussed together with other factors at the end of this section.

Shape of fundamental diagram

This section evaluates the impact of different shapes of FD on bus service regularity. To the best of our knowledge, there have been no prior studies on the relationship between different FD shapes and bus service regularity. Section 3.4.2 shows that the VMBus platform can effectively capture different degrees of platoon dispersion by piecewise linear FDs with multiple segments. This section is based on Section 3.4.2 by further evaluating how buses are affected by different FDs.

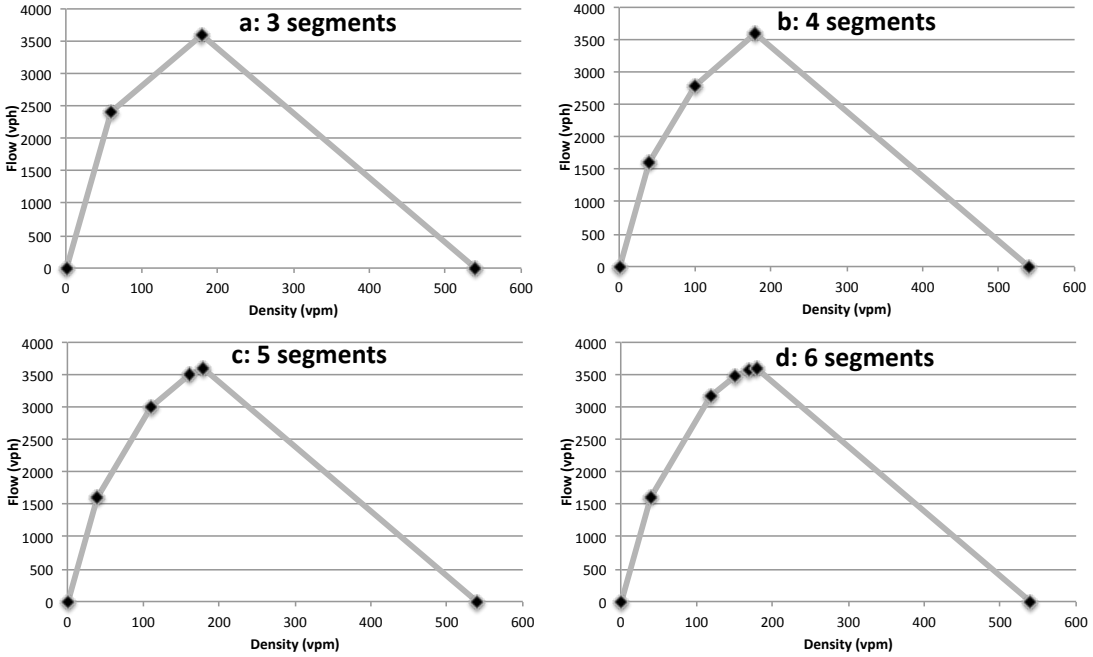

FIGURE 4.20: Specification of piecewise linear FDs with multiple segments

Different multi-segment FDs to be tested are shown in Figure 4.20. In order to eliminate impacts of other factors and focus on the shape of FD, several parameters including the saturation flow, jam density and backward wave speed all remain the same across different FDs as illustrated by Figure 4.21. Table 4.2 lists the parameter specifications of different FDs.

TABLE 4.2: Summary of different FD specifications

Case	**Wave speed (mph)**	**Cost rate (vph)**	**Critical density [1] (vpm)**
3-segment FD	[40 10 -10]	[0; 2700]	90;270
4-segment FD	[40 20 10 -10]	[0 900 2700]	30;90;270
5-segment FD	[40 20 10 5 -10]	[0 400 950 1350 2700]	20;55;80;;90;270
6-segment FD	[40 20 10 5 2 -10]	[0 400 990 1365 1620 2700]	20;59;75;85;90;270

Figure 4.22 shows the average HD under different control strategies with different FDs. A peak of HD can be observed with the 3-segment FD, especially under the no-control scenario. Since FD determines bus cruising speed, it indicates that bus cruising time under the 3-segment FD has the highest deviation compared to that

[1]The term critical density here is different from the traditional one used in triangle FD which divides forward wave speed and backward speed. The critical density here refers to the density which divides two different wave speeds.

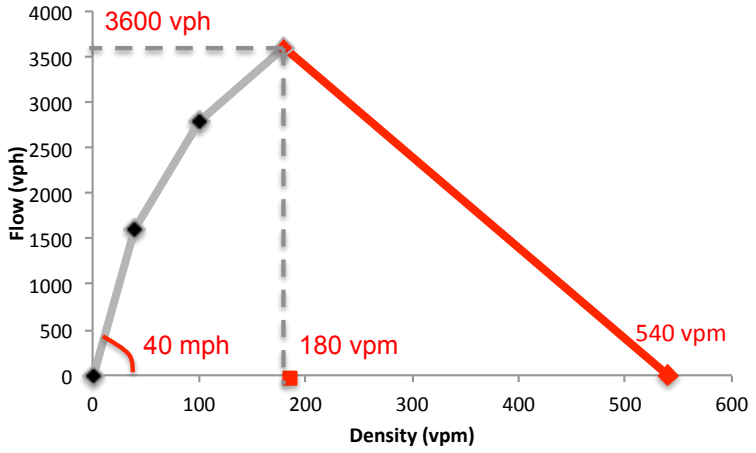

FIGURE 4.21: Fixed parameters of multi-segment FDs

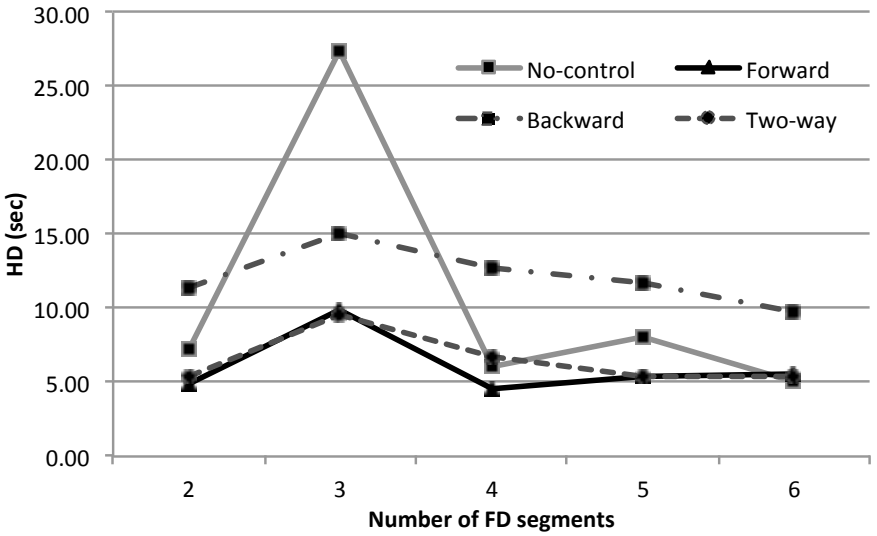

FIGURE 4.22: Bus HD with multi-segment FDs

of other FDs. Table 4.3 presents the deviation of dwelling time and cruising time in the no-control scenario. It can be seen that the average dwelling time deviation for the 3-segment FD is 3.1 sec and the average cruising time deviation is 14.1 sec. Deviation of bus cruising time is significantly higher than deviation in bus dwelling time because FDs strongly affect road traffic characteristics. Thus different FD specifications can generate greater impact on bus cruising time in the road than bus dwelling time at bus stops.

The 3-segment FD leads buses to operate with the highest cruising speed deviation compared to other FDs because of the associated platoon dispersion effect. Compared to the 3-segment FD, the 2-segment FD allows buses to instantaneously

TABLE 4.3: Average deviation of dwelling time and cruising time (sec)

Number of FD Segments	Deviation of dwelling time					Deviation of cruising time				
	Stop 1	Stop 2	Stop 3	Stop 4	Avg	Stop 1-2	Stop 2-3	Stop 3-4	Stop 4-5	Avg
2	0.8	1.0	1.0	1.4	1.0	0	0	0	0	0
3	0.8	2.7	4.2	4.8	3.1	12.3	13.9	15.1	15.3	14.1
4	0.8	0.8	0.4	1.1	0.8	0.5	2.8	5.3	6.6	3.8
5	0.6	0.8	1.2	1.8	1.1	1.7	2.2	2.2	2.2	2.1
6	0.6	0.8	0.8	0.8	0.7	2.4	2.9	2.4	2.5	2.6

reach the equilibrium free-flow speed after they departure from bus stops. In this case, bus cruising speed deviation is 0 and there is no variance in bus cruising time. When the FD has more than 2 segments, buses can have various cruising speeds.This research assumes that the free-flow speed[2], the saturation flow, the critical density[3] and the jam density are the same for each FD in every test. Therefore, the upper boundary and the lower boundary of bus cruising speed is fixed at 40 mph and 20 mph ($Q/\rho_k = 20$) respectively. With more segments in the FD free-flow section, buses can change between the boundary speeds more smoothly with more transitioning speeds. This contributes to lower bus cruising speed deviation. Thus, the 3-segment FD has the highest cruising speed deviation compared to 4-segment, 5-segment and 6-segment FDs. In general, the 3-segment FD has the worst performance in regulating buses and the 2-segment (triangular) FD has the best.

Figure 4.22 also shows that bus holding strategies can reduce the impact of FD shapes on bus regularity. The forward holding strategy and the two-way holding strategy can achieve similar bus service regularity which is better than the backward holding strategy and the no-control scenario.

Discussion

Table 4.4 compares bus regularity with different holding strategies under the impact of different factors as listed in Table 4.1. The notation "=" and "≈" mean equivalent or similar performance on regularity. The strategy on the left of the

[2]the speed associated with the lowest range of density

[3] the density associated with the switching point from forward wave speed to backward wave speed at constant levels

TABLE 4.4: Comparative performance ranking

Passenger demand	
• Spatial deviation	For = Two = Back = No
• Temporal deviation	Two > For > Back > No
Traffic demand	
• Fixed high demand	For > Two > No > Back
• Stochastic demand	Two > For > No > Back
• Midblock inflow	For > Two > No > Back
Traffic characteristics	
• Passing rate	For > Two > No > Back
• Multi-segment FDs	For ≈ Two > No > Back
Note: = means equivalent performance; > means better performance	

notation ">" has a better performance on regularity compared to the one on the right.

It can be seen that spatial deviation of passenger demand at different bus stops alone does not cause bus service irregularity. All holding strategies and the no-control scenario have the same HD which equals to 0.

With the incorporation of stochasticity as in the case of temporal deviation of passenger demand and stochastic demand of road traffic under low traffic saturation, the two-way holding strategy achieves lower HDs compared to the forward holding strategy. The two-way holding strategy considers both forward bus headway and backward bus headway as indicated by Equation 4.20. This makes it more flexible and hence more effective to regulate bus headways than forward or backward holding strategy, especially when bus holding does not affect their following buses under the prevailing traffic congestions. This finding is consistent with research results from Hounsell *et al.* (2008*b*), Daganzo and Pilachowski (2011) and Argote *et al.* (2012).

In the case of temporal deviation of passenger demand with low road traffic demand, the backward control can improve bus regularity compared to the no-control scenario since the bus speed is constant with the free-flow traffic condition. This

justifies the assumption in Bartholdi III and Eisenstein (2012) to use a constant bus speed in estimating the backward bus headway. However, if the bus speed becomes unstable with stochastic traffic demands or high saturation level, the backward holding strategy becomes ineffective.

Table 4.4 also shows that when the road traffic is in a heavy condition, either caused by high road traffic demand (the case of fixed high demand of road traffic and the case of midblock inflow) or limited road capacity (the case of passing rate), the forward holding strategy outperforms the two-way holding strategy and the backward holding strategy is not effective. This difference of bus holding strategy performance can be explained by bus holding effect on their following buses in a heavy traffic condition. Both the two-way holding strategy and the backward holding strategy use the estimated headway of their following (backward) bus to calculate the holding time to apply to the current bus. Equation 4.20 can be reformatted as Equation 4.30 which shows that the holding time of two-way control can be broken down into the holding time to regulate forward headway discrepancy and the holding time to regulate the backward headway discrepancy.

$$T_n^H = T^S - (\alpha + \beta)(h_n - h^T) + \alpha(h_{n+1} - h^T) \tag{4.30}$$

Based on Equation 4.30, Equation 4.31 shows the analytical relationship between two-way holding time and forward holding time.

$$T_n^H|_{\text{Two-way}} = T_n^H|_{\text{Forward}} + \alpha(h_{n+1} - h^T) \tag{4.31}$$

It can be seen the last term $\alpha(h_{n+1,s} - h^T)$, which is the only factor that differentiates calculation of bus holding time under two-way control from the forward control, causes the control performance difference. This term suggests that if the backward headway between bus n and its following bus $n+1$ is longer than the target headway with $h_{n+1} - h^T > 0$, bus n will be held for a longer time for $\alpha(h_{n+1} - h^T)$.

However, the actual effect of the term $\alpha(h_{n+1} - h^T)$ can be opposite to its original intention to regulate buses. If the road traffic is heavy and congestion delays bus n, this leads to $\alpha(h_{n+1} - H) > 0$. In this case, the objective of holding bus n for longer time is to reduce h_{n+1}. However, bus n dwelling for extra time can further reduce road capacity and worsen traffic conditions. For high-frequency bus routes with short headways, it is quite possible for the following bus $n+1$ to be trapped in traffic congestion with further delay which increases the backward headway h_{n+1}. This effect is the opposite as the objective to reduce h_{n+1}. Thus, the term $\alpha(h_{n+1} - h^T)$ to increase holding time of bus n fails to shorten its headway with bus $n+1$. Similarly, if $(h_{n+1,s} - h^T) < 0$ and bus n is held for shorter time to increase headway h_{n+1}, reduced traffic impact on bus $n+1$ movement could shorten h_{n+1} instead. In general, the term $\alpha(h_{n+1} - h^T)$ which considers the backward bus headway can reduce bus service regularity under congested traffic conditions.

4.4.2 Evaluation of holding strategies

Upon understanding sensitivity of bus HD with different factors in Section 4.4.1, this section aims to evaluate bus holdings strategies more comprehensively from various aspects including: bus journey time, traffic delay and journey time deviation.

Test setting

Bus route configuration of the simulation test is the same as the base case as in Section 4.4.1. A total of 4 scenarios are carried out in order to fully evaluate holding strategy performance and its impact on the surrounding traffic. Different scenarios vary from each other in terms of road traffic demand and passenger demand dynamics. The passenger demand is temporally dynamic so that it can create bus bunching in order to fully evaluate holding strategy effectiveness and impact. On top of the initialized mean value of the passenger demand, a stochastic term is added in different scenarios. Specific information regarding each scenario is presented in Table 4.5. The road traffic of different volumes is loaded into the

network in different tests. The standard deviation of stochastic traffic demand is 25% of its mean value. The standard deviation of stochastic passenger demand is 25% of its mean value as well. The passing rate is fixed at $q_B/Q = 50\%$

TABLE 4.5: Specification of test scenario

	Scenario 1	Scenario 2	Scenario 3	Scenario 4
Traffic Load	Deterministic	Stochastic	Deterministic	Stochastic
Passenger demand	Deterministic	Deterministic	Stochastic	Stochastic

In each scenario, 5 cases are tested with the average underlying traffic load d at 0 vph, 900 vph, 1800 vph, 2700 vph and 3600 vph, of which d/Q ratios are 25%, 50%, 75% and 100% respectively.

Average bus journey time

Bus average journey time (AJT) is used in this section to evaluate bus system efficiency.

Figure 4.23 compares bus AJTs of different cases with underlying traffic. It can be observed that ATJ is not sensitive to the increase of traffic demand when $d/Q \leq q_B$. With $d/Q > q_B$, bus AJTs become longer and commercial speeds become slower as d/Q increases.

The no-control case has the lowest AJTs compared to the case with holding strategies as buses are not held at bus stops for regularity control. Among different holding strategies, the forward holding strategy has the shortest AJT. The two-way holding strategy has the longest AJT.

Average traffic delay

The average traffic delay is used to measure impact of different bus holding strategies on the road traffic.

Figure 4.24 illustrates the average delay of road traffic incurred in different scenarios. A consistent trend of increasing total delay can be observed with the increase of road traffic load. If d/Q ratio is smaller or equal to 50% of road capacity, which

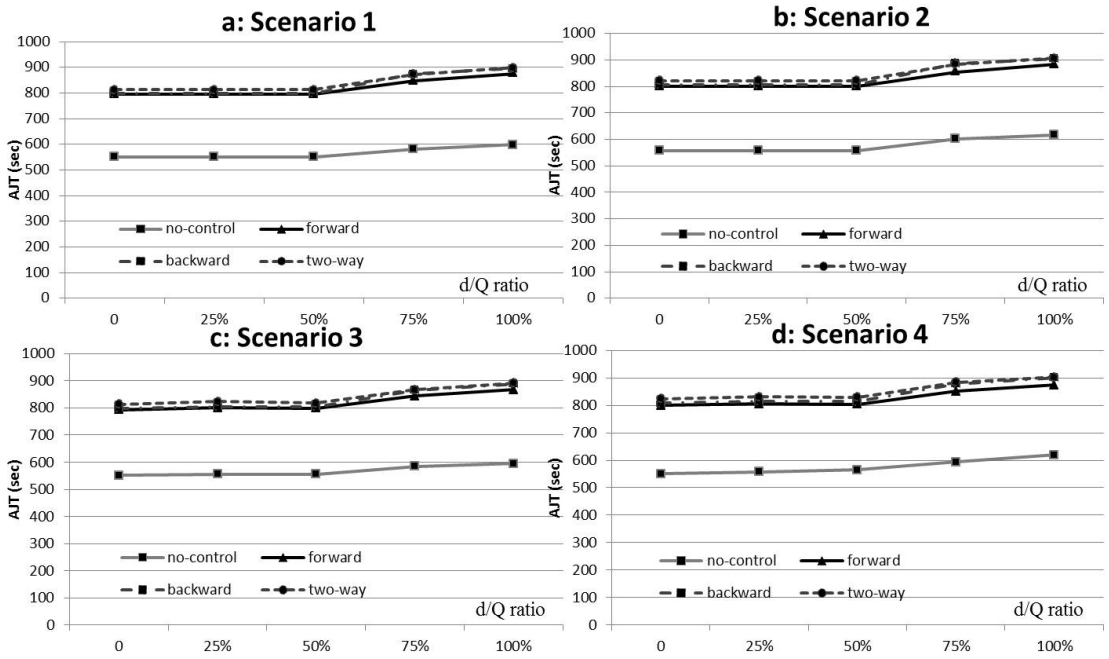

FIGURE 4.23: AJT of buses with underlying traffic

is the passing rate, traffic flow can surpass dwelling buses at bus stops without getting delayed. The average traffic delay is thus 0. When $d/Q > q_B$, average traffic delay increases as the road traffic demand grows.

It can be seen that average delay in the no-control scenario is the lowest. Among different bus holding strategies, the two-way control leads to the longest average delay and the forward control the shortest. Average delay under the forward control is 12.3% shorter than the average delay under two-way control and 10.1% shorter than the average delay under the backward control.

Deviation of bus journey times

Bus journey time deviation (JTD) is used to measure bus service regularity at the route level.

Figure 4.25 shows JTDs with different underlying traffic loads. A general trend can be observed that JTD decreases with the increase of road traffic volume when $d/Q > q_B$. This is because of the fact that the bottleneck effect can slow down the traffic following a dwelling bus. It makes a bus unlikely to bunch into its leading bus due to the traffic congestion. Thus, the overall JTD is reduced. When

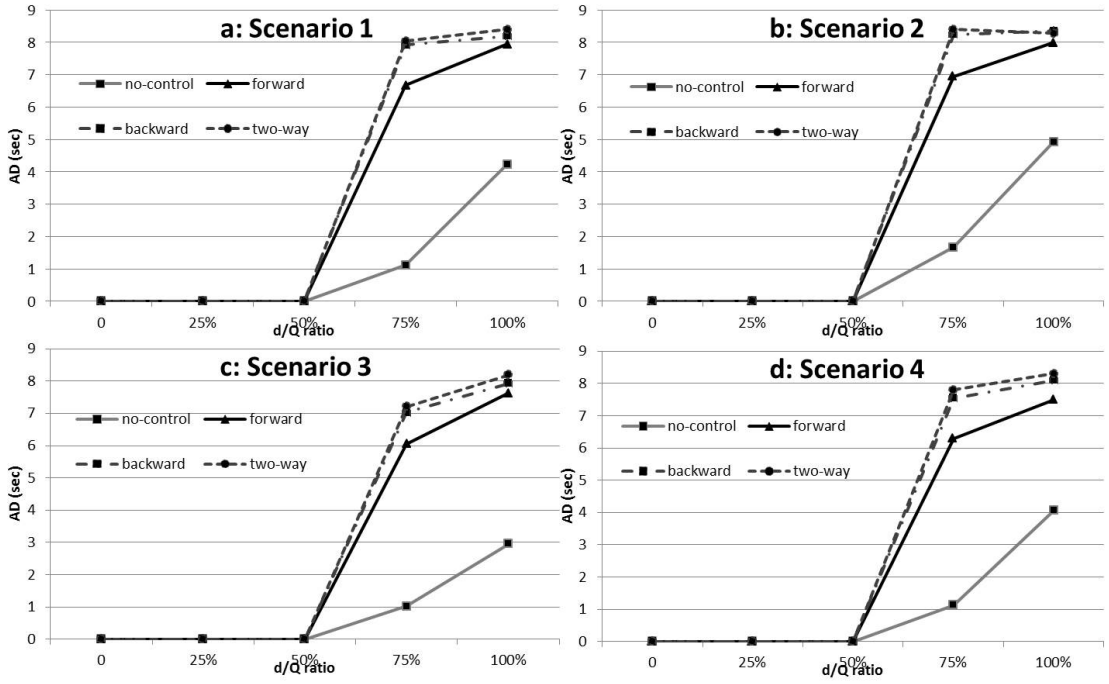

FIGURE 4.24: Average traffic delay of different scenarios

$d/Q \leq q_B$, JTD is relatively stable with the change of road traffic volume. However, the non-monotonic lines of the no-control JTD in Scenario 2 and Scenario 4 suggest that passenger demand deviation at bus stops can significantly affect bus irregularity at the route level without any bus holding control.

The two-way holding strategy is the most effective strategy to regulate the bus service with the lowest JTD at different levels of the road traffic volume. With $d/Q \leq q_B$, JTD under the forward control is 23.0% less than that under the backward control on average. However, when $d/Q > q_B$, no significance can be observed between the forward and backward holding strategies.

Deviation of bus headways

Headway deviation (HD) is often used as the performance metric of bus regularity at stop level. HD can be calculated by Equation 4.22. Effectiveness of different holding strategies is evaluated and compared at different traffic levels.

Performances of different bus holding strategies are related to the underlying traffic demand volumes. Figure 4.26 shows HD at the low-traffic level with $d/Q = 25\%$

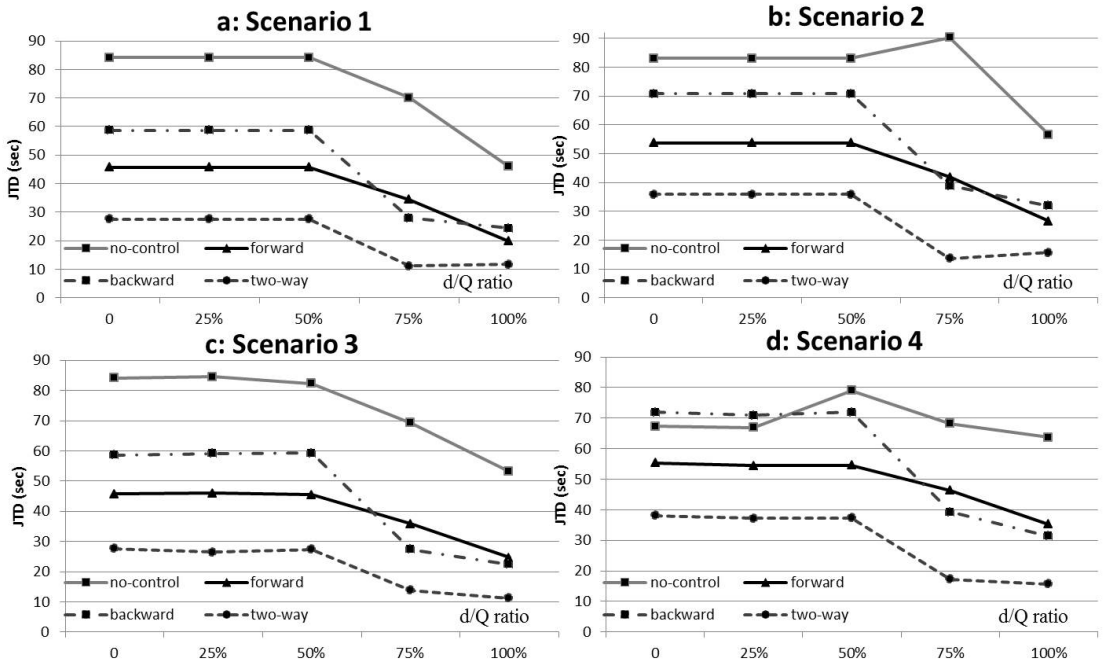

FIGURE 4.25: JTD of bus operation with different traffic loads

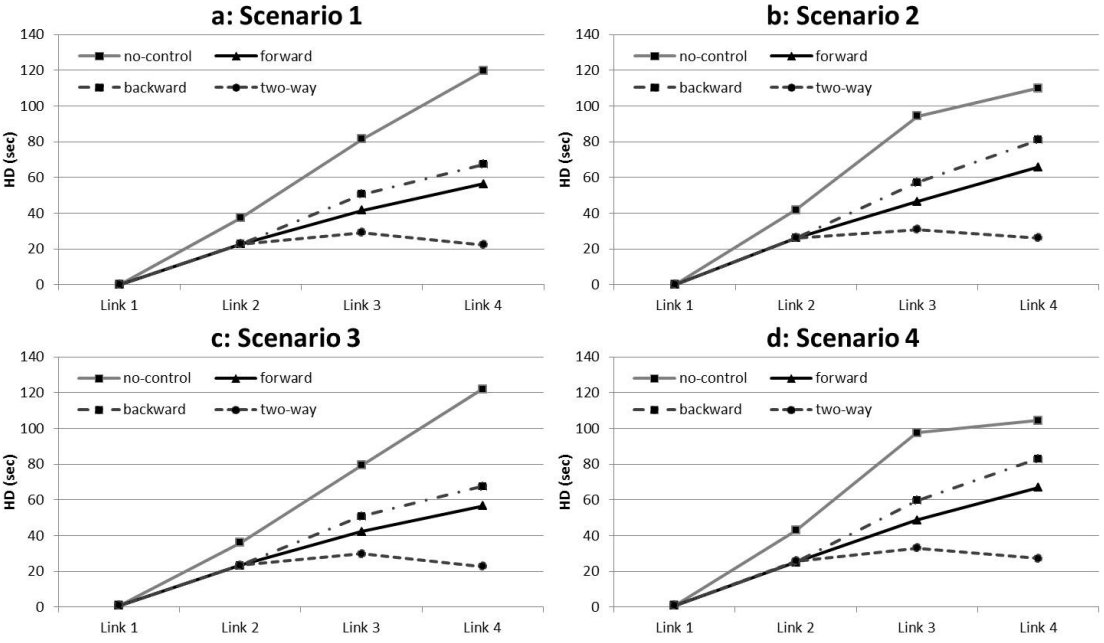

FIGURE 4.26: HD of buses operation with $d/Q = 25\%$

before buses reach their destination. From Figure 4.26, it can be seen that the two-way holding strategy is most effective to regulate bus service at the stop level. The two-way holding strategy can also prevent HD from getting larger as buses travel along the route. In comparison, an increasing trend of HD along the bus route can

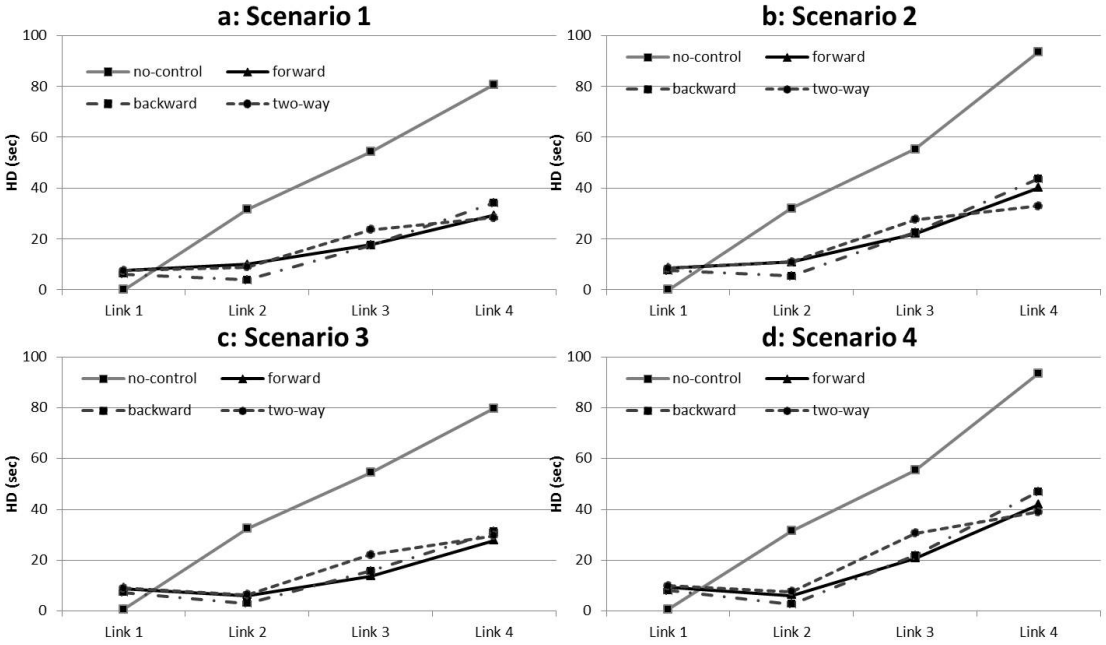

FIGURE 4.27: HD of buses operation with $d/Q = 75\%$

be observed in the forward control, backward control and no-control cases. HD at the high-traffic level with $d/Q = 75\%$ is presented by Figure 4.27. There are no clear differences among performances different holding strategies. An increasing trend can be observed in all cases. In general, with the road traffic volume lower than the passing rate, the two-way holding control is the most effective strategy in regulating bus service at the stop-level. The forward holding control is the second, and the backward control the third. With $d/Q > q_B$, control performances of the forward holding strategy and the two-way holding strategy are similar in reducing bus HD.

Discussion

Section 4.4.2 evaluates various dynamic headway-based bus holding strategies with consideration of underlying traffic demand and dynamic passenger demand, as suggested by Daganzo and Pilachowski (2011), it is necessary to have a *'a systematic understanding'* of *'more complex scenarios'* which involves *'demand and cruising speeds'*.

Table 4.6 summarises the impact of different bus holding strategies on bus service regularity and transport system efficiency.

TABLE 4.6: Impact of different bus holding strategies

	Performance comparison
Average journey time	No > For > Back > Two
Traffic delay	No > For > Back > Two
Deviation of bus journey times	Two > For > Back > No
Deviation of bus headways (low-traffic level)	Two > For > Back > No
Deviation of bus headways (high-traffic level)	Two ≈ For ≈ Back > No
Note: > means better or more efficient	

At the low-traffic level when bus cruising time is not affected by road traffic conditions, the two-way holding strategy works the best to improve bus service regularity. This agrees with previous research findings as in Daganzo and Pilachowski (2011) and Argote *et al.* (2012) which assumed bus cruising speed to be independent of road traffic conditions. With a low traffic volume, the two-way control works better than forward control which is better than the backward control.

Moreover, it is shown that the forward holding strategy is similar to the two-way holding strategy in improving bus service regularity at the high-traffic level. This can be explained by the aforementioned traffic impact on bus regularity as discussed in Section 4.6. This study also complements previous evaluation studies from perspectives of route-level regularity and transport efficiency. Forward holding strategy demonstrates better results, average delay and AJT compared to the two-way holding strategy under all these evaluation metrics.

4.5 Real-world application

Tottenham Court Road (TCR) in central London is selected as the real-world test bed to evaluate different bus holding strategies. Configuration of the transport

FIGURE 4.28: Bus stops in TCR (1:10000)

links, junctions, signal timing plan and traffic demand are the same as in Section 3.5.

There are 7 different bus routes travel throughout TCR which are Bus 10, 14, 24, 29, 73, 134 and 390. For simplicity, they are referred as Route 1 to Route 7 as specified in Table 4.7.

Bus target headways at each stop are between 5 to 8 minutes from 8:00 to 21:00 according to TfL website[4]. There are 4 bus stops in the selected road section which are TCR stop, Percy Street stop. Goodge Street stop and Warren Street stop as indicated by Figure 4.28.

[4]https://tfl.gov.uk/travel-information/timetables/

TABLE 4.7: TCR Bus route ID

Route ID	Actual route number
1	10
2	14
3	24
4	29
5	73
6	134
7	390

In the simulation test, a total of 49 buses are loaded into the network with an initial headway of 1 minute. Buses of different routes enter the network in a fixed cyclical order from Route 1 to Route 7. There are 7 buses for each route and their initial headways are fixed at 7 minutes.

Passenger demand at bus stops is assumed to be stochastic with $\bar{\beta} = 0.18$ and $\sigma(\beta)/\bar{\beta} = 25\%$. The simulation test runs 20 times for each of the control strategy and the no-control scenario. Average results of outputs from 20 tests are presented in this section which measure the transport efficiency and bus regularity under different holding strategies in a real-world environment.

Bus efficiency

AJT of different bus routes are presented in Table 4.8. Without any holding strategy, Route 1, 3 and 4 have the shortest AJTs between 244 and 248 sec. Route 2 and 6 have the longest AJT around 273 sec. Different bus routes have different AJTs to travel through TCR due to actual traffic conditions and signal timing plan. The average value of bus journey time of all routes is 256 sec. Bus holding strategies increase bus AJT and reduce their commercial speed.

TABLE 4.8: AJT of TCR bus route under different holding strategies (sec)

	Route 1	Route 2	Route 3	Route 4	Route 5	Route 6	Route 7	Route Average
No-control	244	274	245	248	250	273	260	256
Forward	283	280	257	248	257	279	269	267
Backward	359	377	368	371	385	381	348	370
Two-way	291	292	278	258	265	290	285	280

Different holding strategies result in significantly different AJTs. The forward holding strategy operates buses the fastest with the 267-second AJT. It is consistent with findings from Section 4.4.1 that the forward holding strategy operates buses with the highest efficiency. It is 13 sec (5%) lower than the AJT achieved by two-way holding strategy and 93 sec (25%) lower than the backward holding strategy.

Buses operated under the backward holding strategy have significantly longer AJTs. This is due to the heavy road traffic and delay from traffic signal control which extend bus headways to be larger than the target headway. Thus, it leads to the control term $h_{n+1,s} - h^T > 0$ and buses are held for longer time. Therefore, the backward holding strategy results in the longest AJTs compared to other holding strategies.

Average traffic delay

Average delays of road traffic in the main arterial and cross streets are presented in Table 4.9. Similar results as Section 4.4.1 and 4.4.2 can be observed that the

TABLE 4.9: Average traffic delay on TCR under different holding strategies (sec)

	Main arterial	Cross streets	Whole TCR
No-control	89	34	52
Forward	89	34	52
Backward	92	34	53
Two-way	89	34	52

forward holding strategy causes the least traffic delay compared to the two-way and the backward holding strategy.

As the backward holding strategy has the longest holding time, it causes the longest delay to the road traffic which is 3 sec longer per vehicle than the forward holding strategy and the two-way holding strategy.

Journey time deviation

TABLE 4.10: JTD of the bus routes under different holding strategies (sec)

	Route 1	Route 2	Route 3	Route 4	Route 5	Route 6	Route 7	Route Average
No-control	54	53	40	42	61	42	54	49
Forward	35	55	44	37	59	38	47	45
Backward	48	42	48	67	37	34	51	47
Two-way	29	44	41	31	51	29	40	38

All holding strategies show improvement of route-level regularity with lower JTD compared to the non-control scenario. The two-way holding strategy is the most effective strategy which reduces JTD from 49 sec in the no-control scenario to 38 sec. JTD under the forward holding strategy is 2 sec lower than that under the backward holding strategy.

Headway deviation

Table 4.11 shows HD of different routes under different control strategies. It can be seen that the Warren Street stop, the two-way holding strategy has the lowest HD which is 60 sec compared to the 68-second HD in the no-control scenario at the Warren Street stop. The forward holding strategy works slightly better than the backward holding strategy with 1 sec lower in HD.

TABLE 4.11: TCR bus route HD under different holding strategies (sec)

Strategy	Stop	Route 1	Route 2	Route 3	Route 4	Route 5	Route 6	Route 7	Route Average
No-control	TCR	0	0	0	0	0	0	0	0
	Percy	14	7	6	11	5	8	5	8
	Goodge	32	60	48	55	31	25	38	41
	Warren	83	77	63	65	70	61	58	68
Forward	TCR	0	0	0	0	0	0	0	0
	Percy	15	7	5	11	5	8	5	8
	Goodge	29	61	48	55	31	25	38	41
	Warren	48	74	76	61	71	61	57	64
Backward	TCR	0	0	0	0	0	0	0	0
	Percy	10	11	10	18	7	12	7	11
	Goodge	48	45	68	76	35	40	37	50
	Warren	73	67	69	77	47	60	61	65
Two-way	TCR	0	0	0	0	0	0	0	0
	Percy	15	7	5	11	5	8	5	8
	Goodge	29	61	48	55	31	25	37	41
	Warren	45	71	77	55	70	48	51	60

It is interesting to note that reduction of bus HD achieved by different holding strategies is about 4% to 12% lower compared to the no-control scenario in the TCR environment. This rate is not as significant as the 50% reduction in Section 4.4.2 which is based on a hypothetical bus route. This performance variance can be explained by the complexity of the real-world environment in TCR which has more dynamic road traffic during the peak hour and the existence of traffic signal plan. For example, there are three intersections with inflow traffic and dynamic signal timing between the Goodge Street stop and the Warren Street stop. All these disruptions can affect bus service regularity at the Warren Street stop and compromise effectiveness of bus holding strategies.

4.6 Conclusion

This chapter presents an analysis of bus holding strategies with consideration of surrounding traffic. This study complements and differentiates from previous studies such as Daganzo (2009), Daganzo and Pilachowski (2011), Argote *et al.* (2012) and Cats *et al.* (2012). These differences originate from the incorporation of underlying road traffic conditions and bus interaction with their surrounding traffic

which affect the effectiveness of bus holding strategy based on the proposed VMBus platform. Moreover, this research also expands previous evaluation framework by Cats *et al.* (2012), Argote *et al.* (2012) and Toledo *et al.* (2010) by taking into consideration more evaluation indicators. Bus holding strategies are assessed from the perspectives of non-public users sharing the road and the route-level regularity. Forward holding strategy demonstrates the best performance under these criteria compared to two-way and backward holding strategies.

This chapter first documents the development of the VMBus simulation platform which is used to evaluate bus service regularity under different bus holding strategies and road traffic conditions. Various dynamic headway-based bus holding strategies are implemented on the VMBus simulation platform to evaluate their effectiveness in bus regularity improvement and impact on transport efficiency.

It is shown that forward strategy can operate buses with the highest service efficiency and least delay impact on the surrounding road traffic than the backward and two-way holding strategy. If the road traffic volume is low and does not affect bus movement, two-way control is the most effective strategy to improve bus regularity. However, at the high-traffic level, performance of the forward holding strategy in terms of regulating bus headways is similar to the two-way control and backward control.

Findings from this research motivate the development of more innovative bus holding strategies which are responsive to different road traffic conditions in order to effectively improve bus service regularity without compromising bus commercial speeds or causing significant urban traffic delay.

Chapter 5

Signal-based control

5.1 Introduction

This chapter presents a set of signal-based bus holding strategies with the objective of improving bus service regularity through transit signal management in an urban traffic control system.

A comparative evaluation of different proposed control strategies is carried out on the VMBus simulation platform to systemically analyse their performance. Signal-based control strategies were also compared with stop-based holding control and iBus priority control to identify their advantages and disadvantages. Findings based on numerical results generated by the VMBus platform are discussed.

Section 5.2 presents the background and motivation for the proposed study. Section 5.3 documents the development of proposed signal control rules and strategies. Section 5.4 implements the proposed control strategies on the VMBus simulation platform and evaluates their performance with a hypothetical network. Section 5.5 validates the proposed holding strategy in a real-world setting. Section 5.6 concludes this chapter.

5.2 Background

5.2.1 Stop-based holding strategies

In order to improve bus service regularity, bus stops are frequently selected as the control points where bus holding strategies are applied (Turnquist, 1981; Eberlein *et al.*, 2001; Cats *et al.*, 2012; Xuan *et al.*, 2011; Fu and Yang, 2002). The length of holding time is usually dependent on headway discrepancies and predefined slack time.

Stop-based holding control strategies insert predefined slack time at each stop control point. In order to ensure effectiveness, the slack time is set to be sufficiently large so that calculated bus holding time is always positive to be applied in practice. To meet this condition, the selected slack time value is calculated as the upper boundary of the headway variance in Daganzo (2009). As Section 4.6 concludes, the introduction of slack time significantly increases bus journey time and reduces bus commercial speed. Furthermore, conventional scheduled-based holding control builds the slack time into the bus schedule time table which results in buses being held even if their journeys have no disruptions.

Section 2.4.1 identifies that stop-based holding strategies are developed with the assumption that bus cruising speed in the road is deterministic or independent from the prevailing road traffic conditions (Turnquist, 1981; Eberlein *et al.*, 2001; Cats *et al.*, 2012; Xuan *et al.*, 2011; Fu and Yang, 2002; Daganzo, 2009). There is little research to establish an effective bus holding strategy in the context of an integrated multi-model transport system with consideration of bus-traffic interaction. When the road is congested, bus holding at in-line stops can lead to further traffic delay and even adversely affect their following buses.

To mitigate the challenges of stop-based bus holding strategies, a range of innovative signal-based control strategies have been proposed to apply bus holding through traffic signal adjustment. Performance of the proposed bus control strategies is compared with the stop-based holding strategy in Section 5.4.2.

5.2.2 iBus

The iBus system is developed and operated by TfL for the purpose of continuous location monitoring and management of London buses. The iBus system detects bus location through an onboard Global Positioning System (GPS) every second and stores the location information locally in the bus. This onboard device of iBus also carries out the communication function between buses and a central server by sending out bus location information every 30 seconds. Based on the received real-time bus location information, bus service performance is evaluated and compared with a benchmark so that bus control actions can be derived.

Since the initiation of the iBus project in 2003, the iBus has been used mainly for improving bus service efficiency through priority assignment in London transport system. Bus control and management are carried out by iBus in corporation with SCOOT Urban Traffic Control (UTC). The system architecture which integrates iBus and UTC allows traffic signal priority to be responsive to real-time bus dynamics. Components of the iBus system and related transport infrastructure are illustrated in Figure 5.1. Empirical data have shown that iBus can enhance bus service efficiency. TfL (2006) reported that the bus journey time saving is between 4 to 9 seconds at each junction with the iBus system.

Recent development of the iBus system is to assign differential priorities rather than the unified priority to buses which are running late behind their schedules as identified by Hounsell *et al.* (2009) in the Nearctis project. Differential priority control assigns priority to buses based on their degree of lateness(Gardner *et al.*, 2009). iBus and SCOOT work together to implement the differential priority strategy through signal adjustment as illustrated in Figure 5.2. iBus monitors bus trajectory information at an interval between 30 sec to 60 sec and reports bus arrival time at a bus stop. This information is used to determine bus priority level. Upon receiving the bus priority levels, SCOOT sends out specific control actions to either extend the green light or to recall the green light early in order to prioritize target buses. The advantage of differential priority is to increase bus

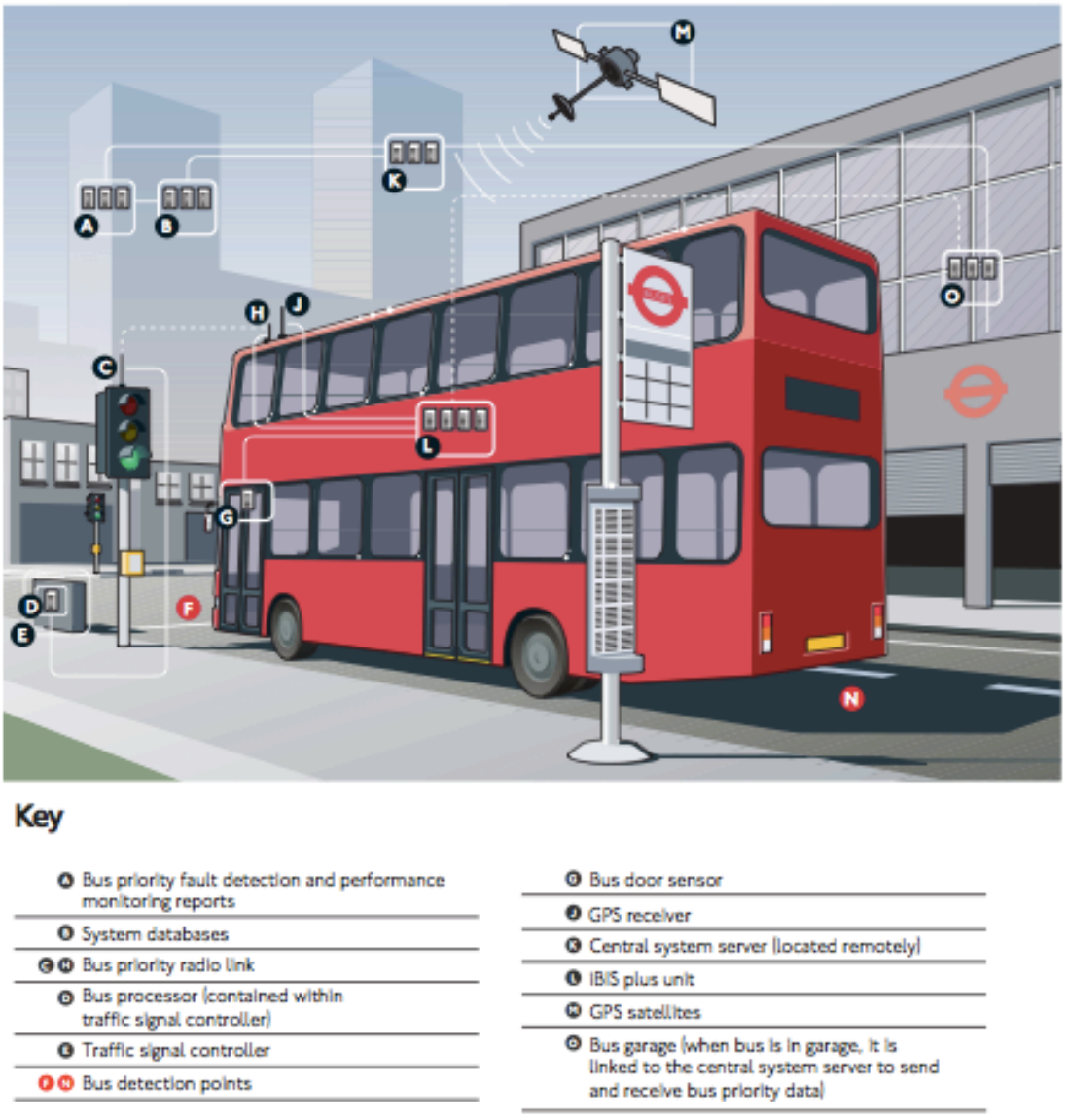

FIGURE 5.1: iBus architecture for bus priority. Source: TfL (2006)

efficiency without severely delaying other vehicles sharing the road together. It can also improve bus service regularity and reduce passenger waiting time.

There are two main ways to determine the priority level which are mainly based on either bus schedule adherence or headway discrepancy compared to the target headway. Other factors that contribute to the priority level include the bus importance factor as perceived by users and road-specific requirement set up by various stakeholders such as policy makers and site engineers (Gardner *et al.*, 2009). In Hounsell *et al.* (2008*a*) and Hounsell *et al.* (2008*b*), the priority level is calculated based on bus headway comparison with the target headway as bus headways are

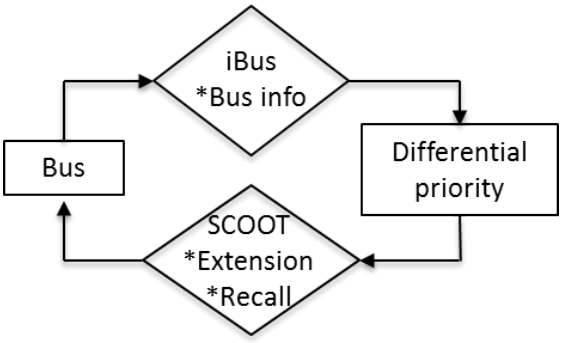

FIGURE 5.2: Implementation of differential priority by iBus and SCOOT

more related to high-frequency urban buses. D'Souza *et al.* (2010) claimed that at present iBus can classify up to 4 priority levels as indicated by Table 5.1. Numerical tests also suggested that bus operations experienced increased delay savings and reduced standard deviation of bus headways when late buses receive high priority and other buses do not receive any priority.

TABLE 5.1: Differential priority levels of iBus

Priority Level	Criteria	Implemented control
0	Early buses	No control
1	Buses on time	Extension
2	Buses with slight delay	Extension and recall
3	Buses with severe delay	Extension and recall

Compared to the automatic process to derive iBus-based priority strategies, iBus-based strategies to reduce bus bunching and improve service regularity rely on a manual process which is labour intensive and subject to human biases. The iBus system is leveraged in presenting bus information through the visualization of their location information. After the central server receives bus location information, it presents buses in a digital time-space map. If buses of the same route become close to each other on the map, bus bunching is identified by the bus controllers and corresponding regularity control strategies will be applied (Bellinger, 2011). Bus controllers are usually former bus drivers who determine the appropriate control strategy to apply based on their previous bus driving experience. Each controller is in charge of 1 to 3 bus routes depending on route frequency. Various

regularity improvement strategies to apply include bus holding, stop skipping and curtailment.

In conclusion, the iBus system is used primarily in cooperation with London UTC to monitor buses and reduce bus delays through automatic traffic signal extension and recall. The proposed signal-based control strategies leverage the iBus infrastructure in detecting bus locations and derive bus holding strategies through traffic signal adjustment. Therefore, they are responsive to real-time bus dynamics and road traffic conditions. Performance of the proposed bus control strategies is compared with the iBus differential priority strategy in Section 5.4.2.

5.3 Control rules

There are various ways to adjust signal timings. These specific control ways are called control actions in this research, and they are the basic elements of signal-based control strategies.

This section first identifies the basic control actions that can be applied through traffic signal adjustment. The signal-based holding strategies are then developed by integrating different control actions and control objectives.

Section 5.3.1 describes the fundamental control actions which can be applied to adjust traffic signals. Section 5.3.2 proceeds with developing signal-based holding strategies which incorporate different control actions and control objectives.

5.3.1 Control actions

Green extension

Green extension is applied to prioritize buses which are detected at the end of an upstream approach and about to lose their right of way due to signal change. The green phase is thus extended to allow the controlled buses to travel through the signalised junction. The green extension is a common action deployed by

iBus and London UTC to assign priority to buses (Gardner *et al.*, 2009). It is of significant value for short road or bus stops located close to traffic signals. Figure 5.3 demonstrates the extension of green light for the length of Δg_e from the original signal timing plan.

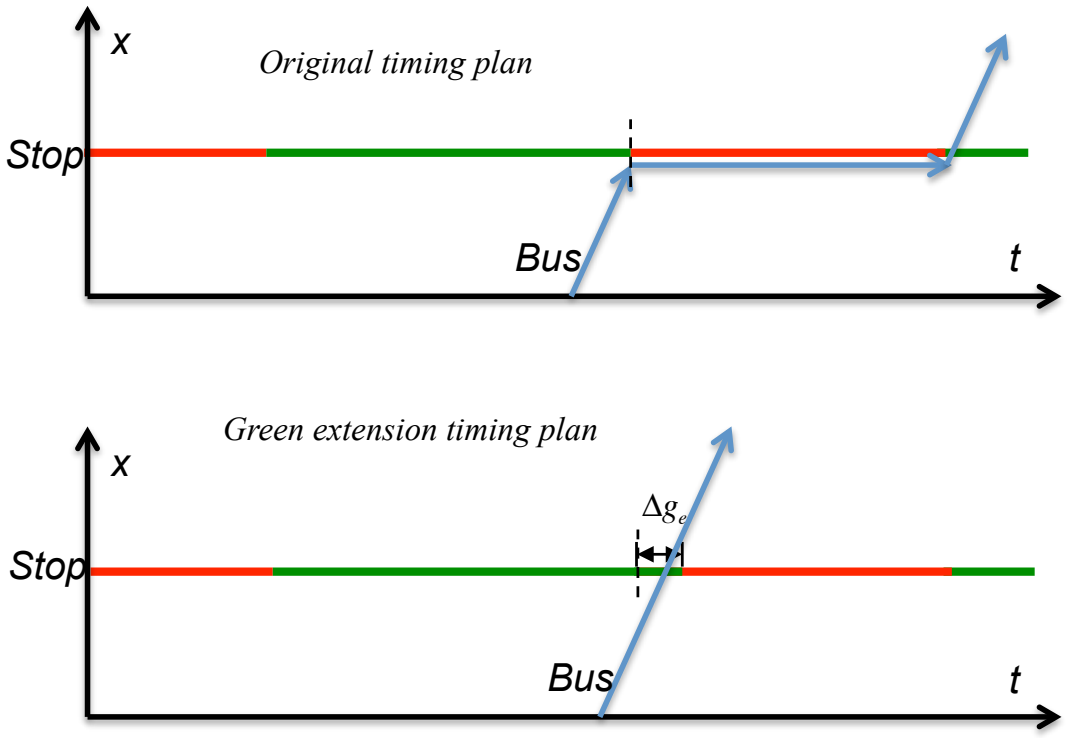

FIGURE 5.3: Extension of green light

Few buses can meet the implementation requirement to apply green extension because it requires buses arriving at the junction and the traffic signal switching from green to red concurrently. However, if green extension can be properly implemented, it can significantly reduce bus delay caused by the red light with little interruption to the transport system.

Green recall

Green recall is applied if buses are detected to be located in the traffic queue due to red light timing without the right of way. It is also implemented by iBus and London UTC to grant priority to buses. The remaining duration of red light is reduced to release buses earlier. Figure 5.4 shows the recall of green light for the duration of Δg_r.

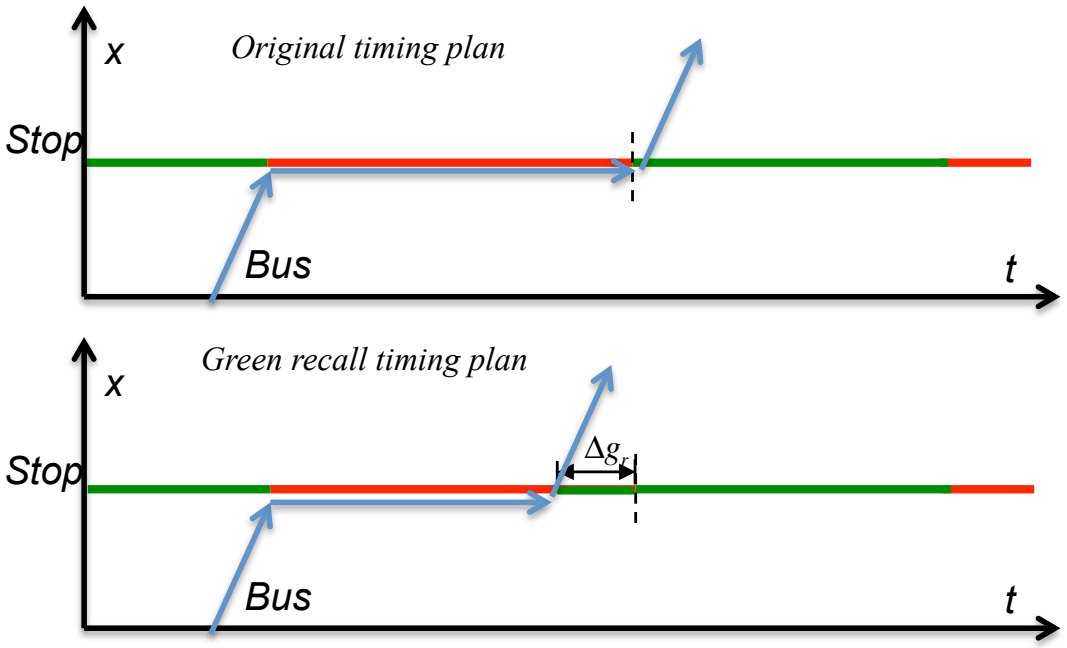

FIGURE 5.4: Recall of green light

Compared to green extension, more buses can benefit from priority assigned by red recall since its requirement is less restrictive. As long as buses meet the traffic queue during red light phases and other related requirements such as the minimum safety green light time are satisfied, red recall can be implemented. However, buses under red recall do not receive as much priority as green extension due to the elapsed red light time.

Red extension

Red extension is applied during the time when buses do not have the right of way and their headways need to be extended. The effect of bus efficiency under the red extension is contrary to that under the green recall. It is used for the purpose to regulate bus service rather than to prioritize buses. Figure 5.5 shows that the red light is extended for the duration of Δr_e. An extended red light can hold buses so that their forward headways are extended and backward headways are reduced. Since red extension increases bus journey time by holding buses for a longer amount of time, it is contradictory to prioritizing buses and currently not used by iBus or London UTC.

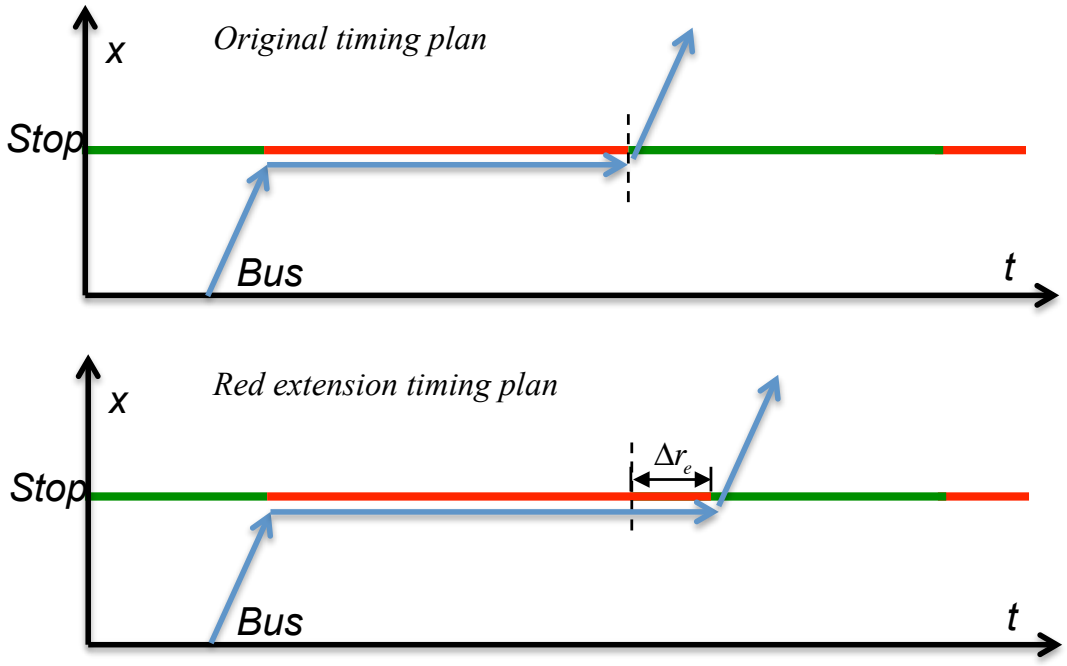

FIGURE 5.5: Extension of red light

Compared to stop-based bus holding strategies, red extension might not be effective because it requires buses meeting the traffic queue. If buses travel through signalized junctions without meeting the red light, red extension cannot be applied.

Red recall

To mitigate the limit that red extension may not be implementable if buses do not meet the red light, the red recall action is developed to guarantee that necessary bus holding can be applied as buses travel through signalized junctions. Red recall is applied when buses are about to cross the junction with the right of way and their headways need to be extended. Figure 5.6 shows the recalled red light for the duration of Δr_r.

Red recall is the most effective way to regulate bus headways since all buses will travel through junctions. However, its effectiveness is achieved at the expense of traffic signal order disruptions and further delay of road traffic and bus journeys. Similar to red extension, red recall is also not implemented by iBus or London UTC.

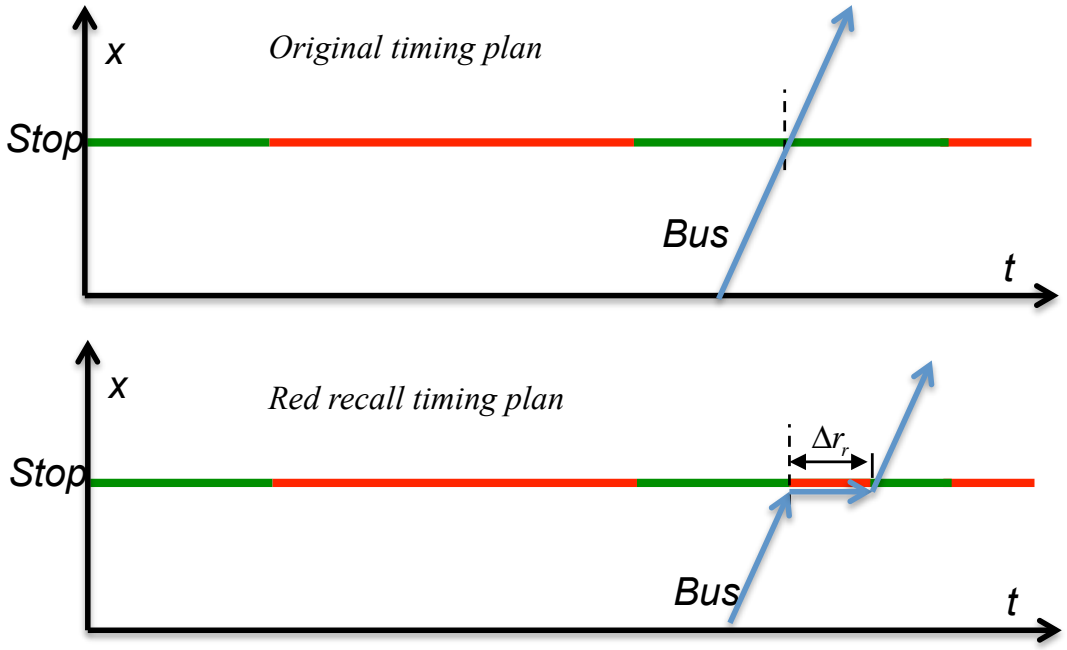

FIGURE 5.6: Recall of red light

5.3.2 Control strategies

Once buses are detected by the inductive loop detectors or the iBus system, various traffic control actions can be deployed depending on real-time bus information and specific control strategy. London iBus has implemented green extension and green recall with the objective of prioritizing buses and improving their efficiency. In addition to iBus, the proposed signal-based bus control strategies also deploy red extension and red recall with dual objectives to improve both bus service regularity and transport system efficiency.

This research proposes three signal-based control strategies which are referred to as SIG-1, SIG-2 and SIG-3. All control strategies aim at improving bus service regularity, while SIG-2 and SIG-3 strategies also consider transport efficiency factor. As road traffic becomes increasingly congested, objectives of SIG-2 and SIG-3 strategies are gradually shifted to focus on reducing overall road traffic delay.

Control actions and objectives of different control strategies are summarised in Table 5.2. London iBus is also included in the table for comparison. The symbol '✓' labels factors included in development of the corresponding strategy.

TABLE 5.2: Signal-based control strategies

Strategy Symbols	Control actions				Control objectives	
	Green extension	Green recall	Red extension	Red recall	Regularity	Efficiency
SIG-1	V	V	V		V	
SIG-2	V	V	V		V	V
SIG-3	V	V	V	V	V	V
iBus	V	V				V

SIG-1 strategy

SIG-1 strategy is applied when a bus meets a traffic queue during the red light phase. Therefore, only green recall and red extension actions are deployed.

Figure 5.7 shows the scenario when SIG-1 strategy can be applied. The bus trajectory (represented by the black line) shows that a bus approaches towards a signalized junction. Bus n joins the traffic queue at location x and time t when the signal is red. At time t, the remaining length of red light is r and the length of upcoming green light is g.

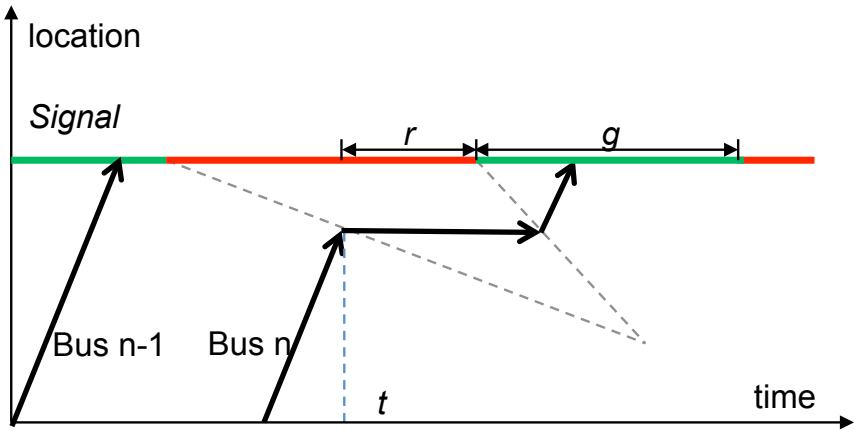

FIGURE 5.7: Scenario to apply SIG-1 control

By retrieving the trajectory information of bus $n-1$ stored in the central server, the time $t^A_{n-1,x}$ of bus $n-1$'s arrival at location x can be identified. Thus the headway of bus n at location x with its leading bus $n-1$ can be calculated by Equation 5.1.

$$h_{n,x} = t^A_{n,x} - t^A_{n-1,x} \tag{5.1}$$

Based on $h_{n,x}$ and the target headway h_T, the adjusted signal timing Δr can be calculated based on Equation 5.2.

$$\Delta r = (\alpha + \beta_n)(h_{n,x} - h_T) \tag{5.2}$$

where α is the control parameter ranging from 0 to 1 and h_T is the target headway to maintain for different buses. Proposed strategies here focus on adjusting the forward bus headway because holding based on two-way or backward headway could be ineffective under high-volume road traffic as identified in Ch 4.

If $\Delta r = 0$, it means that the actual headway equals to the target headway and buses do not need to be held.

If $\Delta r > 0$, it means that actual bus headway is larger than target headway. It is necessary to recall the green light earlier in order to reduce bus headway with its leading bus. The length of the recalled green light time Δg_r is calculated as Equation 5.3.

$$\Delta g_r = \min\{r, \Delta r\} \tag{5.3}$$

If $\Delta r < 0$, it means that actual bus headway is smaller than the target headway. Thus it is necessary to extend the red light in order to increase the headway. The length of extended red light time is Δr_e calculated as Equation 5.4.

$$\Delta r_e = \min\{g - g_M, \Delta r\} \tag{5.4}$$

where g is the remaining green time in current cycle and g_M is the minimum green light time assigned to the transport link to ensure traffic movement.

SIG-2 strategy

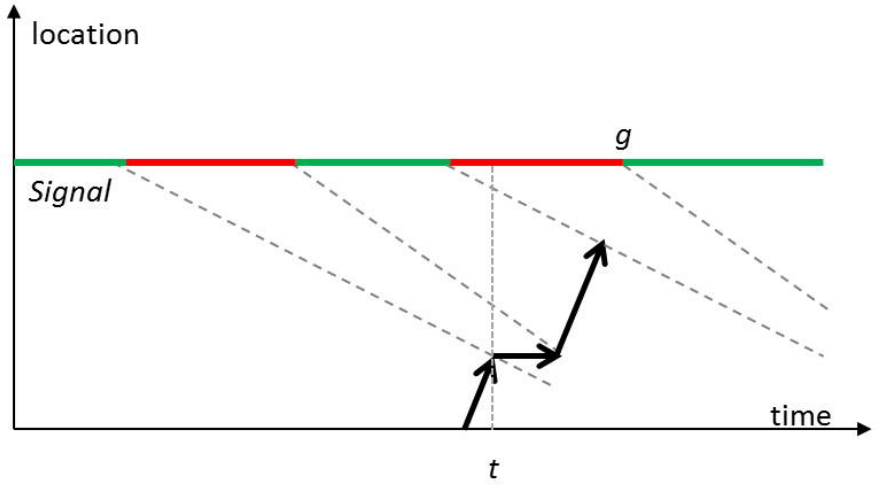

FIGURE 5.8: Scenario to consider traffic factor

SIG-2 strategy extends SIG-1 strategy by not only considering the variance of bus headways, but also road traffic conditions. If the road traffic volume is low, SIG-2 control works in the same way as SIG-1 control and the scenario to apply SIG-2 control is illustrated in Figure 5.7. When the road traffic condition reaches a congestion threshold, signal priority will be assigned to ensure road traffic movement to reduce traffic delay. In this case, the extension component will not be carried out as it further reduces effective road capacity and worsens traffic congestion. Only the recall component or nothing is applied to adjusting signal timing.

The congestion threshold is considered to be reached if road traffic volume exceeds the effective road capacity in the signal cycle during which the controlled bus joins a traffic queue. When the road traffic demand is above the effective capacity that the traffic queue cannot be fully dissipated within the same cycle, the traffic condition threshold is considered to be reached. Figure 5.8 illustrates a scenario when the threshold is reached. The trajectory of a bus is represented by the black line. At time t, the bus joins the traffic queue formulated in the last cycle which indicates that the road traffic demand exceeds effective road capacity. In this case, the traffic factor is considered by the SIG-2 control strategy when adjusting traffic signals.

SIG-3 strategy

Since SIG-1 and SIG-2 strategies are applied when buses meet traffic queues, they might not be effective if buses do not meet a red light and cruise at free-flow speed throughout the whole journey. If buses do not meet traffic queues, which is more common in the case of low traffic volume, SIG-1 control and SIG-2 control strategies may not be effective. To mitigate this disadvantage, the SIG-3 control is developed which extends SIG-2 strategy by incorporating the red recall action.

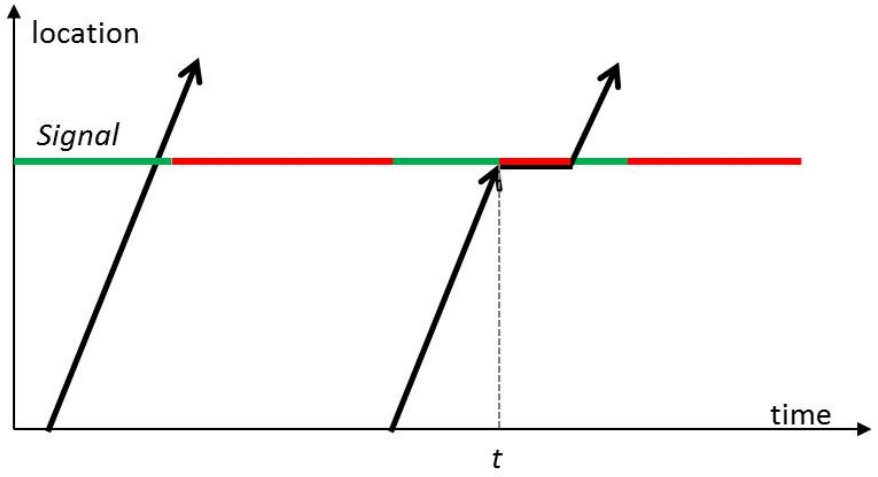

FIGURE 5.9: Scenario to apply insertion in SIG-3 control

Figure 5.9 illustrates the scenario when insertion is applied to a bus. If a bus is running a short headway with its leading bus and does not meet the traffic queue while travelling through the transport link, the recall of red control action is applied when it arrives at the downstream boundary in front of the traffic signal. A period of red light will be inserted into the green light to hold the bus. The length of the inserted red period is subject to actual headway discrepancy, control parameter and the length of remaining green light period.

iBus differential priority strategy

The implemented iBus differential priority on the simulation platform is based on bus headway discrepancy compared to the target headway as proposed by Hounsell *et al.* (2008*a*) and Hounsell *et al.* (2008*b*). If buses are delayed with longer headways than the target, green recall and green extension will be applied. The amount of adjusted traffic timing follows Equation 5.2. When buses are

running early with shorter headways compared to the target, no control actions are taken.

5.4 Numerical test

A range of numerical tests are carried out in the VMBus simulation platform for three purposes:

1. To evaluate and compare different signal-based control strategies (SIG-1, SIG-2 and SIG-3)
2. To compare signal-based control strategies with the stop-based holding strategy (Stop)
3. To compare signal-based control strategies with the iBus-based differential priority strategy (iBus)

The research also ran a simulation of the scenario without any control strategy (NO) in the VMBus as the benchmark to quantify performance improvement of different strategies. For the stop-based holding strategy, buses are held at bus stop 1 for a period of time determined by the forward holding strategy.

Performance evaluation is conducted from both the efficiency perspective and the regularity perspective. The efficiency perspective is represented by average bus journey time (sec) and average traffic delay (sec). Bus service regularity is measured by the bus journey time deviation (sec) and headway deviation (sec).

5.4.1 Test setting

The road configuration is the same as the one tested in Section 3.4. Two bus stops are added in order to apply the stop-based holding strategy for comparison with proposed signal-based holding strategies. Buses cruise towards Stop 1 first,

dwell there to pick up passengers, go through a signalized junction and then reach Stop 2. Due to the passenger variation at Stop 1 and traffic signal control at the junction, buses arrive at Stop 2 with various headways.

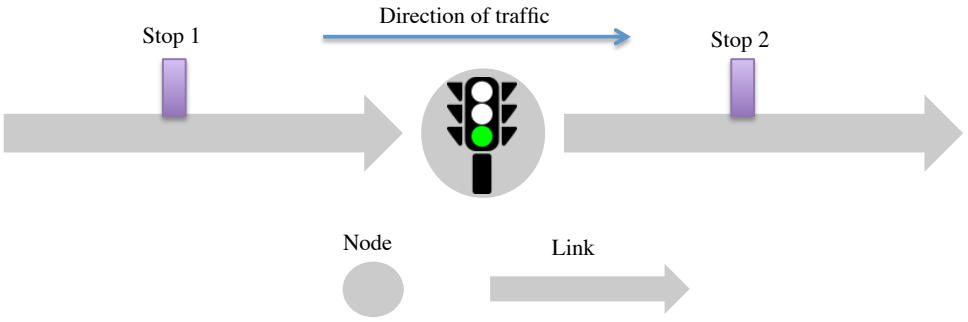

FIGURE 5.10: Numerical Test Setting

A two-lane road is constructed with an identical triangular fundamental diagram with saturation flow 3600 vph, jam density 540 vpm, free-flow speed 20 mph and backward shock wave speed 10 mph. Predefined green/cycle time ratio (g/c) is 0.5. The cycle length c is fixed at 60 sec. Each link is 0.5 mile long and each bus stop is located in the middle of a link.

A total of six buses enter the network with a headway of two minutes and the target headway to maintain is two minutes. Two-minute headway is categorised as high-frequency service in Turnquist (1982). This value is relatively low compared to the real-world situation; nevertheless, the bus bunching problem is more severe for high-frequency routes and performance difference among different holding strategies can be clearly presented with a two-minute headway.

A total of 164 numerical tests are carried out for each control strategy or the no-control scenario. The ratio of traffic volume d over road capacity Q, d/Q ratio, increases from 0 to 1 at an increment of 0.025. The road capacity is represented by saturation flow Q. When the d/Q ratio equals to 0, there are only 6 buses in the network and no other vehicles. When the d/Q ratio equals to 1, the network is fully saturated with vehicles. At each level of d/Q ratio, 4 tests are conducted for each control strategy or the no-control scenario with evenly distributed starting times of the first bus at every 15 sec of the fixed one-minute signal cycle. Average

output values from these 4 tests are regarded as the control output at the given d/Q ratio so that the traffic light offset effect is mitigated.

5.4.2 Test results

This section first presents all the simulation output against different traffic volumes ranging from $d/Q = 0$ to $d/Q = 1$ in Section 5.4.2. Section 5.4.2 evaluates and compares performance of different signal-based control strategies. Section 5.4.2 compares proposed signal-based control strategies with the stop-based holding strategy. Section 5.4.2 compares proposed signal-based control strategies with the iBus priority strategy.

General results

All the simulation outputs for different control strategies and the no-control scenario at different levels of d/Q ratios are plotted in Figure 5.11, 5.12, 5.13 and 5.14.

A general trend can be observed that transport efficiency remains stable with $d/Q \in [0, 0.5)$ and relatively insensitive with the change of d/Q ratio. As d/Q reaches above 0.5, traffic delay and bus journey time become longer and bus service becomes increasingly unregulated. The reason why d/Q ratio above 0.5 causes reduced efficiency and unstable service is that the g/c ratio is set as 0.5. The g/c ratio measures the percentage of green light time assigned to a transport link. Since traffic can only move when the road receives green light, g/c determines effective road capacity. This numerical test assumes a fixed signal timing with $g/c = 0.5$. The effective capacity is thus 50% of the saturation flow. With $d/Q > 50\%$, the road traffic volume is actually larger than the amount of vehicles it can transport. Traffic delay and unstable bus service hence occur.

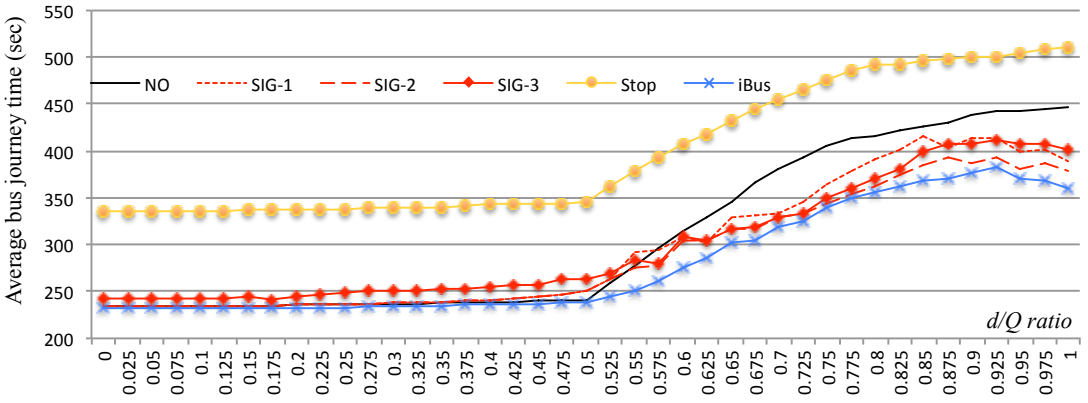

FIGURE 5.11: Average bus journey time

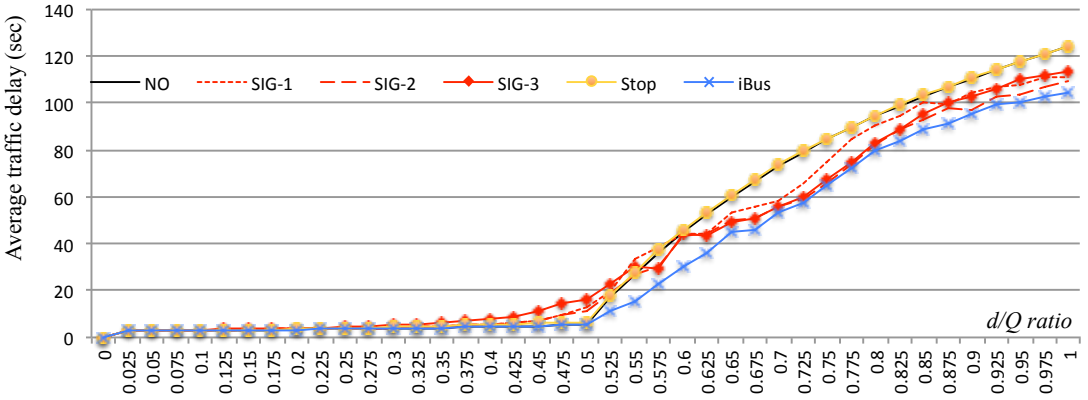

FIGURE 5.12: Average traffic delay

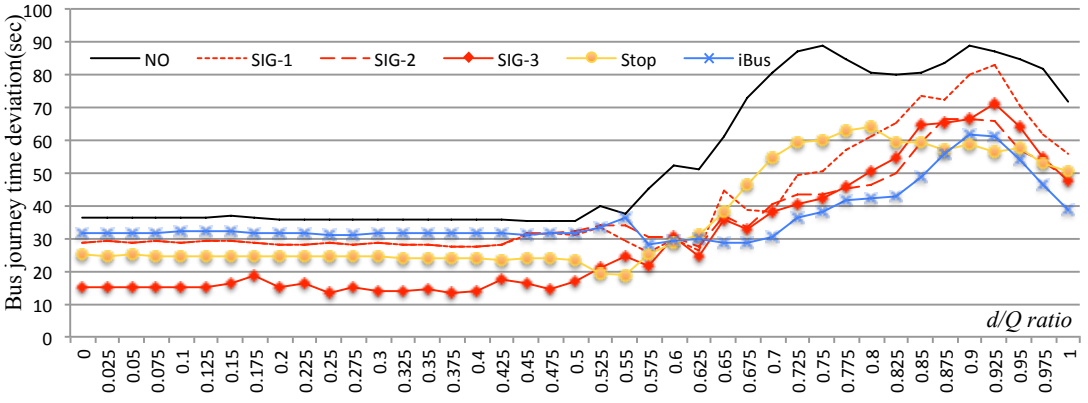

FIGURE 5.13: Bus journey time deviation

Evaluation of SIG

Control comparison of different signal-based strategies are compared with the no-control scenario to identify whether they are effective to improve bus regularity

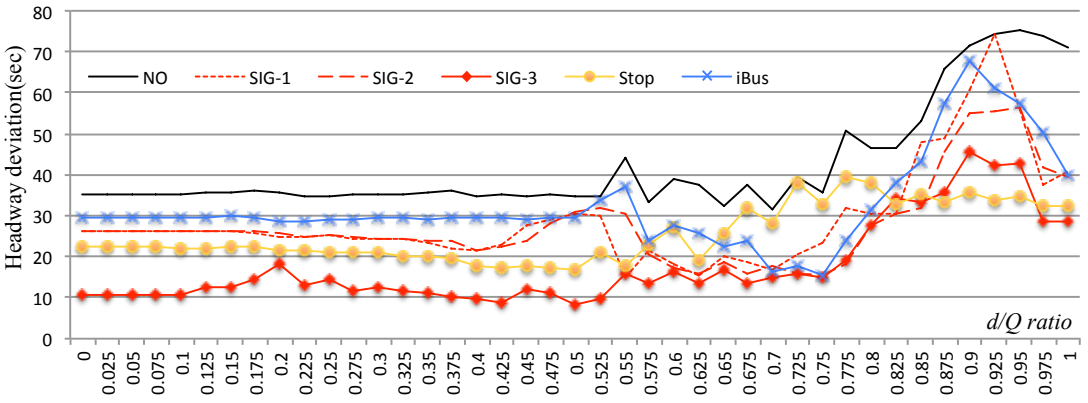

FIGURE 5.14: Bus headway deviation

TABLE 5.3: Evaluation of different signal-based control strategies

	All Cases	Under-saturation	Over-saturation
Average bus journey time (sec)			
SIG1 - No	-12	1	-24
SIG2 - No	-20	1	-39
SIG3 - No	-9	12	-30
Average traffic delay (sec)			
SIG1 - No	-3	1	-5
SIG2 - No	-5	1	-10
SIG3 - No	-3	2	-8
Variance of bus journey times (sec)			
SIG1 - No	-13	-7	-19
SIG2 - No	-17	-7	-25
SIG3 - No	-24	-21	-27
Variance of bus headways (sec)			
SIG1 - No	-13	-10	-16
SIG2 - No	-15	-10	-19
SIG3 - No	-24	-23	-26

and transport efficiency. Differences of mean value associated with various evaluation metrics are presented in Table 5.3. All the mean differences are calculated as the signal-based control output minus the no-control output. Therefore, negative values with efficiency metrics suggest less delay, journey time, journey time variance and headway variance under the signal-based control compared to the no-control scenario.

The average control performance of all cases suggests that proposed signal-based control strategies can effectively improve transport efficiency and bus service regularity in general. Savings of average bus journey times range between 9 sec to 20

sec and average traffic delay between 3 sec to 5 sec. Variance of bus journey times is reduced by 13 sec to 24 sec, and bus headways 13 sec to 24 sec.

A further comparison under different traffic levels shows that signal-based control strategies decrease traffic efficiency when the road is under saturated and increases traffic efficiency when the road is over saturated. This is due to the fact that proposed signal-based control strategies focus on regulating bus service at low-traffic level and on reducing traffic delay at high-traffic level. With $d/Q < 0.5$, proposed strategies implement bus holding actions to regulate their services and result in average bus journey time increasing and their commercial speed decreasing. The trade-off between efficiency and regularity at low-traffic level can be quantified that 1 sec to 12 sec increase in average bus journey time and 1 sec to 2 sec increase in average traffic delay are compensated by 7 sec to 21 second reduction in bus journey time variance and 10 sec to 23 sec reduction in bus headway variance. Under over-saturated traffic conditions, proposed signal-based controls can improve transport efficiency and bus regularity concurrently since priority is assigned to the transport approach where buses are located.

Among different signal-based control strategies, SIG-3 is the most effective strategy to improve bus service regularity with the largest amount of reduction in bus headway variance and bus journey time variance. Especially when the road is under saturated, reduced headway variance under SIG-3 is 130% (13 sec) more than that under SIG-1 and SIG-2, and the reduced journey time variance is 200% (14 sec) more than under SIG-1 and SIG-2. However, improvement in bus service regularity comes at the expense of increased bus journey times and traffic delay. SIG-3 causes an 11-second longer bus journey and a 1-second longer delay per vehicle than SIG-1 and SIG-2 at low-traffic level.

Comparison of SIG and Stop

Performance differences of signal-based control strategies and the stop-based control strategy are presented in Table 5.4. All the mean differences are calculated as the signal-based control output minus the stop-based control output.

TABLE 5.4: Comparison and signal-based control and stop-based control

	All Cases	Under-saturation	Over-saturation
Average bus journey time (sec)			
SIG1 - Stop	-102	-102	-102
SIG2 - Stop	-110	-102	-117
SIG3 - Stop	-99	-90	-108
Average traffic delay (sec)			
SIG1 - Stop	-3	0	-6
SIG2 - Stop	-5	0	-11
SIG3 - Stop	-4	1	-9
Variance of bus journey times (sec)			
SIG1 - Stop	4	4	5
SIG2 - Stop	1	4	-2
SIG3 - Stop	-6	-10	-3
Variance of bus headways (sec)			
SIG1 - Stop	4	5	3
SIG2 - Stop	2	5	0
SIG3 - Stop	-8	-9	-7

From the bus service efficiency perspective, it can be seen that all signal-based control strategies can improve bus commercial speed compared to the stop-based holding strategy. This is due to the fact that the slack time used in the stop-based holding strategy is not needed in signal-based control strategies. Savings of bus journey times generally range from 99 sec to 110 sec depending on deployed control strategies. SIG-2 and SIG-3 result in longer bus journey time savings at high-traffic level than low-traffic level because the traffic factor is considered.

In terms of traffic delay caused by different control strategies, signal-based control strategies have less average delay between 3 sec to 5 sec than stop-based holding control. At low-traffic level, the signal-based holding strategy does not result in less traffic delay than the stop-based holding strategy because bus regularity is the primary focus of proposed signal management. By holding buses at the stop, other road traffic is also held. Differences in average traffic delay are more significant at high-traffic level. SIG-2 saves the most traffic delay of 11 sec per vehicle.

As for bus service regularity, stop-based control has a better performance at low-traffic level with bus journey time variance 4-second less and bus headway variance 5-second less than SIG-1 and SIG-2. This is due to the fact that buses do not meet the traffic light in the test setting. SIG-1 and SIG-2 are thus ineffective to regulate

buses. SIG-3 operates buses at higher regularity than Stop at all traffic levels with a 6-second reduction in bus journey time variance and 8-second reduction in bus headway variance.

Comparison of SIG and iBus

Performance comparison between signal-based control and the iBus control is presented in Table 5.5. All the mean differences are calculated as the signal-based control output minus the iBus control output.

TABLE 5.5: Comparison of signal-based control and iBus

	All Cases	Under-saturation	Over-saturation
Average bus journey time (sec)			
SIG1 - iBus	17	4	29
SIG2 - iBus	9	4	14
SIG3 - iBus	20	15	24
Average traffic delay (sec)			
SIG1 - iBus	5	1	10
SIG2 - iBus	3	1	5
SIG3 - iBus	5	2	7
Variance of bus journey times (sec)			
SIG1 - iBus	4	-3	11
SIG2 - iBus	1	-3	5
SIG3 - iBus	-6	-17	3
Variance of bus headways (sec)			
SIG1 - iBus	-3	-4	-2
SIG2 - iBus	-5	-4	-5
SIG3 - iBus	-14	-17	-12

Buses and road traffic operating under the iBus scheme have higher speed and shorter delays compared to signal-based control strategies. Bus journey time with signal-based control is 9 sec to 20 sec longer than that with the iBus on average. Road traffic experiences 3 sec to 5 sec longer delay. Moreover, efficiency performance difference is greater at the high-traffic level than at the low-traffic level. Higher transport efficiency is expected as bus priority is the primary focus of the iBus control scheme. The proposed strategies implement red extension and red recall actions to hold buses which results in longer bus journey times and average traffic delay.

In terms of route-level regularity, signal-based holding strategies have less bus journey time variance than iBus with $d/Q < 0.5$. Reduction in bus journey time

variance is 3 sec with SIG-1 and SIG-2, and 17 sec with SIG-3. With $d/Q \leq 0.5$, iBus control has lower bus journey time variance than signal-based control strategies because traffic congestion becomes the main factor to disrupt bus cruising time between stops and bus dwelling time. Thus, signal priority aimed at improving bus efficiency can lead to service regularity improvement at the route level. Higher priority at the approach where buses are located means higher bus commercial speed and more consistent bus journey times. Numerical results show that, iBus operates buses with 3-second to 11-second lower bus journey time variance compared to the signal-based strategies at the high-traffic level.

Bus regularity at the stop level is better with the signal-based control strategies than the iBus control. Average headway variance reductions by SIG-1, SIG-2 and SIG-3 are 3 sec, 5 sec and 14 sec respectively. Stop-level regularity performance difference is more significant at the low-traffic level than at the high-traffic level. This is because signal-based control strategies primarily focus on regulating bus service when the road traffic volume is lower than effective capacity. Bus headway variance saving compared to the iBus is between 4 sec to 17 sec when the road is under saturated. When the road is over saturated, bus headway variance saving is between 2 sec to 15 sec.

5.4.3 Discussion

Table 4.6 ranks different control strategies with an evaluation score assigned to each strategy in various criteria. The no-control scenario is also assigned with a score as a benchmark for comparison. The numerical score values are ordinal data which indicate quantitative ranking of different control strategies based on findings from Section 5.4.2. 1 is the best score which indicates the highest service regularity or transport efficiency. 6 is the worst score with the lowest bus regularity or transport efficiency. Strategies of the same score suggest that their performance in the corresponding criterion has no significant difference. For the under-saturation category, $d/Q < 0.5$; and for over-saturation category, $0.5 \leq d/Q$. Table 4.6 can

TABLE 5.6: Summary of control strategy effects

		SIG-1	SIG-2	SIG-3	Stop	iBus	NO
Average bus journey time	Under-saturation	3	3	5	6	1	2
	Over-saturation	4	2	3	6	1	5
Total traffic delay	Under-saturation	1	1	6	1	1	1
	Over-saturation	4	2	3	6	1	5
Bus journey time variance	Under-saturation	3	3	1	2	5	6
	Over-saturation	5	3	2	4	1	6
Bus headway variance	Under-saturation	3	3	1	2	5	6
	Over-saturation	4	2	1	2	5	6

be used by policy makers to select appropriate strategies based on road traffic condition and control objectives.

It can be seen from Table 4.6 that iBus is most effective to prioritize buses and improve bus service efficiency. This is because only green extension and green recall are implemented by iBus to adjust traffic signals. iBus also contributes to improving bus service regularity compared to the no-control scenario which agrees with findings in Hounsell *et al.* (2008*b*). Especially with a high traffic demand, iBus can enhance bus mobility in the road through priority assignment and reduction in bus journey time variance.

SIG-3 is the most effective strategy to improve bus service regularity, especially at the stop level. With a low traffic demand, SIG-3 applies red recall and red extension to hold buses based on their headway variance which regulates bus service. With a high traffic demand, SIG-3 considers traffic congestions factor and assigns more priority to reduce road traffic flow. This strategy further improves bus regularity.

SIG-1 and SIG-2 have similar performance compared to the stop-based holding strategy in terms of regularity improvement. Differences in bus journey time

variance and headway variance are within 5 seconds. However, SIG-1 and SIG-2 can achieve significant bus journey time savings and reduce road traffic delay, especially at high-traffic level. When the road traffic volume exceeds the passing rate caused by bus dwelling at in-line stops, the stop-based bus holding strategy can also increase road traffic delay compared to the no-control scenario.

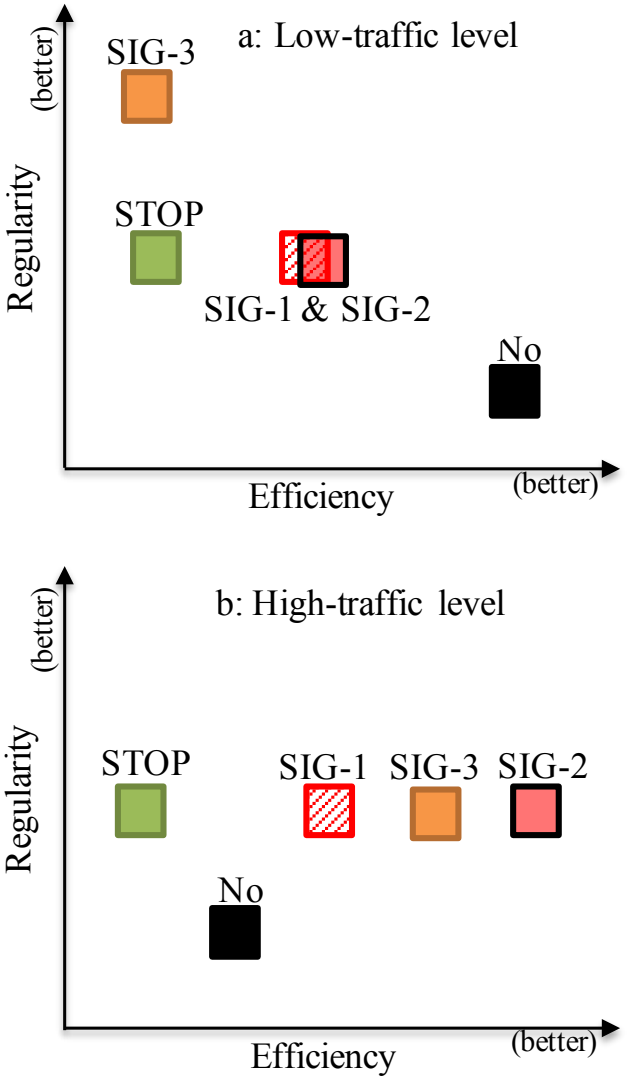

FIGURE 5.15: Recommendation chart of holding strategies

A recommendation chart is presented in Figure 5.15.

At the low-traffic level, SIG-3 strategy works the best with significantly lower headway deviation and the longest average bus journey time. SIG-3 achieves 70% headway deviation reduction with the cost of 10% increase in average bus journey time. SIG-1 and SIG-2 have the same performance because the congestion factor

is not considered by SIG-2 at low-traffic level. The performance of the regulating bus service is similar among SIG-1, SIG-2 and Stop strategies. However, SIG-2 and SIG-1 strategies significantly reduce average bus journey time compared to the Stop holding strategy.

Despite the unstable performance at high-traffic level, Stop strategy delivers relatively more stable headway deviation compared to other strategies since the impact on road traffic by bus dwelling is much less than traffic signal adjustment. With consideration of the congestion factor, SIG-2 outperforms SIG-1 with lower headway deviation. Since signal-based control strategies assign road traffic priorities and bus dwelling at the stop introduces the bottleneck effect, signal based control strategies are able to improve transport system efficiency compared to Stop control.

Policy makers can select appropriate strategies based on road traffic conditions and control objectives. At low-traffic level, trade-off can be observed between achieved bus regularity and transport efficiency by different signal-based holding strategies. To achieve the highest bus service regularity, SIG-3 is recommended which outperforms other strategies with 70% reduction in headway deviation at the cost of 10% increase in average bus journey time. At high-traffic level, different strategies cannot differentiate themselves in terms of regularity improvement. Nevertheless, SIG-2 is the most efficient one to minimize traffic delay.

5.5 Real-world application

The proposed signal-based bus holding strategies are implemented in TCR signalised junctions on the VMBus simulation platform in order to evaluate their effectiveness and impact in an environment similar to the real world. Road traffic characteristics and traffic demand are the same as in Section 3.5 which are calibrated based on the actual loop detector data provided by TfL. The signal timing plan deployed in Section 3.5 serves as the original input to be adjusted by the

proposed holding strategies with objectives to improve bus service regularity and transport efficiency.

The bus route setting and passenger demand profile at each bus stop are the same as Section 4.5. The simulation test runs 20 times with stochastic passenger demand and mean values of different outputs are presented in this section to quantify efficiency and impact of different proposed control strategies.

Average bus journey time

TABLE 5.7: Average bus journey time under signal-based control (sec)

	Route 1	Route 2	Route 3	Route 4	Route 5	Route 6	Route 7	Route Average
No-control	244	274	245	248	250	273	260	256
SIG-1	213	207	207	200	206	205	212	207
SIG-2	215	208	206	200	206	205	212	207
SIG-3	218	207	207	200	212	204	211	208
iBus	202	204	197	193	205	204	195	200
Stop	283	280	257	248	257	279	269	267

Table 5.7 presents bus AJT under different signal-based holding strategies in comparison with the no-control scenario. It can be seen that bus AJT can be reduced by 18.8% to 19.0% with the signal-based holding strategies. iBus has the lowest average bus journey time of 200 sec as it only prioritizes buses and does not hold buses. The stop-based bus holding strategy has the longest average journey time because the bus holding time is the longest.

Average traffic delay

TABLE 5.8: Average traffic delay under signal-based control (sec)

	Main arterial	Cross streets	Whole TCR
No-control	89.32	33.73	52.28
SIG-1	53.71	35.69	41.70
SIG-2	53.72	35.67	41.70
SIG-3	54.18	33.74	40.56
iBus	53.47	35.92	40.27
Stop	88.95	33.73	52.46

Table 5.8 shows the average traffic delay under different signal-based holding strategies. This table presents the experiment results in 2 decimal places in order

to show the difference in cross street traffic delay which is relatively negligible. It can be seen that the average traffic delay in the main TCR decreases from 89.32 sec to around 54 sec with 38% savings under the proposed signal-based holding strategies. In cross streets, SIG-1, SIG-2 and SIG-3 result in 1.96, 1.94 and 0.01 sec increase in average traffic delay compared to the no-control scenario. In terms of traffic delay in the whole TCR, SIG-1 and SIG-2 can achieve 21.0% reduction compared to the no-control scenario. SIG-3 can save the average traffic delay by 22.0%. iBus leads to slightly lower average traffic delay which is 40.27 sec. Compared to signal-based control strategies, the stop-based bus holding strategy increases average traffic delay marginally by 0.18 sec in the main TCR. Delay in cross streets remains unchanged.

It is interesting to note that traffic journey time savings in the main route is much larger than the increased traffic delay in the cross streets. This is due to the fact that traffic inflow from cross streets is of a lower volume than the main arterial. Increasing the green light in the main road and reducing the green light in cross streets can improve overall efficiency in the studied TCR network.

Journey time deviation

TABLE 5.9: Journey time deviation under signal-based control (sec)

	Route 1	Route 2	Route 3	Route 4	Route 5	Route 6	Route 7	Route Average
No-control	54	53	40	42	61	42	54	49
SIG-1	28	31	33	16	24	26	30	27
SIG-2	33	30	33	16	24	26	30	27
SIG-3	33	32	33	15	26	25	28	27
iBus	31	27	22	21	25	27	26	26
Stop	35	55	44	37	59	38	47	45

Table 5.9 presents bus JTDs under different control strategies. It can be seen that all proposed signal-based holding strategies can achieve the same level of JTD which is 45.8% lower than the JTD in the no-control scenario. The iBus system achieves a slightly higher journey time regularity which is 1 sec less than signal based holding strategies on average. This is because the underlying traffic in the main road is of a relatively high volume and strong priority assigned to buses can

improve their overall route regularity. The finding here is consistent with that in Section 5.4.2. The stop-based bus holding strategy has the longest journey time deviation compared to signal-based control strategies.

Headway deviation

Table 5.10 shows HD of buses arriving at different stops under various signal-based holding strategies. Proposed holding strategies are effective to reduce bus HD at Percy Street stop, Goodge Street stop and the Warren Street stop. Reduction of bus HD ranges from 4 sec to 32 sec. At the Warren Street stop, the SIG-3 strategy is the most effective one with the lowest HD. It is because that there are 3 signalized junctions between Goodge Street and Warren Street which effectively adjust bus headways along the route. All proposed strategies have smaller or equal standard deviation of bus headways at Goodge Street stop and Warren Street Stop compared to the iBus differential priority strategy. In addition, bus stop-level regularity is the worst under the stop-based holding strategy compared to signal-based control strategies.

5.6 Conclusion

This chapter proposes a range of signal-based bus control strategies with different focuses and objectives to regulate the bus service and reduce traffic delay. The proposed strategies are evaluated on the VMBus macroscopic simulation platform in an integrated multi-modal transport system. Various numerical tests have been carried out with different signal-based control strategies, stop-based bus holding strategy and the no-control scenario. Different evaluation criteria include average bus journey time, average traffic delay, bus journey time variance and bus headway variance. These numerical results are analysed statistically in order to compare control performances among different signal-based strategies, between signal-based strategies and the stop-based holding strategy, and between signal-based strategies and the iBus priority strategy in a systematic approach.

TABLE 5.10: Average bus journey time under signal-based control (sec)

Strategy	Stop	Route 1	Route 2	Route 3	Route 4	Route 5	Route 6	Route 7	Route Average
No-control	TCR	0	0	0	0	0	0	0	0
	Percy	14	7	6	11	5	8	5	8
	Goodge	32	60	48	55	31	25	38	41
	Warren	83	77	63	65	70	61	58	68
SIG-1	TCR	0	0	0	0	0	0	0	0
	Percy	4	2	4	4	3	3	4	3
	Goodge	27	13	20	8	15	7	17	15
	Warren	30	46	60	18	37	30	42	38
SIG-2	TCR	0	0	0	0	0	0	0	0
	Percy	6	2	4	4	3	3	4	3
	Goodge	27	13	19	8	15	7	17	15
	Warren	32	43	60	18	37	30	42	37
SIG-3	TCR	0	0	0	0	0	0	0	0
	Percy	6	2	4	4	3	3	4	4
	Goodge	28	13	19	8	15	7	17	15
	Warren	29	45	60	18	33	29	40	36
iBus	TCR	0	0	0	0	0	0	0	0
	Percy	5	2	4	4	3	2	4	3
	Goodge	29	18	22	7	15	12	18	17
	Warren	45	39	44	32	34	28	42	38
Stop	TCR	0	0	0	0	0	0	0	0
	Percy	15	7	5	11	5	8	5	8
	Goodge	29	61	48	55	31	25	38	41
	Warren	48	74	76	61	71	61	57	64

It has been identified that signal-based control strategies can deliver a bus service with higher speed and more regularity compared to the no-control scenario. Buses under the proposed control schemes can achieve higher regularity without compromising their commercial speed as the stop-based holding strategy does. Test results also show that the existing iBus priority control is the most effective strategy to improve bus efficiency compared to stop-based and the proposed strategies. However, this research provides insights from another perspective to use the iBus system and traffic signal management to achieve stronger bus regularity improvement. It is interesting to conduct field tests to validate proposed strategies in real-world application.

Upon understanding performance and impact of signal-based holding control strategies based on the hypothetical bus route, this research implement them in the TCR with actual traffic demand and signal timing plan to validate their effectiveness and impact in a real-world environment. Test results show that proposed control

strategies can effectively improve bus service regularity and enhance transport system efficiency for both buses and road traffic.

Chapter 6

Conclusions

6.1 Summary

This thesis investigates multi-modal traffic modelling and bus regularity management with consideration for the interaction between buses and their surrounding traffic in an integrated urban transport system.

First, this research has established a macroscopic simulation platform based on the variational formulation of the LWR model to estimate urban traffic conditions and multi-modal traffic interactions. In Chapter 3, the proposed simulation framework is compared with the CTM-based simulation framework (coded by Andy Chow) systematically through a range of numerical experiments and a real-world case based on TCR in Central London to identify the advantages and disadvantages of the variational formulation of the LWR model. Empirical results suggest that the proposed simulation framework is easy to implement and accurate to reproduce dynamic traffic conditions, especially in modelling platoon dispersions and bus-traffic interactions. Moreover, experiment results from the real-world data supported by TfL validate the feasibility to apply the proposed simulation platform in the modelling of large-scale urban transport systems and multi-modal traffic flows.

Second, the bus system is further incorporated into the variational framework for the development of a VMBus simulator which can estimate bus movement and evaluate the bus service in a multi-modal transport system. In Chapter 4, VMBus is applied to evaluate the impact of road traffic conditions on bus service regularity through a range of numerical tests. Different headway-based bus holding strategies are also implemented in TCR to evaluate their performances in a real-world environment. It is shown that the forward strategy can operate buses with the highest service efficiency and the least delay impact on the surrounding road traffic than the backward and two-way holding strategy. If the road traffic volume is low and does not affect bus movement, two-way control is the most effective strategy to improve bus regularity. However, at the high-traffic level, the performance of the forward holding strategy in terms of regulating bus headways is similar to the two-way control and backward control. This evaluation study complements previous research with consideration of buses as an integrated traffic flow in a multi-modal system rather than as an independent traffic flow.

Third, a range of signal-based bus control strategies are proposed with the main objective to improve bus service regularity while maintaining transport system efficiency. In Chapter 5, proposed control strategies, the stop-based holding strategy and iBus priority strategy are all implemented in the VMBus to identify their advantages and disadvantages. Compared to stop-based bus holding strategies, signal-based holding strategies can regulate the bus service without significantly reducing their commercial speed. Among them, SIG-3 is the most effective control strategy to reduce bus journey time variance and headway variance. The iBus differential priority strategy is the most effective control to increase average bus commercial speed and reduce traffic delay. Proposed holding strategies are further implemented in TCR to validate their performances in a real-world environment. Empirical results show that proposed control strategies can effectively improve bus service regularity and enhance transport system efficiency for both buses and road traffic.

6.2 Contribution

First, this study establishes an effective macroscopic simulation platform to estimate road traffic conditions and represent bus-traffic interaction in an integrated urban transport system. Compared to the classical CTM-based macroscopic simulation, the proposed platform can produce more accurate traffic estimation by overcoming the viscosity issues of the CTM method. It can also produce more accurate solutions to model traffic flow dispersion, slow-moving or dwelling buses among other traffic.

Second, this study develops a parsimonious and cost-efficient evaluation framework to access the effectiveness of bus holding strategies and their impact on the surrounding traffic. Rather than assuming buses as a separate system as in previous studies, this study extends them with consideration of dynamic road traffic conditions and bus-traffic interaction. By implementing different bus holding strategies in a multi-modal urban transport system, a systematic study is conducted to evaluate the sensitivity of bus regularity with different factors such as passenger demand, road saturation levels and road transport characteristics. Furthermore, bus control performance is assessed from the perspectives of both public transport agency and other road drivers in terms of bus commercial speeds, traffic delay and journey time deviation.

Third, this study proposes a range of innovative bus headway control strategies which can respond to traffic dynamics and effectively improve bus service regularity and transport efficiency. Compared to classical stop-based holding strategies, these rule-based strategies innovatively deploy signal adjustment to regulate the bus service which does not require predefined slack time. The impact of bus holding on other traffic sharing the road is also managed with reduced traffic delay and improved transport system efficiency.

6.3 Assumption and limitation

This research work is built upon the LWR model which assumes that the equilibrium of traffic conditions can be achieved instantly. Therefore, acceleration and deceleration of road traffic are not considered by the proposed simulation framework. This limitation in an urban transport network is not as critical as in a freeway since urban traffic conditions are largely determined by traffic signals. However, the application of the proposed simulator in a more detailed transport network and traffic condition study might be constrained by this assumption.

Second, the VMBus simulation platform assumes that bus speeds during their cruising between stops are determined by traffic flow speeds. This assumption is necessary to enable this research to exclude bus driver influence and to focus on bus holding impact on the whole transport system. However, the actual bus cruising speeds can be altered by bus drivers and further affect their surrounding traffic in practice. If future research needs to investigate into the interaction between slow-moving buses and their other road traffic, more simulation components need to be developed in the existing VMBus platform.

Third, the proposed bus holding strategies through traffic signal adjustments assume that the volume of traffic flows can be changed instantly. No start or end lags are necessary. This ideal scenario helps identifying the effectiveness and efficiency of the proposed holding strategies without interruptions caused by other factors. This scenario, nevertheless, does not exist in reality. To make the proposed control strategies more implementable, more practical elements need to be taken into consideration such as the time lag for the discharge traffic flow to reach road saturation level.

6.4 Future work

Short term: 0 - 1 year

The short-term plan identifies research tasks which can be taken immediately and play an instrumental role in fulfilling mid-term and long-term plans. Selected short-term tasks include incorporating moving bottlenecks in the VMBus simulation platform, deploying more traffic modes and evaluating the impact of uncertain factors on proposed control strategy effectiveness.

First, it is rather common to have buses move slowly among road traffic in urban transport systems. Slow-moving buses form moving bottlenecks which reduce road capacity. It has been proven that the proposed simulator in Chapter 3 is effective and accurate to capture buses as moving bottlenecks among other road traffic compared to the CTM-based simulator. To further incorporate the proposed simulation in the VMBus, more development and configuration need to be carried out and implemented. Slow moving buses can be represented as internal boundaries which change road capacity in a time-space plane. The slope of bus trajectories and the associated traffic overtaking rates can be collected from real world observations.

The second direction to develop the established simulation platform is to incorporate other traffic modes such as bicycles and pedestrians in an integrated urban transport network. The modelling of multi-modal urban traffic flow in this research focuses on buses and takes the rest of road traffic as an integrated part. However, bicycles and pedestrians are considered as important components of an urban transport system which can have strong impacts on road traffic conditions. For example, separate bicycle lanes reduce road capacity and pedestrian-actuated signals directly affect road traffic. It is thus interesting to model bicycle and pedestrian flows and understand their impact on transport systems.

Third, the impact of uncertain factors on proposed control strategy effectiveness and efficiency needs to be fully evaluated and understood. The impact of the proposed bus holding strategies is evaluated in an ideal scenario where traffic

signal changes can affect road traffic flow instantaneously. However, it takes time for drivers to react to signal changes and for the discharge traffic flow to reach the saturation level in reality. Moreover, the proposed holding strategy also relies on accurate measurements of bus headways and bus locations in traffic links. The impact and sensitivity of this measurement accuracy on control performance need to be studied.

Middle term: 1 to 2 years

The mid-term task is identified as a continuation of short-term tasks and the basis for long-term tasks.

Upon completion of short-term tasks, a critical area to explore is to implement the proposed signal-based control strategies in practice and measure their actual performance in a real-world environment. Although the simulation platform is capable of representing the actual transport system with essential features of research interests, it does not consider exogenous interruptions which might arise from various sources as in the real-world practice. Performance of the proposed control strategies under uncertainty and external interruptions remains an interesting topic for future research. Validation of the proposed simulation platform is essential to carry out before its application in a large-scale network.

Long term: 2 to 3 years

The long-term task is identified based on an objective to commercialize the proposed simulation platform and increase its social and the economical impact. The following action items need to be carried out in order to fully commercialize the simulator.

From a technical perspective, the simulator needs to be further developed and packaged in a user-friendly manner for practical application. The simulator is currently written in Matlab. Despite the core algorithm being mostly developed and implemented, its interface with end users is yet to be addressed. Moreover, the work flow for calibrating the simulator to fit site-specific situations needs to be properly defined and configured in the software.

From a business perspective, the business model of the commercialized software needs to be defined. It is necessary to identify potential clients and develop client-oriented functions. The competitive situation faced by this product should also be evaluated in about 2 years.

From a financial perspective, how to raise the capital to grow the business needs to be studied. In order to launch the product at different stages to attract different investor funding, the ongoing business should be planned out and implemented.

References

Abkowitz, M. and Tozzi, J. (1987), 'Research contributions to managing transit service reliability', *Journal of Advanced Transportation* **21**(1), 47–65.

Adebisi, O. (1986), 'A mathematical model for headway variance of fixed-route buses', *Transportation Research Part B: Methodological* **20**(1), 59–70.

Allsop, R. (1977), Priority for buses at signal-controlled junctions: some implications for signal timings, *in* 'Proceedings of 7th International Symposium on Transportation and Traffic Theory', pp. 247–270.

Argote, J., Xuan, Y. E. and Gayah, V. V. (2012), 'Comparative analysis of various bus control strategies', *12th Conference on Advanced Systems for Public Transport, Santiago, Chile* .

Balcombe, R., Mackett, R., Paulley, N., Preston, J., Shires, J., Titheridge, H., Wardman, M. and White, P. (2004), 'The demand for public transport: a practical guide', *TRL Report 593* .

Balijepallia, N. C., Ngoduy, D. and Watling, D. (2013*a*), 'The two-regime transmission model for network loading in dynamic traffic assignment problems', *Transportmetrica A* **1**(1), 1–22.

Balijepallia, N. C., Ngoduy, D. and Watling, D. (2013*b*), 'The two-regime transmission model for network loading in dynamic traffic assignment problems', *Transportmetrica A* **1**(1), 1–22.

Barnett, A. (1974), 'On controlling randomness in transit operations', *Transportation Science* **8**(2), 102–116.

Barnett, A. and Kleitman, D. J. (1973), 'Optimal scheduling policies for some simple transportation systems', *Transportation Science* **7**(1), 85–99.

Bartholdi III, J. J. and Eisenstein, D. D. (2012), 'A self-coördinating bus route to resist bus bunching', *Transportation Research Part B: Methodological* **46**(4), 481–491.

Bates, J., Polak, J., Jones, P. and Cook, A. (2001), 'The valuation of reliability for personal travel', *Transportation Research Part E: Logistics and Transportation Review* **37**(2), 191–229.

Becerik-Gerber, B., Siddiqui, M. K., Brilakis, I., El-Anwar, O., El-Gohary, N., Mahfouz, T., Jog, G. M., Li, S. and Kandil, A. A. (2013), 'Civil engineering grand challenges: Opportunities for data sensing, information analysis, and knowledge discovery', *Journal of Computing in Civil Engineering* **28**(4), 401–413.

Bellinger, D. (2011), Bunching behaviour in London buses, Master's thesis, University of Westminster, UK.

Bellomo, N. and Dogbe, C. (2011), 'On the modeling of traffic and crowds: A survey of models, speculations, and perspectives', *SIAM review* **53**(3), 409–463.

Benn, H. (1995), 'Bus route evaluation standards: A synthesis of transit practice', *Transportation Research Board Report, Washington, DC* .

Bly, P. and Jackson, R. L. (1974), 'Evaluation of bus control strategies by simulation', *TRRL laboratory report, 637* .

Bowman, L. A. and Turnquist, M. A. (1981), 'Service frequency, schedule reliability and passenger wait times at transit stops', *Transportation Research Part A: General* **15**(6), 465–471.

Boyle, D. K. (2006), 'Fixed-route transit ridership forecasting and service planning methods', *Transit Cooperative Research Program (TCRP) Synthesis 66* .

Carey, M. and Bowers, M. (2012), 'A review of properties of flow–density functions', *Transport Reviews* **32**(1), 49–73.

Cats, O., Larijani, A. N., Ólafsdóttir, Á., Burghout, W., Andréasson, I. J. and Koutsopoulos, H. N. (2012), 'Bus-holding control strategies', *Transportation Research Record: Journal of the Transportation Research Board* **2274**(1), 100–108.

Ceder, A. and Stern, H. I. (1981), 'Deficit function bus scheduling with deadheading trip insertions for fleet size reduction', *Transportation Science* **15**(4), 338–363.

Chen, C., Skabardonis, A. and Varaiya, P. (2003), 'Travel-time reliability as a measure of service', *Transportation Research Record: Journal of the Transportation Research Board* **1855**(1), 74–79.

Chen, X., Yu, L., Zhang, Y. and Guo, J. (2009), 'Analyzing urban bus service reliability at the stop, route, and network levels', *Transportation research part A: policy and practice* **43**(8), 722–734.

Chin, K., Mundy, J. and Thompson, T. (1992), 'Control of the light rail transit/-traffic conflict: an update from Hong Kong, and simulation using the FLEXSYT program', *Traffic engineering & control* **33**(2).

Chow, A. (2007), System optimal traffic assignment with departure time choice, PhD thesis, University of London, UK.

Chow, A. (2013), 'Lecture 13-14: Bus priority and operations', *Lecture notes, University College London, UK* .

Chow, A. H. F. (2009), 'Dynamic system optimal traffic assignment: a state-dependent control theoretic approach', *Transportmetrica* **5**(2), 85–106.

Chow, A. H. F., Dadok, V., Dervisoglu, G., Gomes, G., Horowitz, R., Kurzhanskiy, A., Kwon, J., Lu, X., Muralidharan, A., Norman, S., Sanchez, R. and Varaiya, P. (2008), 'TOPL: Tools for operational planning of transportation networks', *Proceedings of the 1st ASME Dynamic Systems and Control Conference (CD-ROM), October 20-22. Ann Arbor, MI, USA.* .

Chow, A. H. F., Gomes, G., Kurzhanskiy, A. A. and Varaiya, P. (2010), 'Aurora RNM - a macroscopic tool for arterial traffic analysis', *Proceedings of 89th Annual Meeting of Transportation Research Board. Washington, DC, USA* .

Chow, A. H. F. and Lo, H. (2007), 'Sensitivity analysis of signal control with physical queuing: delay derivatives and an application', *Transportation Research Part B: Methodological* **41**(3), 462–477.

Chow, A. H., Li, Y. and Gkiotsalitis, K. (2015), 'Specifications of fundamental diagrams for dynamic traffic modeling', *Journal of Transportation Engineering* **141**(9), 04015015.

Chow, A. H., Santacreu, A., Tsapakis, I., Tanasaranond, G. and Cheng, T. (2014), 'Empirical assessment of urban traffic congestion', *Journal of Advanced Transportation* **48**(8), 1000–1016.

Courant, R., Friedrichs, K. and Lewy, H. (1928), 'Über die partiellen differenzengleichungen der mathematischen physik', *Mathematische Annalen* **100**(1), 32–74.

Daganzo, C. (1997), *Fundamentals of transportation and traffic operations*, Pergamon, Oxford.

Daganzo, C. F. (1994), 'The cell transmission model: A dynamic representation of highway traffic consistent with the hydrodynamic theory', *Transportation Research Part B: Methodological* **28**(4), 269–287.

Daganzo, C. F. (1995), 'The cell-transmission model, part II: network traffic', *Transportation Research Part B: Methodological* **29**(2), 79–93.

Daganzo, C. F. (2005*a*), 'A variational formulation of kinematic waves: basic theory and complex boundary conditions', *Transportation Research Part B: Methodological* **39**(2), 187–196.

Daganzo, C. F. (2005*b*), 'A variational formulation of kinematic waves: solution methods', *Transportation Research Part B: Methodological* **39**(10), 934–950.

Daganzo, C. F. (2006), 'On the variational theory of traffic flow: well-posedness, duality and applications', *Networks and heterogeneous media* **1**(4), 601–619.

Daganzo, C. F. (2009), 'A headway-based approach to eliminate bus bunching: Systematic analysis and comparisons', *Transportation Research Part B: Methodological* **43**(10), 913–921.

Daganzo, C. F. and Laval, J. A. (2005), 'On the numerical treatment of moving bottlenecks', *Transportation Research Part B: Methodological* **39**(1), 31–46.

Daganzo, C. F. and Menendez, M. (2005), 'A variational formulation of kinematic waves: bottleneck properties and examples', *In: Transportation and Traffic Flow Theory* pp. 345–364.

Daganzo, C. F. and Pilachowski, J. (2011), 'Reducing bunching with bus-to-bus cooperation', *Transportation Research Part B: Methodological* **45**(1), 267–277.

Danaher, A. R. (2010), *Bus and rail transit preferential treatments in mixed traffic*, Vol. 83, Transportation Research Board.

Delgado, F., Munoz, J. C. and Giesen, R. (2012), 'How much can holding and/or limiting boarding improve transit performance?', *Transportation Research Part B: Methodological* **46**(9), 1202–1217.

Delle Site, P. and Filippi, F. (1998), 'Service optimization for bus corridors with short-turn strategies and variable vehicle size', *Transportation Research Part A: Policy and Practice* **32**(1), 19–38.

DfT (2012*a*), Britain transport statistics: 2012, Technical report, Department for Transport, UK.

DfT (2012*b*), Green light for better buses, Technical report, Department for Transport, UK.

DfT (2013), Road transport forcasts 2013, Technical report, Department for Transport, UK.

Diab, E., Badami, M. and El-Geneidy, A. (2015), 'Bus transit service reliability and improvement strategies: Integrating the perspectives of passengers and transit agencies in north america', *Transport Reviews* **35**(3), 292–328.

Diab, E. I. and El-Geneidy, A. M. (2013), 'Variation in bus transit service: understanding the impacts of various improvement strategies on transit service reliability', *Public Transport* **4**(3), 209–231.

D'Souza, C., Gardner, K., Hounsell, N. and Shrestha, B. (2010), 'New developments for bus priority at traffic signals in London using iBus', pp. 72–77.

Eberlein, X. J., Wilson, N. H. and Bernstein, D. (2001), 'The holding problem with real–time information available', *Transportation science* **35**(1), 1–18.

Edie, L. C. (1961), 'Car-following and steady-state theory for noncongested traffic', *Operations Research* **9**(1), 66–76.

Fellendorf, M. (1994), Vissim: A microscopic simulation tool to evaluate actuated signal control including bus priority, *in* '64th Institute of Transportation Engineers Annual Meeting', pp. 1–9.

Fu, L. and Yang, X. (2002), 'Design and implementation of bus-holding control strategies with real-time information', *Transportation Research Record: Journal of the Transportation Research Board* (1791), 6–12.

Gardner, K., Souza, D, C., Hounsell, N., Shrestha, B. and Bretherton, D. (2009), 'Interaction of buses and signals at road crossings', *TRL Report* .

Gerlough, D. L. and Huber, M. J. (1975), *Traffic flow theory: a monograph*, Vol. 165, Transportation Research Board, National Research Council Washington, DC.

Geroliminis, N. and Daganzo, C. F. (2008), 'Existence of urban-scale macroscopic fundamental diagrams: Some experimental findings', *Transportation Research Part B: Methodological* **42**(9), 759–770.

Geroliminis, N. and Skabardonis, A. (2005), 'Prediction of arrival profiles and queue lengths along signalized arterials by using a Markov decision process', *Transportation Research Record* **1934**, 116–124.

Geroliminis, N. and Sun, J. (2011), 'Hysteresis phenomena of a macroscopic fundamental diagram in freeway networks', *Transportation Research Part A: Policy and Practice* **45**(9), 966–979.

Godunov, S. K. (1959), 'A difference method for numerical calculation of discontinuous solutions of the equations of hydrodynamics', *Matematicheskii Sbornik* **89**(3), 271–306.

Gomes, G. and Horowitz, R. (2006), 'Optimal freeway ramp metering using the asymmetric cell transmission model', *Transportation Research Part C: Emerging Technologies* **14**(4), 244 – 262.

Goodwin, P. (2012), 'Peak travel, peak car and the future of mobility'.

Greenberg, H. (1959), 'An analysis of traffic flow', *Operations research* **7**(1), 79–85.

Greenshields, B. D., Bibbins, J., Channing, W. and Miller, H. (1935), A study of traffic capacity, *in* 'Highway research board proceedings', Vol. 14, pp. 448–477.

Gu, W., Cassidy, M. J., Gayah, V. V. and Ouyang, Y. (2013), 'Mitigating negative impacts of near-side bus stops on cars', *Transportation Research Part B: Methodological* **47**, 42–56.

Hall, F. L. and Agyemang-Duah, K. (1991), 'Freeway capacity drop and the definition of capacity', *Transportation Research Record* (1320).

Han, K., Friesz, T. L. and Yao, T. (2013*a*), 'A link-based mixed integer LP approach for adaptive traffic signal control', *Transportation Research Board 92nd Annual Meeting, Washington, DC, USA* .

Han, K., Friesz, T. and Yao, T. (2013*b*), 'A partial differential equation formulation of Vickrey's bottleneck model, part I: Methodology and theoretical analysis', *Transportation Research Part B: Methodological* **49**, 55–74.

Han, K., Friesz, T. and Yao, T. (2013*c*), 'A partial differential equation formulation of Vickrey's bottleneck model, part II: Numerical analysis and computation', *Transportation Research Part B: Methodological* **49**, 75–93.

Hau, T. (1998), 'Congestion pricing and road investment', *Road Pricing, Traffic Congestion and the Environment* pp. 39–78.

Henn, V. (2005), 'Tracking waves through spatial discontinuities: boundary conditions in the wave tracking resolution of the LWR model', *Mathematics in Transport* pp. 349–362.

Hensher, D. A., Stopher, P. and Bullock, P. (2003), 'Service quality—-developing a service quality index in the provision of commercial bus contracts', *Transportation Research Part A: Policy and Practice* **37**(6), 499–517.

Heydecker, B. (1983*a*), *Mathematical analysis of responsive priority for buses at traffic signals*, Doctoral Thesis, University College London, UK.

Heydecker, B. and Addison, J. (2011), 'Analysis and modelling of traffic flow under variable speed limits', *Transportation research part C: Emerging Technologies* **19**(2), 206–217.

Heydecker, B. G. (1983*b*), 'Capacity at a signal-controlled junction where there is priority for buses', *Transportation Research Part B: Methodological* **17**(5), 341–357.

Heydecker, B. G. (1984), Delay at a junction where there is priority for buses, *in* 'Ninth International Symposium on Transportation and Traffic Theory', pp. 113–132.

Heydecker, B. G. and Addison, J. D. (2005), 'Analysis of dynamic traffic equilibrium with departure time choice', *Transportation Science* **39**(1), 39–57.

Hickman, M. D. (2001), 'An analytic stochastic model for the transit vehicle holding problem', *Transportation Science* **35**(3), 215–237.

Hill, S. A. (2003), 'Numerical analysis of a time-headway bus route model', *Physica A: Statistical Mechanics and its Applications* **328**(1), 261–273.

Hollander, Y. (2006), 'Direct versus indirect models for the effects of unreliability', *Transportation Research Part A: Policy and Practice* **40**(9), 699–711.

Hossain, M. and McDonald, M. (1998), 'Mixnetsim: A mixed traffic network simulation model for developing countries', pp. 722–733.

Hounsell, N. B., Shrestha, B. P., Bretherton, R. D., Bowen, T. and D'Souza, C. (2008*a*), Exploring priority strategies at traffic signals for London's ibus, *in* 'European Congress and Exhibition on Intelligent Transport Systems and Services, 7th, June 2008, Geneva, Switzerland'.

Hounsell, N. B., Shrestha, B. P., Bretherton, R. D., Bowen, T. and D'Souza, C. (2008*b*), 'New strategy options for bus priority at traffic signals in London', *European Transport and contributors Association Report* .

Hounsell, N., Kaparias, I., Cohen, S., Hoogendoorn, S. and Shrestha, B. (2009), 'Review of available case studies and related scientific knowledge', pp. 160–174.

Hundenski, R. (1998), 'A matter of time: Cultural values and the " problem" of schedules', *Transportation Research Board Report: 99* .

Hunter-Zaworski, K. (2003), 'Transit capacity and quality of service manual', *TCRP Report* .

Jabari, S. E. and Liu, H. X. (2012), 'A stochastic model of traffic flow: theoretical foundations', *Transportation Research Part B: Methodological* **46**, 156–174.

Janos, M. and Furth, P. (2002), 'Bus priority with highly interruptible traffic signal control: simulation of San Juan's Avenida ponce de leon', *Transportation Research Record: Journal of the Transportation Research Board* (1811), 157–165.

Jin, W., Chen, L. and Puckett, E. (2009), 'Supply-demand diagrams and a new framework for analyzing the inhomogeneous Lighthill-whitham-Richards model', *Transportation and Traffic Theory* pp. 603–635.

Koenig, J.-G. (1980), 'Indicators of urban accessibility: theory and application', *Transportation* **9**(2), 145–172.

Koffman, D. (1978), 'A simulation study of alternative real-time bus headway control strategies', *Transportation Research Record* (663), 41–46.

Kometani, E. and Sasaki, T. (1961), 'Dynamic behaviour of traffic with a non-linear spacing-speed relationship', *Proceedings of theory of traffic flow* pp. 105–119.

Kosonen, I. (1999), 'Hutsim-urban traffic simulation and control model: principles and applications', *Transportation Engineering Publication of Helsinki University of Technology* **100**.

Kuhne, R. D. (2011), 'Greenshields' legacy: Highway traffic', *Transportation Research E-Circular* (E-C149).

Kurzhanskiy, A. A., Kwon, J. and Varaiya, P. P. (2009), Aurora road network modeler, *in* 'Control in Transportation Systems', pp. 204–210.

Laval, J. (2004), 'Hybrid models of traffic flow: Impacts of bounded vehicle accelerations', *PhD thesis, University of California Berkeley, CA, USA* .

Laval, J. A. and Leclercq, L. (2013), 'The Hamilton–Jacobi partial differential equation and the three representations of traffic flow', *Transportation Research Part B: Methodological* **52**, 17–30.

Law, A. M., Kelton, W. D. and Kelton, W. D. (2015), *Simulation modeling and analysis, Fifth Edition*, McGraw-Hill New York.

Lebacque, J. P., Lesort, J. B. and Giorgi, F. (1998), 'Introducing buses into first-order macroscopic traffic models', *Transportation Research Record* **1644**, 70–79.

Leclercq, L., Laval, J. A. and Chevallier, E. (2007), The lagrangian coordinates and what it means for first order traffic flow models, *in* 'Transportation and Traffic Theory 2007. Papers Selected for Presentation at ISTTT17, London, England'.

Leutzbach, W. (1988), *Introduction to the theory of traffic flow*, Berlin: Springer.

LeVeque, R. J. (1992), *Numerical methods for conservation laws*, Basel: Birkhauser Verlag.

Li, J., Chen, Q.-Y., Wang, H. and Ni, D. (2012), 'Analysis of LWR model with fundamental diagram subject to uncertainties', *Transportmetrica* **8**(6), 387–405.

Li, M. Z. (2008), 'A generic characterization of equilibrium speed-flow curves', *Transportation Science* **42**(2), 220–235.

Lighthill, M. J. and Whitham, G. B. (1955), 'On kinematic waves. ii. a theory of traffic flow on long crowded roads', *Proceedings of the Royal Society of London. Series A. Mathematical and Physical Sciences* **229**(1178), 317–345.

Lin, J., Wang, P. and Barnum, D. T. (2008), 'A quality control framework for bus schedule reliability', *Transportation Research Part E: Logistics and Transportation Review* **44**(6), 1086–1098.

Lo, H. K. (1999), 'A novel traffic signal control formulation', *Transportation Research Part A: Policy and Practice* **33**(6), 433–448.

Lo, H. and Szeto, W. Y. (2002), 'A cell-based variational inequality formulation of the dynamic user optimal assignment problem', *Transportation Research Part B: Methodological* **36**(5), 421–443.

May, A. D. (1990), *Traffic flow fundamentals*.

Mazare, P., Dehwah, A., Claudel, C. G. and Bayen, A. M. (2011), 'Analytical and grid-free solutions to the lighthill-whitham-richards traffic flow model', *Transportation Research Part B: Methodological* **45**, 1727–1748.

Mehran, B. and Kuwahara, M. (2013), 'Fusion of probe and fixed sensor data for short-term traffic prediction in urban signalized arterials', *International Journal of Urban Sciences* **17**(2), 163–183.

Mehran, B., Kuwahara, M. and Naznin, F. (2012), 'Implementing kinematic wave theory to reconstruct vehicle trajectories from fixed and probe sensor data', *Transportation research part C: Emerging Technologies* **20**(1), 144–163.

Murray, A. T. and Wu, X. (2003), 'Accessibility tradeoffs in public transit planning', *Journal of Geographical Systems* **5**(1), 93–107.

Nam, D., Park, D. and Khamkongkhun, A. (2005), 'Estimation of value of travel time reliability', *Journal of Advanced Transportation* **39**(1), 39–61.

Nanda, S. (1993), 'Teletraffic models for urban and suburban microcells: Cell sizes and handoff rates', *Vehicular Technology, IEEE Transactions on* **42**(4), 673–682.

Newell, G. F. (1974), 'Control of pairing of vehicles on a public transportation route, two vehicles, one control point', *Transportation Science* **8**(3), 248–264.

Newell, G. F. (1993), 'A simplified theory of kinematic waves in highway traffic, part i: General theory', *Transportation Research Part B: Methodological* **27**(4), 281–287.

Newell, G. F. (1998), 'A moving bottleneck', *Transportation Research Part B: Methodological* **32**, 531–537.

Newell, G. F. and Potts, R. B. (1964), Maintaining a bus schedule, *in* 'Australian Road Research Board (ARRB) Conference, 2nd, 1964, Melbourne, Australia'.

Nie, Y., Ma, J. and Zhang, M. H. (2008), 'A polymorphic dynamic network loading model', *Computer-Aided Civil and Infrastructure Engineering* **23**, 86–103.

Noland, R. B. and Polak, J. W. (2002), 'Travel time variability: a review of theoretical and empirical issues', *Transport Reviews* **22**(1), 39–54.

OBR (2014), Economic and fiscal outlook, Technical report, Office for Budget and Responsibility.

ONN (2009), National population projections, 2008-based, Technical report, Office for National Statistics.

Osuna, E. and Newell, G. (1972), 'Control strategies for an idealized public transportation system', *Transportation Science* **6**(1), 52–72.

Perk, V., Flynn, J. and Volinski, J. M. (2008), 'Transit ridership, reliability and retention', *National Center for Transit Research Report* .

Pipes, L. A. (1953), 'An operational analysis of traffic dynamics', *Journal of Applied Physics* **24**(3), 274–281.

PMSU (2009), An analysis of urban transport, Technical report, Prime Minister's Strategy Unit.

Richards, P. I. (1956), 'Shock waves on the highway', *Operations research* **4**(1), 42–51.

Robertson, P. *et al.* (1974), Bus priority in a network of fixed time signals, *in* 'Transportation and Traffic Theory, Proceedings', Vol. 6, pp. 285–306.

Robinson, S. and Polak, J. (2006), 'Overtaking rule method for the cleaning of matched license plate data', *ASCE Journal of Transportation Engineering* **132**(8), 609–617.

Schramm, L., Watkins, K. and Rutherford, S. (2010), 'Features that affect variability of travel time on bus rapid transit systems', *Transportation Research Record: Journal of the Transportation Research Board* **2143**(1), 77–84.

Sibley, S. W. (1985), 'NETSIM for microcomputers', *Public Roads* **49**(2), 54–59.

Siemens (2012), 'SCOOT user guide', *Siemens Mobility, Traffic Solutions UTC System* .

Silcock, J. (1993), 'SIGSIM version 1.0 users guide'.

Silva, P. C. M. (2001), Modelling interactions between bus operations and traffic flow., PhD thesis, University College London, UK.

Strathman, J. G., Kimpel, T. J., Dueker, K. J., Gerhart, R. L. and Callas, S. (2002), 'Evaluation of transit operations: Data applications of tri-met's automated bus dispatching system', *Transportation* **29**(3), 321–345.

Strathman, J. G., Kimpel, T. J., Dueker, K. J. and Northwest, T. (2000), Bus transit operations control: review and an experiment involving tri-met's automated bus dispatching system, Technical report, Transportation Northwest, Department of Civil Engineering, University of Washington, WA.

Szeto, W. Y. (2008), 'The enhanced lagged cell transmission model for dynamic traffic assignment', *Transportation Research Record, Journal of TRB* **2085**, 76–85.

Szeto, W. Y. and Lo, H. (2006), 'Dynamic traffic assignment: properties and extensions', *Transportmetrica* **2**, 31–52.

TfL (2006), Bus priority at traffic signals keeps London's buses moving, Technical report, Transport for London, UK.

TfL (2015), London buses performance, Technical report, Transport for London, UK.

Toledo, T., Cats, O., Burghout, W. and Koutsopoulos, H. N. (2010), 'Mesoscopic simulation for transit operations', *Transportation Research Part C: Emerging Technologies* **18**(6), 896–908.

TRL (2014), 'Modelling bus set-backs', `https://trlsoftware.co.uk/support/knowledgebase/articles/27`. Accessed: 2015-09-05.

Tsapakis, I., Turner, J., Cheng, T., Heydecker, B. G., Emmonds, A. and Bolbol, A. (2012), 'Effects of tube strikes on journey times in the transport network of London', *Transportation Research Record* **2274**, 84–92.

Turnquist, M. A. (1981), 'Strategies for improving reliability of bus transit service', *Transportation Research Record* (818), 7–13.

Turnquist, M. A. (1982), 'Strategies for improving bus transit service reliability', *60th Annual Meeting of the Transportation Research Board, Washington DC, USA* .

Underwood, R. T. (1961), 'Speed, volume, and density relationships', *Quality and Theory of Traffic Flow* pp. 141–188.

Valencia, R. F. A. (2012), Traffic management method to study bus priorities on arterial roads, *in* 'European Transport Conference 2012, Glasgow, UK'.

van Wageningen-Kessels, F., van Lint, H., Hoogendoorn, S. P. and Vuik, K. (2009), Implicit and explicit numerical methods for macroscopic traffic flow models: Efficiency and accuracy, *in* 'Transportation Research Board 88th Annual Meeting, Washington DC, USA'.

van Wageningen-Kessels, F., van Lint, H., Hoogendoorn, S. P. and Vuik, K. (2010), 'Lagrangian formulation of multiclass kinematic wave model', *Transportation Research Record: Journal of the Transportation Research Board, Washington DC* **2188**(1), 29–36.

van Wageningen-Kessels, F., Yuan, Y., Hoogendoorn, S. P., Van Lint, H. and Vuik, K. (2013), 'Discontinuities in the lagrangian formulation of the kinematic wave model', *Transportation Research Part C: Emerging Technologies* **34**, 148–161.

Vickrey, W. S. (1969), 'Congestion theory and transport investment', *American Economics Review* **59**, 251–261.

Vincent, R., Cooper, B. and Wood, K. (1978), 'Bus-actuated signal control at isolated intersections–simulation studies of bus priority', *TRRL report* .

Welding, P. (1957), 'The instability of a close-interval service', *Journal of the Operational Research Society* **8**(3), 133–142.

Wilson, N. H., Macchi, R. A., Fellows, R. E. and Deckoff, A. A. (1992), 'Improving service on the mbta green line through better operations control', *Transportation research record, Journal of TRB* (1361), 296–304.

Wong, S. C. and Wong, G. C. K. (2002), 'An analytical shock-fitting algorithm for LWR kinematic wave model embedded with linear speed-density relationship', *Transportation Research Part B: Methodological* **36**(8), 683–706.

Woodhull, J. (1987), 'Issues in on-time performance of bus systems', *Unpublished manuscript. Los Angeles, CA: Southern California Rapid Transit District* .

Xuan, Y., Argote, J. and Daganzo, C. F. (2011), 'Dynamic bus holding strategies for schedule reliability: Optimal linear control and performance analysis', *Transportation Research Part B: Methodological* **45**(10), 1831–1845.

Yperman, I. (2007), 'The link transmission model for dynamic network loading', *PhD thesis, Katholieke Universiteit Leuven, Belgium* .

Yuan, Y., Van Lint, J., Wilson, R. E., van Wageningen-Kessels, F. and Hoogendoorn, S. P. (2012), 'Real-time lagrangian traffic state estimator for freeways', *IEEE Transactions on Intelligent Transportation Systems* **13**(1), 59–70.

Zhang, H., Nie, Y. and Qian, Z. (2013), 'Modelling network flow with and without link interactions: The cases of point queue, spatial queue and cell transmission model', *Transportmetrica B* **1**(1), 33–51.

Zhao, J., Dessouky, M. and Bukkapatnam, S. (2006), 'Optimal slack time for schedule-based transit operations', *Transportation Science* **40**(4), 529–539.

Ziliaskopoulos, A. (2000), 'A linear programming model for the single destination system optimum dynamic traffic assignment problem', *Transportation Science* **34**(1), 37 – 49.

Journal publication paper